2017

MITOCHONDRIAL TRANSPLANTATION AFTER SPINAL CORD INJURY: EFFECTS ON TISSUE BIOENERGETICS AND FUNCTIONAL NEUROPROTECTION

Jenna L. Gollihue
University of Kentucky, jlva227@uky.edu
Digital Object Identifier: https://doi.org/10.13023/ETD.2017.333

STUDENT AGREEMENT:

I represent that my thesis or dissertation and abstract are my original work. Proper attribution has been given to all outside sources. I understand that I am solely responsible for obtaining any needed copyright permissions. I have obtained needed written permission statement(s) from the owner(s) of each third-party copyrighted matter to be included in my work, allowing electronic distribution (if such use is not permitted by the fair use doctrine) which will be submitted to UKnowledge as Additional File.

I hereby grant to The University of Kentucky and its agents the irrevocable, non-exclusive, and royalty-free license to archive and make accessible my work in whole or in part in all forms of media, now or hereafter known. I agree that the document mentioned above may be made available immediately for worldwide access unless an embargo applies.

I retain all other ownership rights to the copyright of my work. I also retain the right to use in future works (such as articles or books) all or part of my work. I understand that I am free to register the copyright to my work.

REVIEW, APPROVAL AND ACCEPTANCE

The document mentioned above has been reviewed and accepted by the student's advisor, on behalf of the advisory committee, and by the Director of Graduate Studies (DGS), on behalf of the program; we verify that this is the final, approved version of the student's thesis including all changes required by the advisory committee. The undersigned agree to abide by the statements above.

Jenna L. Gollihue, Student

Dr. Alexander G. Rabchevsky, Major Professor

Dr. Kenneth S. Campbell, Director of Graduate Studies

MITOCHONDRIAL TRANSPLANTATION AFTER SPINAL CORD INJURY: EFFECTS ON TISSUE BIOENERGETICS AND FUNCTIONAL NEUROPROTECTION

DISSERTATION

A dissertation submitted in partial fulfillment of the requirements for the degree of Doctor of Philosophy in the College of Medicine at the University of Kentucky

By

Jenna Leigh Gollihue

Lexington, Kentucky, United States of America

Director: Dr. Alexander G. Rabchevsky

Lexington, KY

2017

ABSTRACT OF DISSERTATION

MITOCHONDRIAL TRANSPLANTATION AFTER SPINAL CORD INJURY: EFFECTS ON TISSUE BIOENERGETICS AND FUNCTIONAL NEUROPROTECTION

Contusion spinal cord injury (SCI) results in devastating life-long debilitation in which there are currently no effective treatments. The primary injury site presents a complex environment marked by subsequent secondary pathophysiological cascades involving excessive reactive oxygen and nitrogen species (ROS/RNS) production, glutamate-induced excitotoxicity, calcium dysregulation, and delayed neuronal apoptosis. Many of these cascades involve mitochondrial dysfunction, thus a single mitochondrial-centric therapy that targets a variety of these factors could be far reaching in its potential benefits after SCI. As such, this dissertation examines whether transplantation of exogenous mitochondria after SCI can attenuate secondary injury cascades to decrease the spread and severity of the injury.

Our first experiment tested the dose-dependent effects of mitochondrial transplantation on the ability to maintain acute overall bioenergetics after SCI. We compared transplantation of mitochondria originating from two different sources-cultured PC12 cells or rat soleus leg muscle. 24 hours after injury, State III oxygen consumption rates were maintained to over 80% of sham levels when 100ug of mitochondria was transplanted, regardless of the origin of the mitochondria. Complex I enzyme activity assays corroborated our findings that the 100ug dosage gave optimal benefits compared to vehicle injection.

We also analyzed the rostral-caudal distribution and cell-type colocalization of transplanted transgenically-labeled tGFP mitochondria after SCI. There were greater volumes and rostral-caudal spread of tGFP mitochondria at the 24 hour time point compared to 7 days post injection. tGFP mitochondria had the greatest propensity to colocalize with macrophages and pericytes. Colocalization was evident in endothelial cells, oligodendrocytes and astrocytes, though no such co-labeling was present in neurons. Further, colocalization of tGFP was always greater at the 24 hour time compared to 48 hour or 7days post injection time points. These data indicate that there is a cell-type difference in incorporation potential of exogenous mitochondria which changes over time.

Finally, we tested the effects of mitochondrial transplantation on long term functional recovery. Animals were injected with either vehicle, 100ug cell-derived mitochondria, or 100ug muscle-derived mitochondria immediately after contusion SCI. Functional analyses including BBB overground locomotor scale and von Frey mechanical sensitivity tests did not show any differences between treatment groups. Likewise, there were no differences in tissue sparing when mitochondria were transplanted compared to vehicle injections, though there were higher neuronal cell counts in tGFP mitochondria injected groups caudal of the injury site.

These studies present the potential of mitochondrial transplantation for therapeutic intervention after SCI. While our acute measures do not correspond into long term recovery, we show that at 24 hours transplanted mitochondria do have an effect on bioenergetics and that they are taken into host cells. We believe that further investigation into caveats and technical refinement is necessary at this time to translate the evident acute bioenergetic recovery into long term functional recovery.

KEYWORDS: PC-12 mitochondria, central pattern generators, co-localization, transgenic labeling, oxidative phosphorylation

Jenna L. Gollihue

June 16, 2017

MITOCHONDRIAL TRANSPLANTATION AFTER SPINAL CORD INJURY: EFFECTS ON TISSUE BIOENERGETICS AND FUNCTIONAL NEUROPROTECTION

By

Jenna L. Gollihue

Dr. Alexander G. Rabchevsky
Director of Dissertation

Dr. Kenneth S. Campbell
Director of Graduate Studies

This dissertation is dedicated to my parents, Bud and Lori VanRooyen- their love, support, and guidance has truly made me who I am today.

ACKNOWLEDGEMENTS

My gratitude goes to my mentor, Dr. Alexander “Sasha” Rabchevsky for taking me in as a graduate student in his lab. Sasha’s passion for the research we are doing continually inspires me to work harder, and his mentoring has taught me to be a scientist that is always critical to find the truth. Thank you for instilling in me a drive to be the best scientist I can be. Secondly, I would like to thank the members of the Rabchevsky lab. Dr. Samir Patel, who spent many exhausting “mito days” working beside me in the lab; your friendship, support, and cheerfulness made the long experimental days much more enjoyable. Khalid Eldahan and David Cox, thank you for all of your help over the years, especially with the surgeries that started at dawn and didn’t end until after dark.

I would also like to thank my committee members, who have given me invaluable advice and encouragement when I hit a roadblock. Dr. Bret Smith, Dr. Steve Estus, Dr. John Gensel, and Dr. Pat Sullivan, thank you for always giving me your valuable help and guidance, whether it be science related or not. Our discussions taught me the importance of thinking both critically and creatively.

The Physiology department and the Spinal Cord and Brain Injury Research Center at the University of Kentucky has been a vital part of my education. Thank you to all of the faculty, administrators, lab techs, post docs, grad students, and undergrads. It really does take a village, and without such a great network none of this would have been possible. From you I have found great role models, great friends, and had experiences I wouldn’t change for anything.

My family’s love and support has gotten me through the ups and downs that come with graduate school. All my life, my parents believed in me and pushed me to excel. They gave me the confidence to never doubt that I could do and be whatever I wanted as long as I tried. And thank you for always pushing me to try. My brothers, Alex and Jason, are the best siblings a girl could ask for. Just a phone call away, talking to you guys always made me feel better whenever I was homesick. Which sometimes was a lot.

Thank you to my friends, Erica Littlejohn, Stacy Webb, Caitlyn Reidmann and many others- your friendship has meant the world to me. From hanging out first year to the parades and festivals, craft nights with lots of glitter, coffee breaks and dinners, thank you for the times we just needed a break from science. Even though we all inevitably just ended up talking science anyways.

And last but certainly, definitely, not least- thank you to my amazing husband, Jarrad Gollihue. You have been my rock and my best friend, the shoulder I lean on. After a long day in the lab, you always just know whether I need a hug, a high five, or a jumbo margarita. I am so thankful to have you as my partner through these important life experiences.

TABLE OF CONTENTS

LIST OF TABLES

LIST OF FIGURES

CHAPTER 1

INTRODUCTION AND HYPOTHESIS

1. Introduction to Mitochondria

Mitochondria are located in the cell cytoplasm and often referred to as the powerhouse of the cell, as they produce most of the cell's energy in the form of adenosine triphosphate (ATP). However, they are also referred to as the nuclear power plant of the cell as they can efficiently make ATP while simultaneously producing a small but manageable amount of destructive oxidative agents known as reactive oxygen species (ROS). When mitochondria are damaged they can become extremely reactive and damaging to themselves and surrounding mitochondria, unleashing numerous pathways that can lead to both apoptosis and necrosis. Therefore, a delicate balance must be maintained for these organelles to function at optimal efficiency without devastating consequences.

1.1.1 Mitochondrial DNA

It is theorized that mitochondria were once bacteria that became engulfed by a cell and utilized for its respiratory capabilities. Evidence of this theory lies in the fact that mitochondria have two lipid membranes and their own circular mitochondrial DNA (mtDNA) (Nass & Nass 1963), which allows them to make their own proteins (Mc et al 1958). As evolution progressed, cells became more dependent on mitochondria for their energy supply, even integrating the coding for key mitochondrial proteins within the nuclear DNA. mtDNA only encodes for 13 mitochondrial proteins and needs the cell's nuclear DNA to provide the rest of the mitochondrial proteins.

mtDNA replication and transcription occurs in the S and G2 phases of the cell cycle (Pica-Mattoccia & Attardi 1971, Pica-Mattoccia & Attardi 1972), but mitochondrial protein synthesis doubles during interphase and remains relatively constant during the cell cycle (England & Attardi 1974).

Mitochondria have a distinct DNA polymerase separate from that of nuclear DNA (Ch'ih & Kalf 1969, Meyer & Simpson 1970). mtDNA lacks exons and histones, which protect nuclear DNA by creating a tighter structural formation. Because of this and their proximity to the electron transport chain (ETC) which is prone to release oxidative molecules, mtDNA undergo mutations at a higher rate than nuclear DNA (Brown et al 1979).

Mitochondria are inherited maternally (Hutchison et al 1974), meaning that each offspring will have mtDNA identical to their mother's with no input from the father's mtDNA, making it possible to track familial lineage using the maternal mitochondria. This also implicates maternal inheritance of mtDNA mutations and disorders. It has been suggested that there are no recombinant abilities in mtDNA; when creating mouse x rat somatic cell hybrids and rat cytoplasmic hybrids, Hayashi et al (1985) found that there was no mtDNA recombination even when chloramphenicol (CAP) resistant mtDNA was incorporated into a CAP-sensitive cell. The cell remained resistant to CAP, but the mtDNA was unchanged. The group theorized that since mtDNA is inherited completely maternally, there is no necessity for recombination of mtDNA, and thus it has lost the ability to do so (Hayashi et al 1985). However, the amount of mutated mtDNA in an egg can vary, known as heteroplasmy (Lightowlers et al 1997), resulting in differing phenotypes creating inheritance patterns that may not be obvious.

Interestingly, mitochondrial replacement has been attempted in fertilization techniques to replace defective mtDNA with healthy mtDNA from a donor (Cohen et al 1998, Cohen et al 1997). Mouse models demonstrating the synchronous transfer of cytoplasts from a donor oocyte to a recipient oocyte which led to the development of a healthy zygote (Levron et al 1996) furthered the research efforts of human ooplasmic donation. Clinical studies testing injection of a small portion of cytoplasm which includes mRNA, protein, and mitochondria from a healthy donor oocyte into a compromised oocyte with subsequent fertilization and implantation resulted in successful pregnancy (Cohen et al 1998, Cohen et al 1997). The developing embryo thus contained nuclear DNA from the mother and father, along with mtDNA from the donor egg. While cytoplasmic transfer

therapy resulted in successful births, it was banned in the United States in 2001 for ethical reasons; however the practice is still being performed legally in other countries (Ishii 2014). A similar therapy aimed at avoiding mtDNA mutation inheritance by providing three biological parents uses a nuclear transfer technique- a mother and father providing the nuclear DNA, and a separate donor for the mtDNA (Reardon 2016). The nucleus is removed from the mother's egg (containing unhealthy mitochondria) and implanted into a donor egg (containing healthy mitochondria) in which the nucleus and genetic material has been removed. The resulting egg contains donor mitochondria (with mtDNA) and cytoplasm, and the mother's nucleus (with nuclear DNA). The egg is then fertilized with the father's sperm and an embryo develops with three distinct genetic parents. This therapy has been shown in non-human primates to circumvent the genetic inheritance of mitochondrial disease when the mother's mitochondria carry DNA mutations (Tachibana et al 2009).

1.1.2 Oxidative Phosphorylation

Mitochondria provide for most of the cell's energy needs in the form of ATP (**Figure 1.1A-1**). In the process of oxidative phosphorylation mitochondria use substrates produced by the Kreb's cycle in the mitochondrial matrix, namely reduced nicotinamide adenine dinucleotide (NADH) and flavin adenine dinucleotide (FADH), to power the electron transport system (ETS) located in the inner mitochondrial membrane (IMM). NADH donates an electron to complex I of ETC, an exchange that results in hydrogen atoms being pumped against a concentration gradient from the matrix into the intermembrane space. The electron then passes across the other complexes of the ETC in a series of oxidation/reduction reactions, each time releasing energy and pumping hydrogen from the matrix to the intermembrane space (for comprehensive review see Nicholls & Ferguson 2013). This creates a membrane potential (between 140 and 180 mV) across the inner mitochondrial membrane, which is used by complex V to form ATP from adenosine diphosphate (ADP) with simultaneous passage of hydrogen back into the mitochondrial matrix (Reid et al 1966). When

the electron reaches complex IV, it is released back into the matrix where it joins with oxygen. The oxygen is held at complex IV until enough electrons are present to allow it to form two water molecules. During oxidative phosphorylation, some ROS are created but are in small amounts that can be counteracted by endogenous antioxidant mechanisms within the mitochondria (see Cheeseman & Slater 1993, Droge 2002).

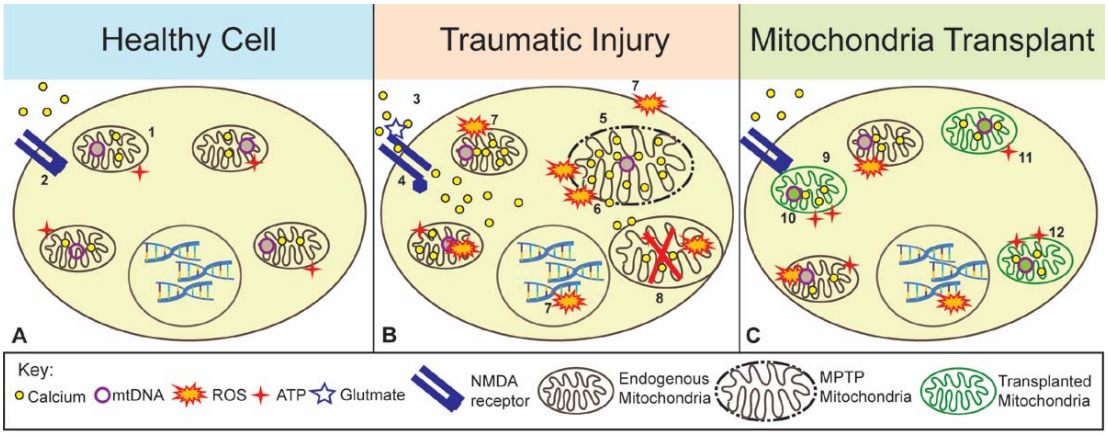

Figure 1.1. Schematic depiction of how mitochondrial transplantation after injury may promote cell survival. A. During normal cellular function, mitochondria sequester and store calcium in their matrix and produce ATP (**1**) while NMDA receptors remain closed (**2**). **B**. After traumatic injury, the cell is subjected to glutamate excitotoxicity mediated by activated NMDA receptors (**3**) which allow massive calcium influx into cells (**4**) and subsequent uptake into mitochondria. This causes a loss of membrane potential across the inner mitochondrial membrane leading to MPTP formation and subsequent swelling of mitochondria (**5**). Consequent bursting of the outer mitochondrial membrane then releases calcium, ROS, and apoptotic factors (**6**). ROS damages membrane lipids, mtDNA, electron transport chain proteins, and nuclear DNA (**7**), which leads to death of adjacent mitochondria (**8**). **C**. After healthy mitochondria, depicted in green, are transplanted into damaged cells they can increase antioxidants to combat ROS release (**9**) and provide new sources of mtDNA (**10**). Further, these mitochondria increase ATP production (**11**) and overall calcium buffering capacity (**12**) in the compromised cells.

1.1.3 Endogenous Antioxidant Systems

During oxidative phosphorylation, electron flow leads to a small amount of ROS production, namely in the form of superoxide radicals. Electrons released from the ETC can reduce oxygen molecules to superoxides (O_2^-). Manganese superoxide dismutase (MnSOD) localized within the mitochondria (Weisiger & Fridovich 1973) can oxidize superoxides into less reactive hydrogen peroxide (McCord & Fridovich 1969). Hydrogen peroxide, however, can undergo the Fenton reaction, creating hydroxyl radicals (OH^-) that can damage lipids, proteins, and nucleic acids (Winterbourn 1995). Alternatively, glutathione peroxidase can convert hydrogen peroxide into water and is present in the intermembrane space of mitochondria (Arai et al 1999). Damage to mitochondria can be countered by an increase of the endogenous antioxidant systems activities. For example, complex I deficiencies increase the expression of MnSOD which turns superoxide into hydrogen peroxide in cultured fibroblasts (Pitkanen & Robinson 1996).

1.1.4 Calcium Buffering

The mitochondrial matrix holds a negative charge of around -240mV, (see Michelakis 2008) allowing the mitochondria to actively sequester positively charged calcium ions into their matrix (**Figure 1.1A-1**). This is important as calcium is involved in various intracellular signaling pathways. Under normal conditions, concentration of cytoplasmic calcium is 0.1μM and extracellular calcium concentration is 1mM, favoring calcium movement into the cytoplasm (see Bianchi et al 2004). The IMM has a potential of -180mV, favoring calcium influx into the matrix through the calcium uniporter (Bygrave & Ash 1977), with equilibrium being reached when the calcium concentration within the mitochondrial matrix reaches 10^6 higher than the cytosol (Bianchi et al 2004). Once inside the matrix, energy is required to export calcium back out of the matrix to overcome the electrochemical force driving calcium influx. It is found that the energy released from ATP hydrolysis (34.1kJ/mol) is sufficient to allow movement of 1 mol of calcium (33kJ) across the inner mitochondrial membrane

and into the intermembrane space (Bianchi et al 2004). Importantly, calcium is required for the activation of different metabolic enzymes such as pyruvate dehydrogenase, α-ketoglutaratedehydrogenase, and isocitrate dehydrogenase. Calcium influx into the mitochondrial matrix leads to increased metabolism through interaction with these metabolic enzymes, increasing ATP production for the cell (Jouaville et al 1999).

1.1.5 Mitochondrial Fusion and Fission

It is not uncommon to see mitochondria depicted in textbooks as small, bean-shaped organelles. To the contrary, mitochondrion are very dynamic organelles that constantly undergo fusion and fission, creating an ever-changing network contained within the cytoplasm. In healthy cells, these fusion/fission events are well-balanced for the turnover of mitochondria and serves multiple purposes pertaining to the health of both the mitochondria and the cell. Fusion can allow for segregation of damaged areas of the mitochondria with subsequent fission and mitophagy (a mitochondrial specific form of autophagy) of this section, serving to maintain a healthy membrane potential of the remaining mitochondria (Twig et al 2008a). This group also found that loss of membrane potential decreased the probability for the mitochondrion to undergo fusion, which could be a protective mechanism keeping damaged mitochondria from joining and affecting the mitochondrial network. Depolarized mitochondria are then targeted for autophagy (Priault et al 2005). Mitochondria will undergo increased levels of fission before apoptosis (Suen et al 2008). Stressed or starved mitochondria can undergo a process known as hyperfusion, in which the mitochondria produce higher amounts of ATP (Tondera et al 2009). Fused mitochondria can share their components such as metabolites, proteins and mtDNA, known as complementation (Arimura et al 2004, Chen et al 2005). Fusion of mitochondria containing mutated mtDNA with mitochondria containing healthy mtDNA could allow a cell to overcome the effects of having mutant mtDNA (Nakada et al 2001). Each of these mechanisms is adapted for maintaining the healthiest possible mitochondrial network for the cell.

1.1.6 Mitochondria Act as a Death Switch

Cell death is a physiologically important and normal occurrence that is used to keep an organism in homeostasis. Without cell death, there would be no opportunities for newer, healthier cells to take over vital functions of the tissue. However, excessive cell death can be detrimental. An early feature of cellular apoptosis is disruption of the ETS. Mitochondrial function is necessary for cells to undergo apoptosis, as this form of controlled cellular death requires energy (see Kroemer et al 1998). Cytochrome c, a protein in the electron transport chain, can act as a signal for apoptosis; when released into the cytosol it can bind to activating factor-1 causing formation of an apoptosome complex that then activates caspases necessary to signal the induction of apoptosis (see Riedl & Salvesen 2007). A consequence of damaged ETS is a drop in ATP production; in cases of extreme ATP depletion the cell undergoes necrosis which is typically detrimental to nearby cells (Ankarcrona et al 1995, Eguchi et al 1997). Acute insult *in vitro* using high concentrations of N-methyl-D-aspartate (NMDA) or free radicals result in necrosis, but the apoptotic pathway is favored when less concentrated NMDA and free radicals are present. Further, NMDA-induced cell death can be prevented with the use of NMDA receptor antagonists, but not when free radicals are simultaneously present (Bonfoco et al 1995).

1.1.7 Mitochondrial Dysfunction

There is an important stability necessary for mitochondria to optimally carry out their biological functions essential to cell survival. Damage to mitochondria can be exponentially devastating as they not only fail to provide these vital biological functions, but they can be extremely hazardous and damaging to nearby mitochondria and cells. Mitochondrial dysfunction is implicated in many disease states such as Parkinson's Disease (Mizuno et al 1989, Winklhofer & Haass 2010), Alzheimer's Disease (Swerdlow & Khan 2004), muscular dystrophy (Onopiuk et al 2009), macular degeneration (Burdon 1995), and ageing-related neurodegeneration (Lin & Beal 2006). Importantly, mitochondria dysfunction is also involved in pathologies seen after many

traumatic insults including cardiac infarctions (Braunwald & Kloner 1985, Ide et al 2001), stroke (Bolanos et al 2009, Krajewski et al 1999, Sims & Muyderman 2010), traumatic brain injury (Aygok et al 2008, Singh et al 2006, Xiong et al 1997), and spinal cord injury (Huang et al 2012, Sullivan et al 2007).

Our lab, in collaboration with others, have shown there is substantial mitochondrial dysfunction after traumatic spinal cord injury (SCI). Studies have shown that mitochondrial ETC functions are compromised and there is increased mitochondrial oxidative stress as soon as 6 hours after injury (Jin et al 2004, McEwen et al 2007, Patel et al 2010, Patel et al 2009b, Sullivan et al 2007). Mitochondrial respiration is significantly decreased as early as 6 hours post injury, with further progressive decline in respiration over 24 hours post injury (Sullivan et al 2007). This group also showed significant increases in markers of oxidation at 24 hours post injury. A different group studying a rat model of spinal contusion injury found that glutathione, an endogenous antioxidant, and ATP levels were significantly decreased as early as 2 hours after injury and that this decrease continued to progress over 24 hours post injury (Jia et al 2016). Interestingly, this group also reported mitochondrial fusion increases immediately after injury, followed by a turn to mitochondrial fission corresponding to decreased ATP and glutathione and increased apoptosis signaling cytochrome c and caspase 3 release. There is evidence that mitochondrial function drastically changes after SCI, thus the next sections will explore the pathophysiology following SCI with emphasis on the role that dysfunctional mitochondria play.

1.2 Introduction to Spinal Cord Injury

Spinal cord injury is a devastating condition with life-long consequences and there are currently no effective treatments for reversing the pathophysiology after injury. In the United States there are approximately 17,000 new cases of SCI each year (Center 2016). There are different types of SCI such as transection, ischemia, and penetration, though a contusion type of injury is most common, where there is a physical compression and bruising of the spinal cord by the bones of the spinal column. Injury progression following the initial

mechanical insult can be separated into two phases commonly referred to as the primary injury and the secondary injury (Norenberg et al 2004). The immediate time point after injury is the primary injury phase and represents the physical destruction and necrosis of tissue (Baptiste & Fehlings 2006, Dumont et al 2001). Even at this early time point, glutamate excitotoxicity and microglial activation are present (Donnelly & Popovich 2008, Wrathall et al 1996). Additionally, vascular hemorrhaging and vasospasms occur resulting in ischemia of the spinal cord (Ducker & Assenmacher 1969). The pathophysiological events at this immediate time point is important, though typically not clinically accessible for treatment interventions. Accordingly, many current treatments aim to address the secondary injury phase.

1.2.1 Secondary Pathophysiological Cascades Following SCI

The secondary injury phase contributes to the spread and severity of tissue damage over time. The progression of the secondary injury phase has been further separated into different sub-phases (Rowland et al 2008). The immediate phase comprises the first 2 hours after injury. The acute phase follows; it is separated into the early acute phase which is 2-48 hours after injury, and the subacute phase which is 2 days to 2 weeks after injury. The early acute phase includes free radical production, delayed cellular apoptosis, excitotoxicity, calcium dysregulation, axonal degeneration, ischemia, and inflammation (Cuzzocrea et al 2001, Faden et al 1988, Fiskum 2000, Lewen et al 2000, Tator & Fehlings 1991). The subsequent intermediate phase is 2 weeks to 6 months post-injury, and the chronic phase begins at 6 after injury. The average time it takes to diagnose a patient after injury is 3.2 hours, which makes the early acute secondary injury phase the earliest clinically feasible target for therapeutic intervention (Bracken et al 1997).

1.2.1.1 Ionic Dysregulation and Excitotoxicity

Ionic imbalance and excitatory molecule release are prevalent manifestations in the secondary injury phase after SCI that potentiate further

damage (Agrawal & Fehlings 1996, Allen 1914, Hall et al 1989, Young & Koreh 1986). Glutamate is an excitatory neurotransmitter that can be neurotoxic in the brain during occurrences of overwhelming exposure (Olney & Sharpe 1969). After SCI, glutamate is released from damaged cells and binds to NMDA and α-amino-3-hydroxy-5-methyl-4-isoxazolepropionic acid (AMPA) receptors located on the membrane of nearby cells (**Figure 1.1A-2**). This causes channel opening and unregulated influx of excessive sodium and calcium into cells, known as excitotoxicity (Hume et al 1991, Lucas & Newhouse 1957, MacDermott et al 1986, Manev et al 1989, Olney 1969, Tator 1991) (**Figure 1.1B-3,4**).

Calcium ionic dysregulation can cause disruptions in cellular signaling processes, mitochondrial function, and increase initiation of apoptotic pathways and neuronal death (Choi 1988, Senter & Venes 1978, Tymianski & Tator 1996). Importantly, mitochondria can sequester large amounts of positively charged calcium ions within their negatively charged matrix. In cases of extreme intracellular calcium concentrations, increased calcium sequestration in the mitochondrial matrix results in a loss of membrane potential across the IMM as the matrix becomes more positively charged (Rottenberg & Scarpa 1974).

Loss of membrane potential then results in decreased calcium buffering capacity with subsequent calcium dysregulation within the cell such as activation of calpains and phospholipases that induce the release of apoptosis inducing factor (AIF) from mitochondria (Polster et al 2005), downstream release of cytochrome c, and formation of the mitochondrial membrane permeability transition pore (MPTP) (Krajewska et al 2004). Formation of the MPTP (**Figure 1.1B-5**) is a phenomenon in which a mega channel forms allowing water, ions, and molecules up to 1500 Daltons to move freely across the inner mitochondrial membrane (Hunter & Haworth 1979, Hunter et al 1976). Upon MPTP formation water will follow its osmotic gradient and pass into the highly concentrated matrix causing swelling of the mitochondria and bursting of the outer mitochondrial membrane (**Figure 1.1B-6**), consequently releasing ROS, reactive nitrogen species (RNS), calcium, and cytochrome c into the cell. Cyclophilin D is a component of the MPTP that interacts with mitochondrial amyloid-beta protein in

Alzheimer's disease (Du et al 2008). This group showed that an Alzheimer's mouse model deficient in cyclophilin D had increased mitochondrial Ca^{2+} buffering capacity and memory and spatial learning scores compared to mice with cyclophilin D. Using a small molecule inhibitor that binds to cyclophilin D such as C-9 decreases the detrimental effects of Aβ and calcium-induced MPTP opening (Valasani et al 2016, Valasani et al 2014), further indicating MPTP as a therapeutic target for neuronal disease states.

In addition to causing potential mitochondrial swelling and MPTP, NMDA receptor activation and calcium influx also leads to activation of nitric oxide synthase, resulting in production of nitric oxide, a powerful oxidant (Dawson et al 1991). Overstimulation of NMDA receptors can also result in ROS production including the formation of superoxide radicals (Lafon-Cazal et al 1993). Superoxide radicals react with nitric oxide to form peroxynitrite (Beckman et al 1990), an oxidant which reacts with lipid membranes, proteins, and DNA and may further cause release of calcium by mitochondria which can be inhibited by cyclosporin A (Packer & Murphy 1994).

Increased glutamate levels in the presence of extracellular calcium *in vitro* causes neuronal degeneration (Choi 1985) that can be inhibited by using NMDA antagonists (Choi 1988). Thus, blockade of excitatory NMDA or AMPA receptors has been a therapeutic target for neuroprotection with promising results (Agrawal & Fehlings 1996, Gill & Lodge 1997, Hall & Braughler 1982, Young & Koreh 1986).

1.2.1.2 Free Radical Release

Free radical production is an important implication after traumatic injury to central nervous system tissue. ROS/RNS are released, oxidizing nearby proteins, lipids, DNA and mtDNA, propagating subsequent reactive species production and increasing the spread of damage (Hall & Braughler 1993). Neurons in the spinal cord are especially vulnerable to oxidative damage. They have a relatively high concentration of polyunsaturated fatty acids in their lipid membrane that contain double bonds easily broken by ROS. Resident microglia

can increase ROS production when activated, and neurons have relatively little endogenous antioxidant mechanisms (for review of CNS tissue vulnerability to ROS, see Friedman 2011). ROS and RNS release from mitochondria may further damage nearby proteins and lipids in the mitochondrial membranes, as well as mtDNA (**Figure 1.1B-7**). When mitochondria undergo oxidative damage they release higher amounts of ROS, and when the ROS overload becomes too much for the endogenous antioxidant systems to handle, these mitochondria will also undergo MPTP. This illustrates how one damaged mitochondria can cause a domino effect resulting in widespread mitochondrial damage within the cell until a threshold is passed to signal the cell to undergo apoptosis or necrosis (**Figure 1.1B-8**).

Xu et al (2005) used a superoxide dismutase (SOD1) overexpressing transgenic mouse model of compression spinal cord injury to investigate ROS-mediated motor neuron death (Xu et al 2005). They found that there was less ROS production and motor neuron cell death in animals overexpressing SOD1 compared to wild type animals. The use of antioxidants such as tirilazad mesylate (Hall 1995) and methylprednisolone have been tested to counter the detrimental effects of reactive species after nervous system trauma (Hall & Braughler 1982, Hall et al 1989, Saunders et al 1987). Clinical trials were performed using methylprednisolone after contusion SCI (Bracken et al 1985, Bracken et al 1997). Importantly, this study found that timing of treatment is crucial, with benefits after treatment more profound with shorter times between injury and treatment. Initial results were promising, though these studies have come under scrutiny for possible side effects leading to controversy and the discontinued clinical use of methylprednisolone.

1.2.1.3 Inflammatory Response

After injury there are remarkable and complex inflammatory responses that can contribute to the escalation of secondary pathophysiology (Blight 1985, Blight 1992, Carlson et al 1998, Fehlings & Nguyen 2010, Fleming et al 2006). The immediate inflammatory response after injury includes neutrophil invasion

and resident microglial activation. Breakdown of the blood brain barrier, coupled with invasion of peripheral immune cells and cytokine activation, causes intricate inflammatory responses in the injured tissue that are both injury-severity and time-dependent (Popovich et al 1996). There is controversy as to the benefits vs detriments afforded by the inflammatory response after SCI. Macrophages can have multiple phenotypes depending on the injury environment and signaling cues. For instance, M1 macrophages produce cytokines and ROS that augment inflammation of the injury site. Inflammation can cause demyelination (Cammer et al 1978, Selmaj & Raine 1988, Wisniewski & Bloom 1975), inhibit axonal growth (Berry & Riches 1974), release ROS/RNS (Griot et al 1989, Merrill et al 1993), release cytokines and increase the progression of injury and cell death (Means & Anderson 1983). Blocking macrophage migration to the injury site helps alleviate some of the secondary injury pathophysiology and improve functional recovery after SCI (Popovich et al 1999). Additionally, immunosuppressants have been used to fight the inflammatory response as a therapeutic treatment after SCI (Bethea et al 1999, Blight 1994, Taoka et al 1997). However, it needs to be noted that the inflammatory response does serve a purpose in tissue healing. M2 phenotype macrophages have anti-inflammatory actions and promote wound healing- for review on macrophage subtypes (see Murray & Wynn 2011). For instance, macrophages can create a permissive environment for neuronal regeneration in a model of optic nerve injury (David et al 1990, Hirschberg et al 1994, Perry et al 1987). Therefore, it is important to understand the complexity of the inflammatory response so that targets can be specifically identified based on the therapeutic goals to counter inflammation but encourage healing.

It is apparent that mitochondria are of bacterial in origin, as evident by common morphological properties including circular DNA, double membranes including cardiolipin, lack of histones, and the ability to form N-formyl peptides. Because these properties are also recognized by the body's immune system as bacterial and thus non-self, or something to be eradicated, the mitochondria can stimulate an immune response similar to that induced by a bacterial infection

(Lotze et al 2007). Damage-associated molecular patterns (DAMPs) are located on the cell surface, secreted into the extracellular matrix, or produced as a byproduct of degradation (Garg et al 2010). Pattern recognition receptors are expressed on dendritic cells and macrophages that recognize DAMPs and cause upregulation of proinflammatory cytokine production (Krysko et al 2011, Rubartelli & Lotze 2007). Some DAMPs associated with mitochondria include mtDNA (Collins et al 2004, Zhang et al 2010b), N-formylmethionyl proteins (Carp 1982), Cytochrome c, ATP (Ghiringhelli et al 2009, Iyer et al 2009), cardiolipin (Sorice et al 2004), carbamoyl phosphate synthase (Struck et al 2005), and ROS (Kazama et al 2008). ATP released from cells into the extracellular matrix acts to recruit monocytes and neutrophils in a model of human neutrophil chemotaxis *in vitro* (Chen et al 2006, Elliott et al 2009) as well as activation of inflammasomes (Schroder & Tschopp 2010). In cases of severe tissue trauma, cellular necrosis can release massive quantities of mitochondrial particles, including mtDNA, which have been found to activate neutrophils and create an immune response in a rat model of trauma/hemorrhagic shock (Zhang et al 2010a, Zhang et al 2010b). Thus, the presence of mitochondria or mitochondrial-derived particles in the extracellular matrix after traumatic tissue damage such as SCI can increase immune and inflammatory responses including macrophage infiltration.

1.2.1.4 Vasculature Changes

Primary injury causes direct mechanical damage to the spinal cord vasculature and subsequent disruption of blood flow within the cord leading to progressive tissue loss (Wolman 1965) which is followed by later reperfusion of the vessels (Senter & Venes 1978). Hemorrhaging after injury can cause prolonged pressure on the spinal cord and cell death (Allen 1914). Damage to vessels results in a breakdown of the blood spinal cord barrier, allowing for unrestricted access of small molecules to the central nervous system (CNS) tissue. There is some disagreement on the length of time between SCI and the reestablishment of the blood spinal cord barrier, which may be due to the different methods of measuring permeability (Matsushita et al 2015).

Reestablishment of the blood spinal cord barrier in a rat model of SCI has been reported as early as 14 days post injury (Noble & Wrathall 1989), though it has been reported that the blood spinal cord barrier is still compromised up 28 days (Popovich et al 1996) or 56 days post injury (Cohen et al 2009). Microvascular damage is thought to exacerbate the secondary injury cascades, and could be a target for early treatment after SCI (Tator 1991, Tator & Fehlings 1991). Gray matter has higher metabolic needs than white matter and is more vulnerable to damage induced by hypoxia and ischemia (Dumont 2001). Ischemia with subsequent reperfusion injury has been shown to increase the production of free radicals such as ROS from complex I of mitochondria (Tompkins et al 2006), and oxidation of lipids and proteins that compromises the integrity of membranes, DNA, and enzymes among other cellular components including mitochondria (Cuzzocrea et al 2001).

1.3 Therapeutic Methods of Targeting Mitochondrial Dysfunction after SCI

As described in the previous section (**Chapter 1.2**), many of the secondary pathophysiological cascades following SCI are closely associated with mitochondrial dysfunction, making these organelles a popular therapeutic target. Accordingly, different treatments for restoring or maintaining mitochondrial function following neurotrauma such as uncoupling agents, antioxidant addition, and biofuel addition have been tested, with varying degrees of effectiveness.

1.3.1 Mild Uncoupling

Drugs that uncouple the mitochondrial ETS have been investigated for their potential benefits in retaining mitochondrial function after different models of traumatic nervous tissue damage *in vivo* (Jin et al 2004, Patel et al 2009b, Rodriguez-Jimnez et al 2012, Sullivan et al 2004). Using drugs to mildly uncouple the ETC from complex V allows hydrogen atoms to diffuse freely from the intermembrane space back into the matrix (see Skulachev 1998). This allows for maximal transport of electrons through the ETC, without conversion of ADP to ATP. When the uncoupling is mild, there can be a buildup and maintenance of

membrane potential across the IMM. This maintenance of membrane potential is beneficial in that the mitochondria are less likely to go through MPTP. Using mild uncoupling proteins (UCP2 and UCP3) has been shown to reduce ROS production and may be beneficial in treating neurodegenerative diseases (see Brand & Esteves 2005). One group found addition of the uncoupler 2,4-dinitrophenol resulted in neuroprotection in a rat model of quinolinic acid- induced Huntington's disease (Maragos et al 2003). Importantly, intraperitoneal injection of 2,4-dinitrophenol was found to maintain mitochondrial bioenergetics and reduce oxidative markers to sham levels when given 15 or 30 min after contusion SCI (Patel et al 2009b).

1.3.2 Antioxidants

The use of antioxidants to supplement the endogenous mitochondrial antioxidant systems have been used to combat free radicals such as ROS and RNS (see Bains & Hall 2012, Smith et al 2008). Reactive species can attack and damage mitochondrial electron transport complexes and mtDNA, further increasing mitochondrial dysfunction. Administration of antioxidants or precursors to antioxidants has been shown to have beneficial effects for Parkinson's disease (Jin et al 2014) and traumatic brain injury (Hall et al 2010). Intraperitoneal injections of N-acetylcysteine amide, a precursor to glutathione, in a rat model of SCI significanlty maintained both mitochondrial respiration and hindlimb functional recovery compared to vehicle (Patel et al 2014). Dietary administration of the antioxidant resveratrol has been shown to increase mitochondrial antioxidant enzyme activity (MnSOD) in mouse brains (Robb et al 2008) and reduce oxidative stress in cultured coronary endothelial cells (Ungvari et al 2009). Tempol treatment is shown to decrease oxidative stress and mitochondrial dysfunction while increasing cell survival and ATP production in a mouse model of nephrotoxicity (Ahmed et al 2014), and partially restore mitochondrial respiration in a model of rat SCI (Xiong & Hall 2009). Intraperitoneal injections of tempol maintained nonsynaptic, but not synaptic, mitochondrial bioenergetics when administered 15 minutes after contusion SCI, and reduced peroxynitrite-

derived 3-nitrotyrosine and protein oxidation (Patel et al 2009b). Further, modified antioxidants can be specifically delivered to mitochondria for optimal effectiveness (see Sheu et al 2006).

1.3.3 Substrate Addition

Substrates that feed into the ETC have also been utilized as mitochondrial therapy. Increasing the amount of substrates such as NADH, acetyl-CoA, and succinate can increase mitochondrial bioenergetics. The subsequent increase in ATP production not only provides more energy to the cell, but helps to maintain a healthy membrane potential across the IMM (for review see Pettegrew et al 2000). Biofuels such as pyruvate and beta-hydroxybutyrate have been found to restore mitochondrial respiration when delivered to cultured neurons after glucose deprivation (Laird et al 2013). Other alternative substrates that can be used by mitochondria for respiration, such as acetyl-L-carnitine, have beneficial effects in clinical trials for Alzheimer's and Parkinson's disease (Carta & Calvani 1991, Puca et al 1990), and it lowers oxidative damage and restores mitochondrial function in rat models of aging (Liu et al 2002, Petruzzella et al 1992). Not only did acetyl-L-carnitine significantly restore mitochondrial bioenergetics compared to vehicle, it also provided significant hindlimb functional recovery and tissue sparing in a rat model of severe SCI (Patel et al 2012, Patel et al 2010).

1.4 Mitochondrial Transplantation

A burgeoning approach used in mitochondrial medicine (Armstrong 2007, Luft 1994) is transplanting mitochondria from a healthy, exogenous source into damaged tissues in the effort to rescue cells or tissues from death. Various models of mitochondrial transplantation have been investigated, each with their own caveats and insights, which is discussed in **Chapter 2**. Many of the 'mitochondrial medicines' that have been explored, such as antioxidants and alternative substrates (biofuels), have a short therapeutic time window in which to treat damaged mitochondria before the oxidative and energy depletion damage

becomes overwhelming. Importantly, they cannot replace mitochondria that are already lost. With transplantation methods to replace damaged mitochondria it may be possible to decrease ROS production within the cell (**Figure 1.1C-9**), provide a new pool of exogenous mtDNA damaged from oxidative processes (**Figure 1.1C-10**), increase energy production **(Figure 1.1C-11)**, and increase calcium buffering capacity (**Figure 1.1C-12**). By providing new mitochondria to the cell it will retain enough energy-producing capacity for survival, thus allowing damaged mitochondria to undergo mitophagy, a form of mitochondria-specific targeted autophagy (see Ding & Yin 2012), to maintain sufficient energy production sources for self-repair. The prospect of replacing damaged and dysfunctional mitochondria with healthy exogenous mitochondria has already been attempted with promising results, though no such intervention has been attempted in models of spinal cord injury.

1.5 Hypothesis of Dissertation

As described above, contusion SCI is a complex and phasic event that results in permanent damage. Mitochondria are implicated in many aspects of the pathophysiological progression, and are therefore a therapeutic target after injury. Pioneering work in our lab characterizing mitochondrial dysfunction after SCI led to the discovery that preservation of mitochondrial function correlates with tissue sparing and better long-term hindlimb recovery after injury (Patel et al 2012, Patel et al 2014). As such, our lab has been actively investigating other methodologies of mitochondrial therapeutics. Early publications describing successful mitochondrial transplantation in models of cardiac tissue *ex vivo* or lung tissue injury *in vivo* (Islam et al 2012, McCully et al 2009) caught our attention as an exciting and novel therapeutic strategy. With the existing experience in our lab of performing microglial cell transplantation into the spinal cord after injury (Rabchevsky & Streit 1997) and extensive knowledge of mitochondrial bioenergetics after SCI, it was a logical step forward to branch out into the field of mitochondrial transplantation.

While the published mitochondrial transplantation approaches showed promise in alleviating tissue damage and mitochondrial dysfunction in different organ systems and pathologies such as cardiac infarction and lung damage, no studies have investigated the potential benefits of supplementing healthy mitochondria into the injured spinal cord. As such, the hypothesis of this dissertation is isolated mitochondria can be successfully transplanted into injured spinal cord tissue and increase overall host mitochondrial bioenergetics and cell survival, resulting in tissue sparing and improved functional recovery. To test our hypothesis, we first characterized and optimized techniques for isolating transgenically-labeled mitochondria from cultured cells for transplantation (**Chapter 4**). We then performed experiments to find the optimal dosage of mitochondria transplantation to maximally restore cellular bioenergetics following acute contusion SCI (**Chapter 5.3.1**). Next, we characterized both time and cell-type dependent incorporation of tGFP-labeled mitochondria after injury (**Chapter 5.3.2**). Finally, we assessed tissue sparing and functional recovery benefits afforded by mitochondrial transplantation (**Chapter 5.3.3**).

Note:

Portions of this chapter were adapted and reprinted by permission from Elsevier: Jenna L. Gollihue and Alexander G. Rabchevsky. (2017) Prospects for Therapeutic Mitochondrial Transplantation. *Mitochondrion.* 2017 May 19 DOI: 10.1016/j.mito.2017.05.007

CHAPTER 2

History of Mitochondrial Transplantation

2.1 Methods of Transplantation

While mitochondrial replacement therapy has been proven successful in embryonic genetic therapies (**see Chapter 1.1.1**), there is a dire need to develop complementary approaches for treating adults who suffer from mtDNA defects and mitochondrial dysfunctions. The transplantation of mitochondria isolated from one source into different recipient cells has been successful in various models and multiple studies have shown incorporation of exogenous mitochondria via direct injection, co-incubation, and cell-mediated transfer, both *in vitro* and *in vivo*. This chapter investigates the techniques used for transplantation of mitochondria into a host cell/tissue, methods used to verify successful transfer, and the benefits that transplantation has afforded various models of mitochondrial dysfunction.

2.1.1 In vitro Transplantation

As early as 1982, the possibility of isolated mitochondrial transplantation into mouse adrenal and embryonal carcinoma cell cultures was shown (Clark & Shay 1982). Chloramphenicol- and efrapeptin-resistant mitochondria were isolated from mammalian cells and co-incubated with cells lacking resistance to the mitochondrial-targeting antibiotics. The isolated mitochondria labeled with rhodamine 123 were not only endocytosed by the cells as visualized by fluorescence microscopy, but they also conferred resistance indicating successful incorporation of the exogenous mitochondria. This resistance was present in 12 passages of the cells as the mtDNA was retained. Damaging the resistant mitochondria with UV light before co-incubation rendered them incapable of conferring resistance to co-incubated cells. Moreover, resistance could not be conferred between species (mouse into human), introducing a caveat in mitochondrial transplantations- that various cell types may have different propensities to take up mitochondria originating from different sources.

Another group that capitalized on conferred resistance via mitochondria transplantation showed that direct injection of isolated mitochondria into cultured cells is a viable technique for replacing endogenous mtDNA (King & Attardi 1988). Using ethidium bromide, mtDNA was reduced in 143B human osteosarcoma cells to 3% of control levels. Mitochondria were then isolated from chloramphenicol-resistant CAP23 cells and microinjected into mtDNA-depleted 143B cells. Subsequent addition of chloramphenicol to the recipient cells failed to kill them, indicating successful incorporation of CAP23 mitochondria. Further, the cells contained CAP23 mtDNA at five weeks after injection while the nuclear DNA was only that of 143B cells, indicating the transfer of only mtDNA.

Direct microinjection of isolated mitochondria into cultured cells was thought to be impractical based on the size of mitochondria compared to the gauge of injection needles (Yang & Koob 2012), despite that previous studies used needles with tip diameter of 1 um or less (King & Attardi 1988). To counteract this, mitochondria were first injected into oocytes to allow larger diameter needles to be used and then a mitocytoplast containing the cell membrane, cytoplasm, and the previously injected mitochondria was taken from the oocyte (Yang & Koob 2012). This mitocytoplast could then be fused with recipient lung carcinoma LL2/rho0 cells that are devoid of mtDNA so that mitochondria were then transferred into the recipient cell cytoplasm. An important finding in this study revealed that when a cell is in the presence of two different species of mtDNA, recipient cells will favor the survival of syngeneic mtDNA, similar to the findings of Clark and Shay (1982).

Others have explored direct injection techniques in which mitochondria were isolated from rabbit heart tissue and injected into regions of ischemic rabbit hearts *ex vivo* shortly before reperfusion (McCully et al 2009). Autologous mitochondria were directly injected into heart tissue following 29 minutes of ischemia, which resulted in decreased infarct size of the post-ischemic tissue. Injections of frozen, non-functional mitochondria into heart tissue showed that functional, respiratory competent mitochondria were necessary to decrease ischemic infarct size and maintain function of cardiac tissues.

In addition to direct transfer approaches into host cells, the possibility of mitochondrial transfer by co-incubation has been investigated. Co-incubation of cultured cells with isolated mitochondria results in successful incorporation of the exogenous mitochondria into host cells, often those that had undergone some sort of insult. Xenogenic transfer of mitochondria was evident when isolated mitochondria were co-incubated with cells *in vitro*, resulting in the successful incorporation of exogenous mitochondria (Katrangi et al 2007). It was shown that healthy murine mitochondria were taken into compromised human mesenchymal stem cells, resulting in their restored respiratory capabilities. The group demonstrated transfer by fluorescently labeling and tracking isolated mitochondria, measuring respiration changes in the cells after transfer, and detecting exogenously-derived mtDNA using polymerase chain reaction (PCR) techniques. These results contrast those found by Clark and Shay (1982) in which mitochondria originating from one species were found not to transfer via co-incubation into host cells of a different species.

Others have studied transfer of isolated mitochondria conjugated to a cell-penetrating peptide, Pep-1 (Chang et al 2013b). Pep-1 causes translocation of its cargo in an endosomal-independent manner and has been used to deliver small peptides and DNA sequences, but never entire organelles (for review see Morris et al 2008). Using mitochondrial specific fluorescent dyes, Chang et al (2013) reported that transplantation of mitochondria into recipient cells was found only when mitochondria were conjugated with Pep-1. Conjugated mitochondria-Pep-1 were isolated and co-incubated either with cells derived from myoclonic epilepsy with ragged-red fibers (MERRF) syndrome that had mutated mtDNA hindering mitochondrial protein synthesis or with cells lacking mtDNA. The exogenous mitochondria-Pep-1 co-localized with host mitochondria and resulted in the recovery of mitochondrial membrane potential in cells, increased oxygen consumption, increased ATP production, and decreased lactate production, all indicating a switch from anaerobic to aerobic respiration. This is in contrast to previous reports (Clark & Shay 1982, Katrangi et al 2007) that showed isolated mitochondria could be taken up by host cells *in vitro* without Pep-1.

In cell-to-cell transfer paradigms, it has been shown that co-culturing human lung epithelial cells containing damaged and/or depleted mitochondria with healthy adult human bone marrow stem cells results in donation of healthy stem cell mitochondria and rescue of epithelial cells that contained functional mitochondria, as indicated by increased ATP production and translation of mitochondrial protein COXII (Spees et al 2006). Microscopy showed that the bone marrow stem cells made cytoplasmic projections towards the epithelial cells, shuttling mitochondria through the extensions between connected cells. In contrast to other studies, this group showed no evidence of isolated mitochondrial transfer into cells using co-incubation methods- when comparing transplantation of isolated mitochondria versus cell-to-cell transplantation, transfer was only attained in a cell-cell fashion, suggesting that movement of exogenous mitochondria into host cells is an active process.

Nanotube formation between cells was reported through which organelles, including mitochondria, were exchanged from one cell to another when co-culturing human bone marrow mesenchymal stem cells with rat embryonic cardiac myocytes (Plotnikov et al 2008). After co-culturing for 24 hours, the cells formed nanotube connections and Tetramethylrhodamine Ethyl Ester (TMRE)-labeled mitochondria were visualized within the nanotubes; TMRE is a membrane potential-dependent mitochondrial dye. Further, the propensity of each cell type to form tunneling nanotubes was higher when co-cultured with the xenogenic cell type compared to a syngeneic cell type. By using calcein-AM, a cell membrane permeant dye, the group was able to demonstrate the movement of cytoplasmic contents in both directions between cultured cells using scanning confocal microscopy, indicating that cytoplasm from both cardiomyocytes and human mesenchymal stem cells was shared. It was also shown that physically disrupting tunneling nanotube formation with gentle shaking inhibited this sharing of cytosolic contents. Using MitoTracker Red and MitoTracker Green FM dyes, each specific for one cell type, they visualized mitochondrial transfer between the co-cultured cells. There was no detectable transfer at 3 hours but was evident after 24 hours of co-culturing. Interestingly, mitochondria movement was

apparent from the mesenchymal stem cells to the cardiomyocytes, but there was no reciprocal movement and no co-localization of the MitoTracker markers, indicating that mitochondria originating from the two different sources did not undergo fusion at 24 hours.

Another group found that co-culturing of rat cardiomyoblasts that had undergone oxygen glucose deprivation (OGD) with healthy mouse mesenchymal stem cells resulted in the formation of 200-500 nm diameter nanotubes between cells after 2 hours, and that after 24 hours these nanotubes contained the membrane potential-dependent dye MitoTracker Red (Cselenyak et al 2010). This indicated the presence of functionally competent mitochondria, although the directionality of movement was not obvious using time-lapse confocal microscopy. Importantly, such co-culturing significantly rescued the cardiomyoblasts from OGD.

Others have reported the formation of tunneling nanotubes in cultured cells that underwent ultraviolet radiation stress (Wang & Gerdes 2015). They showed that PC-12 cells in the beginning stages of apoptosis formed nanotubes that reached out to healthy, unstressed cells and that when UV-stressed cells were co-cultured with healthy cells there was reduced cell death compared to co-culturing with UV-stressed cells. EdU (5-ethynyl-2'-deoxyuridine)-labeled mtDNA could be detected in the stressed cells, indicating transfer had occurred into the damaged cells. They further found that mtDNA-deficient PC-12 cells lacking electron transport function could not rescue UV-stressed cells whereas PC-12 cells with functional mitochondria did.

It is important to note that the reported successful transfer of mitochondria from one cell type to another appears to be most prevalent when transfer occurred from a healthy cell to a cell with dysfunctional and/or depleted mitochondria. While there are many caveats when considering donor vs recipient cell types in the propensity to take up mitochondria, there appear to be mechanisms that allow damaged cells to receive mitochondria more readily than healthy cells. For example, Cho et. al. (2012) found that cell-to-cell mitochondrial transfer occurred via partial cell fusion, but only when the receiving cell had

dysfunctional mitochondria. The group showed that co-culturing of human mesenchymal stem cells with both human osteosarcoma 143B cells lacking mtDNA and cells with severe R6G toxin-induced mitochondrial dysfunction resulted in the transfer of mitochondria accompanied by their increased ATP and oxygen consumption. However, transfer was not evident when recipient cells had mtDNA mutations, leading the group to conclude that mitochondrial transfer occurs only when mitochondrial function is severely hindered or absent (Cho et al 2012).

2.1.2 In vivo Transplantation

Phylogenetic mapping and mitochondrial transplantation methods have been performed in a number of animal models *in vivo*. Interestingly, a study investigating the phylogeny of different canine species with canine transmissible venereal tumor (CTVT) by sequencing their mitochondrial genome (Rebbeck et al 2011) revealed an unexpectedly high polymorphism rate in the CTVT samples thought to be caused by transfer of mitochondria from the dogs into the cancerous tumor cells. The group theorized that host (dog) mitochondria may be healthier than that of the CTVT cells, encouraging transfer of mitochondria and subsequent increase in CTVT metabolic health. This theory reflects an endogenous mechanism of mitochondrial transfer *in vivo*, from one cell to another.

The McCully group who studied direct injection of mitochondria *ex vivo* (McCully et al 2009) also reported successful mitochondrial transplantation *in vivo* using a direct injection technique (Masuzawa et al 2013). Autologous transplantation of isolated mitochondria directly into ischemic rabbit hearts immediately before reperfusion resulted in increased mechanical function as soon as 10 minutes after injection, in addition to significantly higher ATP content at 2 days post injection. Further, they showed via confocal microscopy that cardiomyocytes can take in exogenous mitochondria as early as 2 hours after transplantation and do not illicit an immune response. The group recently compared direct injection mitochondrial transplantation to a more clinically

relevant, less invasive vascular perfusion delivery method (Cowan et al 2016). Rabbit hearts underwent focal ischemia for 30 minutes *in situ* followed by reperfusion and delivery of mitochondria isolated from adult human cardiac fibroblasts. Mitochondria were delivered either by direct injection into the ischemic heart tissue or they were perfused through the coronary artery. They noted that a large amount of mitochondria were found in the interstitial spaces, but some mitochondria were co-localized within cardiomyocytes. Vascular delivery of mitochondria resulted in a larger dispersal area, while direct injection resulted in a higher concentration in smaller regions of tissue. Importantly, this study showed that both direct injection and vascular delivery of mitochondria afforded functional protection in measures of muscle contractility and decreased infarct size after ischemia-reperfusion injury. The group then aimed to show these results in a larger, more clinically relevant animal model. Kaza et al (2016) studied the autologous transplant of mitochondria isolated from the pectoralis major muscle into a porcine model of ischemia reperfusion (Kaza et al 2016). Regional ischemia injury was performed, blocking blood flow for 24 min, after which isolated mitochondria were given to the heart, with reperfusion of the heart following immediately after mitochondrial delivery. The animals then survived for 4 weeks. Results from this study are important as they show that there was no increase in inflammatory or immune reactivity when mitochondria were delivered. There was also significantly larger infarct size in vehicle injected animals compared to mitochondria treated animals. Further, injected mitochondria were still present at the 4 week time point.

In addition to direct injections *in vivo*, cell-to-cell transfer of mitochondria has also been reported *in vivo*. One study instilled mouse bone marrow derived stromal cells (mBMSC) into acutely injured mouse lungs which resulted in connexin pore-dependent attachment of the mBMSC to the injured lung epithelium (Islam et al 2012). This attachment was followed by nanotube formation and delivery of mitochondria-containing vesicles into the injured tissue, leading to increased ATP production and cell survival after injury. The group determined that connexin pore and gap junction channel formation was

necessary for such transfer since blocking connexin pore formation inhibited gap junction channel formation, which was then found to inhibit cytosolic mixing between the two cells. When dynamin, a GTPase responsible for endocytosis in the eukaryotic cell, was inhibited mitochondrial delivery was blocked leading the group to posit endocytosis to be the mechanism responsible for mitochondrial transfer. Again, it is important to note that the mitochondria were transferred to damaged cells or tissues.

Recent compelling studies have shown that endogenous mitochondrial transfer occurs between resident astrocytes and neurons after stroke injury (Hayakawa et al 2016). The investigators stimulated astrocytes *in vitro* to release mitochondria by upregulating the CD38 protein, and found that the addition of these astrocyte-derived mitochondria in a model of neuronal cell injury *in vitro* was successful in increasing neuronal ATP production and cell survival, and that these mitochondria were incorporated into the neuronal cells. They further studied this *in vivo* by directly injecting astrocyte-derived mitochondria into the injury site 3 days after inducing cerebral ischemia in mice and found these mitochondria were taken into neurons. The endogenous transfer of mitochondria was seen in these transgenic mice with labeled astrocytic mitochondria that were found within neurons 24 hours after ischemic stroke, and cell survival signals such as phosphorylated AKT were increased after this transfer (Hayakawa et al 2016).

Direct injection of isolated mitochondria has been explored in a 6-OHDA rat model of Parkinson's Disease (PD) (Chang et al 2013a). Transgenically-labeled GFP-mitochondria were conjugated to Pep-1, a cell penetrating peptide, and injected in a dose dependent manner into the medial forebrain bundle. The group found that GFP labeled mitochondria were evident at 12 weeks post injection using fluorescent microscopy, however, they did not detect foreign mtDNA at these time points. Importantly, they also noted mitochondrial aggregation at the highest dosage used (2.1μg) compared to the lowest dosage (0.525 μg), which was less aggregated and more extensively dispersed. They hypothesized that the aggregation at higher concentrations led to decreased

penetration of mitochondria into host tissues; this is supported by their findings which delineate the lower dosage treatments as having higher efficacy for different outcome measures of recovery including cell survival and behavior. Both the low and middle dosage group (1.05μg) resulted in significantly higher cell body numbers in the substantia nigra compared to vehicle injected animals. Additionally, these two lower dosage groups gave significantly higher mitochondrial complex I, III, and V activity compared to vehicle. Functional recovery was analyzed using apomorphine-induced rotation assessment and showed conjugated mitochondria/Pep-1 injection at the two lower dosages improved rotational scores closer to baseline compared to vehicle injected animals.

In a later study, the same group utilized xenogenic transfer in PD rats (Chang et al 2016). When mitochondria with or without Pep-1 conjugation were injected into the medial forebrain bundle, oxidation of substantia nigra cell DNA was decreased compared to vehicle injection. They simultaneously performed allogeneic transplantation using transgenically-labeled GFP mitochondria isolated from PC-12 cells. 3 months after transplantation, locomotion comparing distance, speed, and amount of movement were analyzed for each animal. After onset of PD by using 6-OHDA, there is significantly decreased locomotor activity. Locomotor scores of 6-OHDA animals were significantly increased when transplanting either allogeneic or xenogenic mitochondria, but only when conjugated with Pep-1; there was not such locomotor recovery when non- Pep-1 conjugated mitochondria were injected. Interestingly, locomotor scores were higher in the allogeneic Pep-1/mitochondria group compared to the xenogenic Pep-1/mitochondria group, suggesting there may be differences when using mitochondria from sources that are unlike the recipient strain or species. Pep-1 conjugated mitochondrial transplant also resulted in significantly increased neuronal survival and tyrosine hydroxylase immunoreactivity, and increased amount of complex I compared to vehicle injection. Importantly, GFP immunofluorescence was apparent in the substantia nigra dopaminergic neurons 3 months after Pep-1 conjugated GFP-mitochondria administration. It should also

be noted that 6-OHDA injury increased inflammatory cytokines such as IL-1a, IL-1b, IL-10, IL-5, and IL-18, and that Pep-1 conjugated mitochondrial delivery significantly decreased these levels.

2.2 Tracking Exogenous Mitochondria after Transplantation

Various methods have been utilized to verify that exogenous mitochondria are successfully transplanted into host cells. One common procedure is to transplant exogenous mitochondria of one species animal into a host cell of a different species, followed by PCR on the host cell mtDNA showing that the exogenous mtDNA is present (Islam et al 2012, Kitani et al 2014b, Yang & Koob 2012). PCR is also performed to show transfer of mtDNA into cells lacking mtDNA (Spees et al 2006) or transfer of mitochondria containing a specific sequence for chloramphenicol resistance (King & Attardi 1988). Alternatively, species-specific mitochondrial antibodies are used to detect exogenous mitochondria (Masuzawa et al 2013). Mitochondria can be fluorescently labeled pre-injection to visualize after uptake into the host cells by either transfection methods (Chang et al 2013b, Islam et al 2012, Kitani et al 2014b, Spees et al 2006, Wang & Gerdes 2015, Yang & Koob 2012), using mitochondrial-specific dyes such as MitoTrackers or rhodamine derivatives (Chang et al 2013b, Clark & Shay 1982, Cselenyak et al 2010, Katrangi et al 2007, Masuzawa et al 2013, McCully et al 2009, Plotnikov et al 2008), or transgenic mice in which a subset of mitochondria are fluorescently labeled (Hayakawa et al 2016). Another method labels mitochondria using pHrodo Red, a pH-sensitive label that indicates proton levels. Using this, increased fluorescence of cardiomyocytes *in vitro* could be measured, indicating mitochondrial internalization that could be quantified as a number of mitochondria per nucleus (Pacak et al 2015).

2.3 Mitochondria Transplantation Increases Health of Host Cells and Tissues

Many different outcome measures are being used to show that transplanted mitochondria have beneficial effects on host tissues. Energy

production, mitochondrial protein translation, and enzyme activities have all been reported to be increased after transplantation. One group found a three-fold increase in ATP levels and a decrease in lactate levels in cells rescued by cell-to-cell mitochondrial transfer, indicating that the host cells with depleted mtDNA were able to switch from anaerobic respiration to aerobic respiration after receiving mitochondria (Spees et al 2006). Further, the host cells that contained extensive mtDNA damage could again translate mitochondrial proteins, namely COXII, after incorporating exogenous mitochondria. Others showed that mitochondrial transplantation into damaged lung epithelia resulted in increased ATP production approaching control levels, not only in the cells that received exogenous mitochondria, but also in juxtaposition alveoli (Islam et al 2012). The increase in ATP to normal levels rescued functional surfactant excretion by the alveolar cells. Increased cellular ATP content and oxygen consumption rates were also reported after exogenous mitochondria internalization into either cultured cardiomyocytes or HeLa cells lacking mtDNA, and PCR confirmed replacement with exogenous mtDNA in the cells (Pacak et al 2015).

Mitochondrial function and ROS production have also been used to assess the benefits of mitochondrial transplantation. For instance, flow cytometry and the fluorescent dyes rhodamine 123 and JCI have been used to determine changes in mitochondrial membrane potential in culture using MERRF cells (Chang et al 2013b). They also measured oxygen consumption rates as well as ATP levels, cell viability, amount of fusion and fission proteins, caspase-3/-7 activity, mtDNA copy number, mitochondrial mass, and mitochondrial calcium uptake. ATP production has also been assessed using fluorometric analyses. TBARS (thiobarbituric acid-reactive substances) has been used to show differences in oxidative damage and TdT-mediated dUTP nick-end labeling (TUNEL) assays have been used to investigate apoptosis (McCully et al 2009). This latter group also employed Mito-Tracker Orange CMTMRos label to show that labeled mitochondria maintained a viable membrane potential and their oxygen consumption rates showed that they were respiration competent.

2.4 Mechanisms for Mitochondrial Incorporation

Cell-to-cell fusion has been disputed as a necessary mechanism of mitochondrial transfer. When co-culturing human mesenchymal stem cells with human alveolar epithelial cells lacking mitochondrial DNA, transfer of mitochondrial but not nuclear DNA was reported (Spees et al 2006). Further, the addition of platelets or isolated mitochondria to cultured cells lacking mtDNA did not result in mtDNA transfer, indicating the incorporation of exogenous mitochondria is not a passive process. In fact, the mesenchymal cells made cytoplasmic extensions towards alveolar cells lacking mtDNA, after which the depleted cells began dividing after being rescued by mitochondrial transfer. It was not shown whether mitochondrial transfer was achieved through nanotube formation or budding of mitochondria-filled vesicles from the donor cells. However, other groups have demonstrated that co-incubation of cells with purified isolated mitochondria results in the uptake of exogenous mitochondria into cells (Clark & Shay 1982, Katrangi et al 2007). This indicates an uncertainty as to whether mitochondria can be passively endocytosed in cell culture. There may be a difference among cell types in the ability to incorporate exogenous materials, as was demonstrated in an earlier study examining incorporation of nuclear DNA among different cell types (Wigler et al 1980). Clark and Shay (1982) similarly showed that different cell lines had a different propensity to uptake co-incubated isolated mitochondria, suggesting that mitochondria are taken up by recipient cells via different endocytic properties according to phenotype.

Islam et al (2012) reported that physical docking of mBMSC to injured lung epithelial cells was necessary for transfer of mitochondria to alveolar cells. mBMSC attachment to injured cells occurred at areas of high CX43 connexin concentration on lung epithelial cells, and specifically blocking CX43 hindered binding and transfer of cytosolic contents from mBMSC to epithelial cells. *In vitro*, mBMSC formed nanotubes with epithelial cells and released microvesicles containing DsRed-labeled mitochondria. They concluded that gap junctional channels are necessary for attachment, while microvesicles and nanotubes are

needed for the movement of mitochondria. Inhibition of dynamin blocked mitochondrial transfer, implicating that endocytosis is responsible for the engulfment of mBMSC microvesicles (Islam et al 2012). Koyanagi et al examined intercellular connections and whether large structures, including organelles such as mitochondria, could be transferred between cells (Koyanagi et al 2005). They found that when human endothelial progenitor cells were co-cultured with cardiomyocytes containing MitoTracker-labeled mitochondria, time lapse imaging showed formation of transient nanotubular structures and the progression of labeled structures moving from the cardiomyocytes to the endothelial progenitor cells. Interestingly, the reverse transport was not evident: when endothelial progenitor cell mitochondria were labeled with MitoTracker there was not transport to the unlabeled cardiomyocytes, indicating there may be cell-type differences that are important to consider for mitochondria transfer. Wang et al showed that tunneling nanotubes can be formed *in vitro*, providing a pathway for mitochondrial transfer (Wang & Gerdes 2015). PC-12 cells stressed by UV created tunneling nanotubes with a larger diameter and containing microtubules that attached to control, unstressed cells. Fluorescence microscopy detected tagged mitochondria located within nanotubes connecting stressed and control cells, but no presence of mitochondria in nanotubes connecting only control, unstressed cells. Live cell imaging techniques allowed tracking of mitochondria from the control cell, through the nanotubes, and into the stressed cells. When tunneling nanotube formation was inhibited using cytochalasin B, an F-actin depolymerizing agent, they found a higher incidence of cell death with the UV stressed/unstressed co-culture suggesting that nanotube formation was necessary for the rescue effect. They also showed positive co-localization of MitoTracker Red-labeled mitochondria with immunostained microtubules located within the nanotubes. They further transgenically labeled mitochondria with DsRed2-mito in the control cells to quantify their transfer into stressed cells. Using cytochalasin B to inhibit the nanotubes decreased the amount of Dsred2-mito in the stressed cells.

A comparative study was performed by the McCully group to determine the mechanism of mitochondrial internalization *in vitro* (Pacak et al 2015). Chemicals were utilized to inhibit different internalization mechanisms, such as cytochalasin D to block actin polymerization, methyl-β-cyclodextrin to block caveola-dependent-clathrin-dependent endocytosis, nocodazole to block tunneling nanotubes, and 5-(N-Ethyl-N-isopropyl) amiloride to block macro-pinocytosis. The only chemical that changed mitochondrial internalization was cytochalasin D, indicating that actin polymerization is involved in mitochondrial uptake into the cardiomyocyte cells, though it was not evident how the mitochondria left the endosomes once they were internalized. The other chemicals had no beneficial effects suggesting that clathrin-dependent endocytosis, tunneling nanotubes, and macro-pinocytosis are not involved. This is in accordance with their previous report that mitochondria were not co-localized with lysosomes, caveolae or autophagosomes upon internalization (Masuzawa et al 2013). In contrast, others utilized fluorescent live imaging to track movement of transgenically-labeled DsRed mitochondria into mesenchymal cells and reported that macropinocytosis is necessary for mitochondrial internalization *in vitro* (Kitani et al 2014b). It should be noted that various dosages of 5-(N-Ethyl-N-isopropyl) amiloride were used in attempts to block macro-pinocytosis in the different cell types used in each study. Recently, mitochondrial incorporation in neurons was theorized to be integrin-mediated, though the authors stated further investigation was necessary (Hayakawa et al 2016).

2.5 Summary

Chapter 1 discussed in detail the intricacies of mitochondrial involvement with the secondary pathophysiological cascades after SCI. Their involvement has made mitochondria a logical target for therapeutic intervention in the acute stages of SCI. Currently, a multitude of treatments are being tested that aim to maintain or increase the integrity of mitochondrial health following injury, though replacement therapies have yet to be investigated. **Chapter 2** investigated the

history of mitochondrial transplantation, including the most recent *in vivo* studies. Though these novel *in vivo* studies are few in number and use other types of injury models, we believe the transplantation paradigm is translatable into our SCI injury models. As we are the first lab to perform such a transplantation after SCI, we had to carefully and methodically choose and characterize multiple procedures to best test our hypotheses, which are delineated in the following chapters.

Note:

Portions of this chapter were adapted and reprinted by permission from Elsevier: Jenna L. Gollihue and Alexander G. Rabchevsky. (2017) Prospects for Therapeutic Mitochondrial Transplantation. *Mitochondrion.* 2017 May 19 DOI: 10.1016/j.mito.2017.05.007

CHAPTER 3

Validation and Optimization of Experimental Models

There are multiple injury models, analytical techniques, and outcome measures that could be used to test our hypotheses. We used historical data from our lab and from other research fields to validate our experimental techniques. There are caveats to consider for each technique, and while these were our first-choice methods, alternatives were considered as discussed in the future directions section (see **Chapter 6.3**).

3.1 Contusion Injury and Behavioral Assessments

The SCI model used in our experiments was a severe contusion injury (250 kDyn) at the L1/L2 spinal level using the force-controlled infinite horizon impactor (Scheff et al 2003), and assessment of hindlimb functional recovery was performed using the Basso, Beattie, Bresnahan (BBB) scale. Our experiments were designed to determine if mitochondrial transplantation could afford functional recovery after severe SCI. We hypothesized that functional recovery would be maintained through increased cell survival including gray matter neurons surrounding the injury site. Therefore, we considered a spinal injury level and behavioral analysis that would elucidate functional recovery based on gray matter sparing.

The BBB open field locomotor scale was developed using a rat model of contusion SCI using the OSU impactor or NYU impactor at the T7-9 level to grade different levels of hindlimb functional recovery (Basso et al 1995). The group also later showed that recovery of hindlimb locomotor function after a complete thoracic transection SCI is dependent upon descending tracts and that at least 10% sparing of the ventral white matter is necessary for weight bearing steps (Basso et al 1996). Others similarly found that in the absence of gray matter loss, a majority of ventral white matter loss is necessary to detect functional deficits in an ethidium bromide demyelinating injury in adult rats (Loy et al 2002). Therefore, using the BBB to measure recovery of function after a

thoracic SCI is a primary measure of white matter sparing of descending spinal tracts. Recovery of BBB scores after an L1/L2 level injury, however, is a measure of gray matter sparing; this was demonstrated when a specifically gray matter injury utilizing spinal injections of kainic acid at T9 did not result in decreased BBB scores, but a gray matter lesion at the L1/L2 level resulted in lasting functional deficits without disrupting descending white matter pathways (Magnuson et al 1999). The Magnuson group later discovered that functional deficits as measured by the BBB were dependent upon loss of intermediate gray matter interneurons at this level, and not ventral motor neurons of the lumbar enlargement (Hadi et al 2000). This indicates that the behavioral recovery relied upon the sparing of the central pattern generator (CPG) interneurons in the intermediate gray matter that are located in lamina VII and X of the L1/L2 spinal level and are responsible for the rhythmic pattern of hindlimb stepping (Grillner 1975, Kjaerulff & Kiehn 1996). Investigators found that a moderate-severe contusion injury at the L2 spinal level resulted in significantly depleted locomotor function that correlates to gray matter tissue sparing, injury level, and injury severity (Magnuson et al 2005). They also found that the amount of spared white matter at this level of injury did not correlate to the functional deficit, further demonstrating gray matter loss was responsible for the low BBB scores. As our mitochondrial transplantation experiments are hypothesized to be neuroprotective, we chose the L1/L2 injury model to measure functional recovery using the BBB scoring system that was sensitive to gray matter sparing.

Further, the BBB scale is a 0-21 point scale that can be split into different segments analyzing 1) joint movements, 2) stepping and coordination, and 3) fine details of paw movements such as toe clearance and balance. Historically we have found that after a 250kDyne L1/L2 injury we can expect a plateau of functional recovery at a score around 7 indicating extensive joint movements with no hindlimb weight bearing or stepping (Patel et al 2012). Increases in recovery by mitochondrial transplantation may increase the scores to the walking and patterned stepping scores. Restoration of function via the CPGs will result in more differences in the upper two thirds of the BBB scale, giving greater

separation of animals that are stepping. Attempts to modify the scale for post hoc analysis have been published, placing more emphasis on certain parts of the scale that are more translational, or making the scale more ordinal by decreasing emphasis on scores that are rarely assigned (Ferguson et al 2004). We reported these post hoc analyses in addition to our BBB testing to further differentiate recovery between treatment groups (**Chapter 5.3.3**).

3.2 Cultured Cells as the Source of Transplanted Mitochondria

From very early stages of our experiments, a major goal was to demonstrate that transplanted mitochondria can be successfully incorporated into host cells *in vivo*. For this purpose, we chose to transgenically label mitochondria in cell culture, allowing us to tag the mitochondria indelibly before their transplantation to track them *in situ*. PC-12-Adh cells were chosen as the cell line to be transfected with the pTurboGFP-mito vector. PC-12 cells originate from the adrenal gland of a *Rattus norvegicus* pheochromocytoma tumor and are neuronal-like in their development. Further, we chose to transplant mitochondria between like species based on studies that showed mitochondrial transplantation *in vitro* was more efficient when the same species of donor mitochondria were used (Clark & Shay 1982, Yang & Koob 2012). For instance, they showed that isolated murine mitochondria were more apt to be incorporated into cultured murine cells, but were not able to incorporate into human cells.

3.3 Stable Selection and Purification of tGFP PC-12 Cells

When first performing these experiments, we used a pTurbo-GFP-mito vector (evrogen cat # FP517 Farmingdale, NY) that contains a neomycin-resistant cassette to transform naïve PC-12 cells. We performed a G418 dose response selection curve, and determined that 400 µg/mL was necessary to kill PC-12 cells that do not have a neomycin resistance cassette. While under constant selection, individual turbo green fluorescent protein (tGFP) positive cells colonies were manually picked from the plates to grow in separate dishes, a technique commonly performed to give a pool of stably transfected cells.

However, we soon noticed that the transfection rate was not 100%, and the cells that were tGFP+ had varying degrees of fluorescence. We then decided to change the antibiotic resistant cassette of the vector to puromycin instead of neomycin and repeat our selection process in the hopes that we could obtain a colony with high tGFP expression rates.

To create our vector, the coding sequence for tGFP and the mitochondrial targeting sequence was removed from the original pTurbo-GFP-mito vector and inserted into a pIRESpuro3 vector (for details see **4.2.1**). The resulting plasmid contained the mitochondrial targeting sequence, tGFP coding sequence, and puromycin resistance sequence. PC-12 cells were transfected with the resultant DNA and the cells were propagated under puromycin selection (concentration for selection curve determined to be 3μg/mL puromycin), first very sparsely. Fluorescent microscopy was used to verify tGFP+ cell colonies, which were then physically selected and re-plated as described. The result was a colony of cells that had close to 100% tGFP-expression at high levels that did not seem to disappear with generations further removed from initial transfection. However, it is important to note that these cells grew more slowly than unlabeled PC-12 cells, and they had overall lower respiration rates (see **Chapter 4.3.4**). Regardless, the tGFP mitochondria had an indelible marker that is critical for tracking purposes. Because we are genetically altering cells and possibly affecting the function of mitochondria destined for transplantation, we had to first characterize the differences between our labeled mitochondria and unlabeled mitochondria. For this, we delved into a series of experiments, which is discussed in detail in **Chapter 4**.

3.4 Muscle Tissue as the Source of Donated Mitochondria

While tGFP-labeled mitochondria are optimal for visualization after transplantation, they respire much more slowly and may have inherently lower metabolic requirements compared to mitochondria isolated from naïve spinal cord tissue. Historically, state III oxygen consumption rates (OCR) of spinal cord mitochondria isolated from naïve SD rats is typically close to 600 pmol

oxygen/min (Patel et al 2014). Typical state III OCR of cell-derived mitochondria labeled with tGFP is closer to 300 pmol oxygen/min (see **Chapter 4.3.4**). As such, we chose to also evaluate the transplantation of mitochondria that had a higher metabolic potential more similar to mitochondria residing in the spinal cord. We therefore tested muscle mitochondria that were isolated from naïve Sprague Dawley rats, and transplanted into a different rat that had received SCI. While this transplantation is syngeneic, and not autologous, it does serve the purpose of transplanting high respiration-competent mitochondria into the spinal cord. In the future, muscle mitochondria transplantation may be clinically relevant- after a patient undergoes a SCI, it may be possible to isolate one's own mitochondria from a muscle biopsy providing for an autologous transplantation.

3.5 Injection Sites

Our mitochondrial injections were performed in the injury penumbra surrounding the primary contusion injury site. The primary injury site is necrotic, while the penumbra contains at-risk tissue that may be salvaged by mitochondrial transplantation therapy (see **Chapter 1.2**). The heterogeneous cell types of the spinal cord are all susceptible to oxidative damage and mitochondrial compromise after SCI, and we hypothesized that mitochondria would be able to incorporate into a variety of cell types in the spinal cord. Affording neuroprotection was a main goal of these experiments, regardless if this is possible directly through transplantation of mitochondria into neurons or indirectly through mitochondrial incorporation into various cell types in the injury penumbra making the environment more favorable for cell survival. Therefore, our injections were made into the medial lateral gray matter near the white matter interface so that injected mitochondria had the opportunity to incorporate into various cell types that are typically found in both the white and gray matter. This also places the injection bolus near lamina VII/X which includes the CPG interneurons critical for patterned locomotor stepping (**Figure 3.1**).

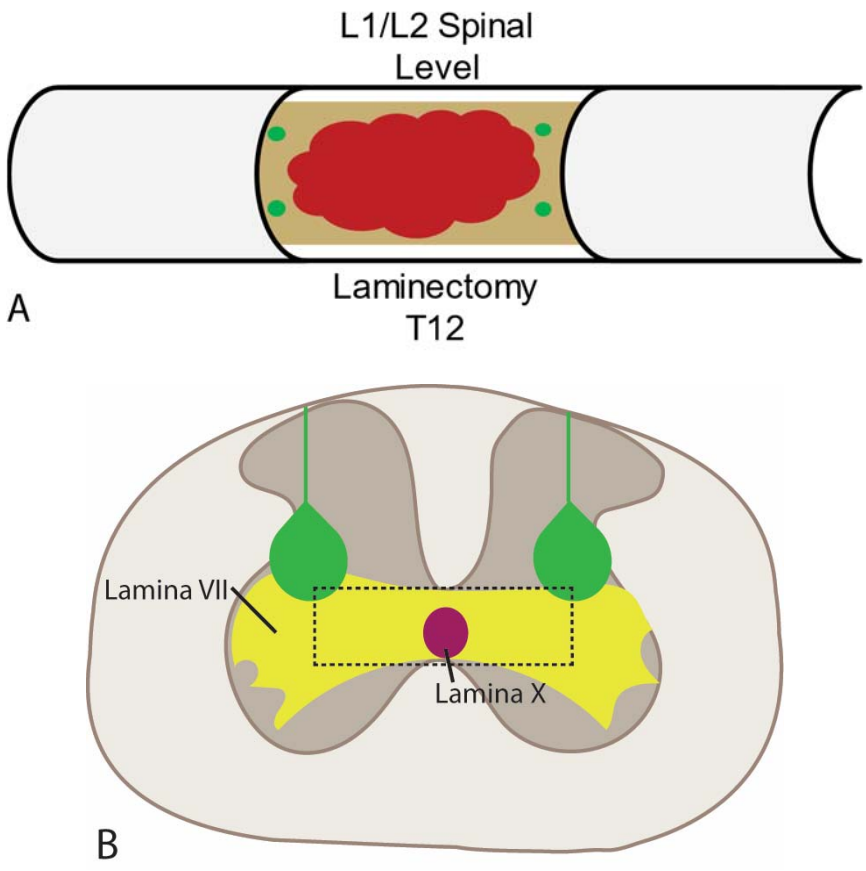

Figure 3.1. Location of mitochondria injections into the injured spinal cord. **A.** Laminectomy was made at thoracic level T12, exposing the L1/L2 spinal level. A 250 kDyne injury was performed, followed within 30 minutes by mitochondrial injections (green). Four injections were made into the injury penumbra, surrounding the injury site at the L1/L2 spinal level. **B.** Injections were targeted to the medio-lateral gray matter. This allowed for the dispersion of exogenous mitochondria into nearby white matter as well as gray matter. Importantly, this placed tGFP mitochondria in close proximity of CPG interneurons (boxed area), which are located within Lamina VII (yellow) and Lamina X (purple).

3.6 Using the Seahorse Flux Analyzer for Respiration Measurements

Function of the mitochondrial electron transport system has been examined using substrates and inhibitors to manipulate different complexes of the ETC and measuring the subsequent oxygen consumption rates. This has historically been done using the popular Clarke-type oxytherm electrode, though a relatively new method that uses the same concept is the Seahorse Flux Analyzer XF^{e} 24. We chose to use the Seahorse for our OCR analysis of mitochondria for its ease of use and higher throughput of samples.

The Seahorse Flux Analyzer XF^{e} 24 is an automated system that was initially developed to assay cultured cells, but techniques were developed to use this device to measure OCR of isolated mitochondria with as little as 5 µg mitochondria protein per well necessary for analysis (Rogers et al 2011). They noted that the optimal concentration of mitochondria to assay is that which will give an increased and sustained OCR with addition of ADP, with a significant decrease after the addition of oligomycin. We have optimized our concentration of isolated mitochondria to be 5- 7.5 µg per well. This allows us to easily run each sample in triplicate, with leftover mitochondria that can be frozen and used for other assays. The oxytherm, on the other hand, requires a relatively large amount of protein per sample, about 80 µg/ sample run.

The time required for a sample run is much lower for the automated Seahorse (about 30 minutes for one plate containing 7 samples in technical triplicate) compared to the oxytherm (15-20 minutes per sample). After the process of mitochondrial isolation, samples are left on ice until they can be analyzed. The order of sample analysis using the oxytherm may influence results, with those run later having been isolated and on ice for much longer, possibly compromising the mitochondria compared to those run first in order.

One benefit that the oxytherm offers is that you can watch and manipulate the trace in real time. For instance, if you have a bad reading in the oxytherm, you can immediately re-start the trace if you have enough sample. There have been mechanical failures in which the seahorse plate got stuck in the reader, or had bad baseline readings ruining all the samples for the day. While there is a

surplus of sample, the plates need to be incubated overnight- so that you do not have a replacement plate if needed. Attempting to prepare for the worst and incubating an extra plate for each experiment can get very costly, as plates and substrates are expensive.

State V.1 should be the maximal respiration rate after addition of the ETC uncoupler protonophore, carbonilcyanide *p*-trifluoromethoxyphenylhydrazone (FCCP). However, while this is always the case in the oxytherm, it is not always the case with the seahorse. On multiple experimental days, the seahorse tended to give lower state V.1 readings compared to state III. One of the theories is that FCCP is interacting with the plastic of the seahorse plate, so that it is not fully interacting with the mitochondria (Sauerbeck et al 2011). While we assume that this interaction is similar in each plate, we have seen plates with very high maximal V.1 rates, and other plates with the same experimental groups have state V.1 lower than state III. This is an important caveat to consider, and for this reason we emphasize state III OCR results when analyzing our results.

3.7 Removing Contamination from Culture-Derived Mitochondria

Many different iterations of mitochondria isolations were performed to increase the yield and health of mitochondria isolated from cell culture. Modifications were made from our usual protocol of mitochondrial isolation from spinal cord tissue, including addition of drill press homogenizations and three rounds of nitrogen bombing (detailed isolation protocol in **Chapter 4.2.2**). In our first mitochondrial transplantation studies, we had difficulty pulling the 100 µg (33.3 µg/µL) dosage into injection needles. We could successfully pull 50 µg (16.6 µg/µL) dosage into the needle- though this still often proved to be difficult with clogging that resulted in bubble formation in the needle. We knew that the clogging issue was specific to cell culture-derived mitochondria, as preliminary feasibility studies used 200 µg (66.6 µg/uL) of spinal cord-derived mitochondria without problems. At this point we assumed that 50 µg was the highest feasible concentration using cell-derived mitochondria, and carried out initial experiments using this dosage including acute bioenergetics and long term behavioral and

histological studies. Preliminary studies indicated that 50 µg tGFP mitochondria injection/cord resulted in significantly maintained state III OCR (**Figure 3.2**).

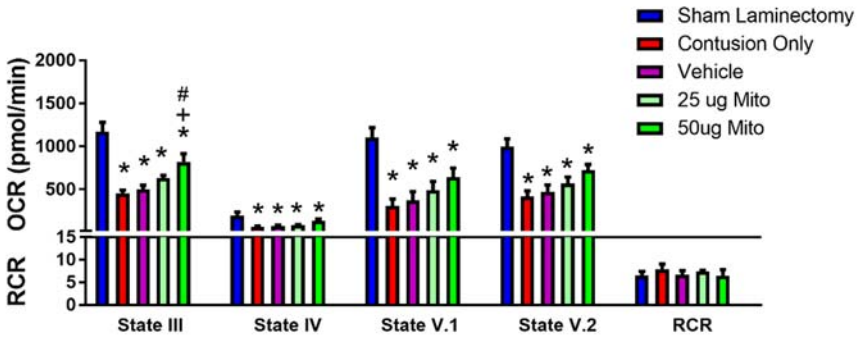

Figure 3.2. Mitochondrial respiration following SCI and tGFP mitochondrial transplant. tGFP-labeled mitochondria were isolated and injected immediately after L1/L2 spinal cord injury. 24 hours later, mitochondria were isolated and analyzed for mitochondrial respiration. State III OCR was maintained with 50 µg tGFP mitochondrial transplantation. Bars are means ± SEM. *p<0.05 vs Sham Laminectomy; #p<0.05 vs Vehicle; + p<0.05 vs contusion only. (one-way ANOVA for each state, Tukey's multiple comparison). N= 4-5/group in triplicate.

During long term transplantation studies, we noted a conspicuous layer of white film on isolated culture-derived mitochondria after ficoll purification steps. Gentle removal of this layer, followed by an additional resuspension and centrifugation step resulted in mitochondria that could be pulled into the needle at a dosage of 150 µg (or 50 µg/µL). At this time, it is not known what comprised the non-mitochondrial fraction that was removed, though all subsequent studies utilized these extra purification steps.

3.8 Conclusions

Using historical data and preliminary studies, we determined the optimal parameters to use for our injury and injections, as well as important outcome measures that were used in the ensuing experiments. As these techniques are being used in a novel paradigm of transplantation, they come with their specific

set of caveats that are discussed further in **Chapter 6**. The studies described in the subsequent chapters provide a foundation for mitochondrial transplantation after SCI, while possible refinements in future studies can continually modify and enhance our mitochondrial transplantation paradigm.

CHAPTER 4

Optimization of Mitochondrial Isolation Techniques for Intraspinal Transplantation Procedures

4.1 Introduction

Mitochondria are widely referred to as the powerhouse of the cell. They sustain life by providing the cell with energy in the form of ATP via a process known as oxidative phosphorylation, and are crucial regulators of calcium buffering and apoptosis (Nunnari & Suomalainen 2012). Since mitochondria are vital to maintain normal cellular functions, their dysfunction can have widespread and devastating effects. Mitochondrial dysfunction has long been associated with neuronal trauma and ischemia/reperfusion damage to central nervous system tissues (Azbill et al 1997, Fiskum 2000, Sullivan et al 2005, Visavadiya et al 2015). Promising pharmacotherapies have been developed to target mitochondrial dysfunction using antioxidants (Bains & Hall 2012, Gilgun-Sherki et al 2002, Jin et al 2014, Patel et al 2014, Smith et al 2008), ETS uncouplers (Cunha et al 2011, Jin et al 2004, Patel et al 2009b, Rodriguez-Jimnez et al 2012, Sullivan et al 2004), and alternative biofuels (Patel et al 2010, Petruzzella et al 1992) to feed into the electron transport system. In the burgeoning field of organelle transplantation, a novel paradigm has emerged to transplant exogenous, well-coupled mitochondria to replace those that are nonfunctional. As evidenced with earlier experiments, not only can this approach supplement the original pool of mitochondria with more endogenous antioxidant systems and improve energy producing capabilities, but it can also replace those mitochondria that are too damaged to function (Chang et al 2016, Hayakawa et al 2016, Islam et al 2012, Katrangi et al 2007, Masuzawa et al 2013, Pacak et al 2015).

Mitochondrial transplantation has been shown to have beneficial effects in different injury models *in vitro* using co-incubation methods (Chang et al 2013b, Clark & Shay 1982, Elliott et al 2012, Katrangi et al 2007), direct injection techniques (King & Attardi 1988) or co-cultured cell delivery approaches (Cselenyak et al 2010, Plotnikov et al 2008, Spees et al 2006, Wang & Gerdes

2015, Yang & Koob 2012); as well as *in vivo* using direct injections (Masuzawa et al 2013) or cell-to-cell transfer (Islam et al 2012). In the emerging field of mitochondrial medicine (for reviews see Armstrong 2007, Luft 1994), mitochondrial transplantation has a unique set of caveats that require careful consideration. Multiple labs have shown that exogenous mitochondria can be integrated into host cells (Chang et al 2013b, Clark & Shay 1982, Cselenyak et al 2010, Islam et al 2012, Katrangi et al 2007, Kitani et al 2014a, Masuzawa et al 2013, Pacak et al 2015, Spees et al 2006). Relevant to the current study, verification of mitochondrial incorporation into host tissues has been performed using various techniques including quantifying transplanted mitochondrial DNA (Islam et al 2012, Spees et al 2006, Yang & Koob 2012) or visualizing mitochondria with transgenic labeling or post-isolation fluorescence tagging (Chang et al 2013b, Clark & Shay 1982, Kitani et al 2014a, Lin et al 2013, Masuzawa et al 2013, McCully et al 2009, Plotnikov et al 2008). More recently, it has been reported that mitochondrial particles are transferred from astrocytes into nearby damaged neurons after ischemic stroke in mice, resulting in neuroprotection (Hayakawa et al 2016). This group also showed that injecting isolated mitochondria particles labeled with MitoTracker Red CMXRos into the mouse brain allows for tracking of mitochondria in the CNS *in situ*.

Using fluorescent mitochondrial labels does not come without its caveats. Different mitochondrial dyes have been utilized when tracking mitochondria *in vitro* (Chang et al 2013b, McCully et al 2009, Plotnikov et al 2008). Transgenic labeling of mitochondria *in vitro* provides a stable alternative to labeling with more photosensitive MitoTracker dyes (Rizzuto et al 1996, Shitara et al 2001). While MitoTracker Green FM is a dye whose fluorescence intensity is altered with changing membrane potentials (Keij et al 2000), it is reported that the MitoTracker dyes can inhibit mitochondrial respiration (Buckman et al 2001). The latter group reported that upon mitochondrial damage, such as uncoupling using FCCP, MitoTracker dyes were released into the cell cytoplasm, indicating that these dyes are not irreversibly bound to the mitochondria. MitoTracker Green FM is reported to be cytotoxic in Hela cells even at low concentrations of 250 nM

(Han et al 2013), and MitoTracker Red CMXRos is toxic to human 143B osteosarcoma cells (Minamikawa et al 1999). CMXRos is a photosensitizer that causes chemical damage when subjected to laser scanning, such as used in confocal imaging.

To address the fidelity of using fluorescent trackers to label exogenous mitochondria, we investigated the use of transgenically-labeled mitochondria isolated from cell culture compared to traditionally labeled MitoTracker mitochondria to ascertain which could provide a non-toxic, indelible tag that allows for long-term visualization of transplanted mitochondria *in vitro*. Our results showed that the tGFP label did not dissociate from isolated transgenic mitochondria, but the MitoTracker Green FM label detached from mitochondria. We then used time-lapse confocal imaging to reveal the incorporation of exogenous tGFP mitochondria into PC-12 cells after brief co-incubation. After we established optimal isolation protocols to obtain well-coupled and easily identifiable mitochondria for characterizing transplantation into cell cultures, we addressed technical hurdles for transplanting mitochondria *in vivo*. Immunohistochemical evidence shows that these transgenically-labeled mitochondria can be injected into the spinal cord with host cellular uptake within 24 hours post injection. In summary, we show successful transplantation of exogenous, transgenically labeled mitochondria both into PC-12 cells *in vitro* and within various host cells in the rat spinal cord *in situ*. These experiments delineate a superior method of using transgenic cell lines for the purpose of isolating well coupled mitochondria that have a permanent fluorescent label that allows real time tracking of transplanted mitochondria. This lays the foundation to apply these techniques of mitochondrial transplantation after SCI to discern cell type incorporation and the effects on overall bioenergetics and tissue sparing.

4.2 Materials and Methods

4.2.1 Transgenic Labeling of PC-12 Cells

The section of the plasmid vector pTurbo-GFP-mito (evrogen cat # FP517 Farmingdale, NY) containing the sequence coding for both tGFP and the mitochondrial targeting sequence was removed and inserted into a pIRESpuro3 vector. Briefly, the restriction enzymes NheI-HF and NotI-HF were used to digest both vectors. NheI cuts the pTurbo-GFP-mito vector at the 591 position, and NotI cuts at the 1406 position. Within these cuts are the mitochondrial targeting sequence and the turbo-GFP coding sequence. This insert was then gel purified and ligated with the PIRESpuro3 vector using a rapid DNA ligation kit (Roche). The resulting plasmid contained CMV promoter, the mitochondrial targeting sequence, tGFP coding sequence, and puromycin resistance sequence. OneShotStbl3 *E. coli* (Invitrogen cat no C7373-03 Carlsbad, CA) were then transformed with the resulting plasmid. Briefly, the plasmid was diluted to 1ng/μL and used according to manufacturer protocol for *E. coli* transformation. One colony from the resulting plate was then selected for plasmid DNA purification using a Miniprep kit (Qiagen 27106 Valencia, CA) according to manufacturer's protocol. PC-12 Adh (ATCC CRL-1721.1 Manassas, VA) cells used in these experiments were grown at 37°C with 95% air, 5% CO_2 in complete growth media consisting of F-12K Medium (ATCC cat # 30-2004 Manassas, VA) with 2.5% fetal bovine serum (Atlanta Biologicals # S1111OH, Atlanta, GA), 15% horse serum (Gibco # 26050-070), and 1.1% penicillin streptomycin (Corning # 30-002-CI, Tewksbury, MA). Cells were passaged every 3-4 days. Transfection was carried out using LipoJet In Vitro DNA and siRNA Transfection kit (SignaGen Laboratories Rockville, MD) according to manufacturer's protocol for transfecting adherent cells. At 24 hours after transfection, selective media (3 μg/mL puromycin in complete media) was applied to the cells. Cells were stably transfected by continual growth in selective media for the remainder of the studies.

4.2.2 Mitochondrial Isolation from Cell Culture

Isolation of mitochondria from cell culture was carried out by using techniques for isolating mitochondria from spinal cords (Patel et al 2014), with modifications for removing PC-12 Adh cells from culture plates and homogenization with additional nitrogen bomb steps to ensure cellular disruption. Briefly, cells were removed from 15cm culture plates at 95% confluence by trypsinization (0.25% Trypsin EDTA) or manual cell scraping, as described for experiments comparing cell removal techniques. Cells were concentrated by centrifugation at 500 x g for 5 min at 4°C and resuspended in 2 mL isolation buffer (215 mM mannitol, 75 mM sucrose, 0.1% BSA, 20 mM HEPES, pH adjusted to 7.2 with KOH) containing 1 mM ethylene glycol tetraacetic acid (EGTA). The solution was centrifuged at 1.8 rcf for 3min, 4°C. The resulting pellet was then resuspended and mechanically homogenized using a drill press with 10 gentle passes of the pestle into and out of the solution. The cells were then nitrogen bombed at 1500 psi, 10 min, 4°C to further release mitochondria from cells and increase yield. Mechanical homogenization was then repeated before the solution was again centrifuged at 1.8 rcf, 3 min, 4°C. The supernatant containing mitochondria was removed and saved in an Eppendorf tube to be combined at later step. To further increase mitochondrial yield, the pellet was resuspended in isolation buffer, and mechanical homogenization and nitrogen bombing steps were repeated. The solution was again centrifuged at 1.8 rcf, 3 min, 4°C, after which the supernatant containing mitochondria was saved and the pellet was again resuspended and underwent mechanical homogenization, nitrogen bombing, and centrifugation at 1.8rcf for 3min, 4°C. Finally, the 3 resulting supernatant portions that had been saved from previous steps were centrifuged at 13,000 rcf for 10 min at 4°C, and the pellets were then resuspended in isolation buffer, combined into one sample, and purified using ficoll gradient (7.5%/10%) centrifugation at 32,000 rpm for 30 min, 4°C. After centrifugation, mitochondria remain in a pellet at the bottom of the tube. Importantly, we found that there is an inconspicuous layer of non-mitochondrial particles lying on top of the pellet that must be aspirated gently prior to removing

the rest of the supernatant. The purified mitochondrial pellet was resuspended 600µL isolation buffer without EGTA and centrifuged at 10,000 rcf, 10 min, 4°C resulting in the final pellet which was then resuspended in 20 µL isolation buffer without EGTA. 2 µL of this was used in the Pierce BCA protein assay kit (Thermo Scientific cat# 23227 Rockford, IL) with the Biotek Synergy HT plate reader (Winooski, VT) measuring absorbance at 560 nm to determine mitochondrial protein concentration.

4.2.3 MitoTracker Green Labeling and Filter Testing

Mitochondria were isolated from naïve, unlabeled PC-12 Adh cell cultures (see previous section **4.2.2**). After centrifugation at 10,000 rcf, 10min, 4°C, the mitochondria were labeled with MitoTracker Green FM (MTG, Invitrogen cat# M7514) according to manufacturer's protocol. Briefly, mitochondria were incubated with 1 uM MTG for 5 min at room temperature, covered from light. The solution was centrifuged at 10,000 rcf, 10 min, 4°C to wash any remaining unbound MTG. The mitochondrial pellet was then resuspended in isolation buffer with EGTA, drawn into a 1mL syringe, slowly passed through a 0.2 µm pore Nalgene filter (Thermo Scientific cat # 723-2520) placed at the end of the syringe, and then seeded onto 35 mm plates containing unlabeled PC-12 Adh cells. The cells were placed in a 37°C incubator for 1 hour, after which they were imaged using a Nikon confocal microscope (see **4.2.7**). In tandem, a filter test was performed on isolated tGFP mitochondria, which were drawn into a separate syringe, passed through a filter and seeded onto naïve cells for imaging.

4.2.4 Transmission Electron Microscopy

For transmission electron microscopy (TEM), tGFP-labeled mitochondria were isolated as described above. After 10,000 rcf centrifugation, the mitochondrial pellet was fixed in 3% glutaraldehyde in sodium cacodylate buffer overnight at 4°C. The pellet was then rinsed in 0.2M sodium cacodylate buffer 3 times for 5 minutes each at 4°C. The pellet was then placed in 2% osmium tetroxide for 1 hour at 4°C, followed by washing in distilled water 5 times for 5

min each at 4°C. The pellet was then placed in 2% uranyl acetate overnight at 4°C. The sample was rinsed in distilled water 5 times for 5 min each at room temperature, followed by sequential ethyl alcohol dehydrations in 30, 50, 70, and 90% ethyl alcohol (EtOH) for 10 min each at room temperature. This was followed by three washes in 100% EtOH for 15 min each wash at room temperature. The pellet was then washed in resin (23.1% ERL 4221 (3,4-Epoxycyclohexylmethyl-3',4'-epoxycyclohexane carboxylate) Electron Microscopy Sciences Hatfield PA), 18.5% DER (Diglycidyl ether of polypropylene glycol, Electron Microscopy Sciences Hatfield PA), 57.7% NSA (Nonenyl succinic anhydride, Electron Microscopy Sciences Hatfield PA), 0.69% DMAE (Dimethylaminoethanol, Electron Microscopy Sciences Hatfield PA) 3 times, each for 1 hour at room temperature with gentle spinning. The pellet was then cut into smaller sections, placed in fresh resin in molded blocks, and incubated at 60°F for 48 hours. Blocks were then trimmed and cut at 90 nm thickness using Ultracut UCT (Leica Microsystems, Buffalo Grove IL). Sections were placed onto copper grids and allowed to dry at room temp, covered to protect from dust accumulation, overnight. The mounted grids were then processed using lead citrate. Briefly, each grid was placed on top of a drop of 0.5% aqueous lead citrate at room temperature in a petri dish containing sodium hydroxide pellets to absorb carbon dioxide. Grids were left on the droplet for 3 minutes, then moved to a new droplet of distilled water, in turn "washing" the grid. The grid was moved to a fresh droplet of water every 5 min, for a total of 5 washes then dabbed with a Kimwipe to remove the excess water and allowed to dry. Grids were then imaged at 60kV on a Philips TECNAI 12 BT transmission electron microscope. Captured images represent the inner portion of the mitochondria pellet.

4.2.5 Assaying Respiration of Isolated Mitochondria

Mitochondria, whether labeled or not, were assayed for OCR immediately after isolation using the Seahorse Bioscience XF^e Flux Analyzer as described previously (Sauerbeck et al 2011, Patel et al 2014). Briefly, isolated mitochondria were applied into cell plate cartridges that were then centrifuged to concentrate

mitochondria to the bottom of each well. Then, automatically 5mM pyruvate/ 2.5 mM malate/ 1mM ADP, 1µg/uL oligomycin, 3 µM FCCP, and 100nM rotenone/10mM succinate were sequentially added to each well. Oxygen levels were measured after each substrate/inhibitor addition over time to obtain OCR in each instance of manipulating different complexes of the electron transport system.

4.2.6 Co-incubation of PC-12 Cells with Transgenically-Labeled tGFP Mitochondria

Transgenically-labeled tGFP mitochondria were isolated from cell culture and then applied to confluent naïve (unlabeled) PC-12 Adh cells. tGFP mitochondria were isolated as described above (section **4.2.2**) and diluted to desired concentrations using complete media at 37°C. Naïve PC-12 cells were plated 24 hours prior in 35mm dishes (MatTek corp. Part no. P35GC-1.5-14-C Ashland, MA) with glass coverslip bottoms for imaging purposes. The media on naïve PC-12 cells was replaced with mitochondrial-supplemented media at concentrations of 5, 10, or 20 µg per 2mL of media, which was left on the cells for 1 or 2 hours dependent on the experimental design at 37°C on a gently rocking platform. The mitochondria-enriched media was then aspirated and the cells were rinsed once, followed by replacement with fresh complete media at 37°C and imaging.

4.2.7 Imaging of PC-12 Adh Cells After Mitochondrial Transplantation

Cells were evaluated using a confocal Nikon Ti-e inverted microscope (Nikon Instruments Melville NY) for high magnification and live imaging purposes or an American Microscopy Group (AMG) Evos fluorescent microscope for low magnification images to verify transfection efficiency of tGFP. For live imaging, the cell plates were placed in an incubation chamber situated above an inverted laser, set to 5% CO2 and 37°C. Cells were imaged using wavelengths for tGFP using excitation laser 488-20 nm (Nikon) or using the green fluorescent protein (GFP) filter cube (EVOS).

4.2.8 Quantification of tGFP Transplantation in vitro

tGFP-labeled mitochondria at three different dosages (5 µg, 10 µg or 20 µg) were applied to and incubated with unlabeled PC-12 Adh cells (Passage 31, 80% confluent in 35 mm dish) for 2 hours before washing and imaging (section **4.2.7**). In each of 3 separate experimental runs performed on separate days, each dosage was applied to 3 different culture dishes, and 4 random non-overlapping fields of view in each dish were captured using Nikon confocal microscopy representing the region of interest (ROI). These images were taken on live, non-fixed cells. After capturing the ROI, the image was thresholded above background fluorescence, and quantification of the number of green fluorescent objects was calculated using Nikon NIS software (Nikon Instruments).

4.2.9 Microinjection of tGFP Mitochondria in vivo

Adult female Sprague Dawley rats (250g, Harlan, n=13) underwent a T12 laminectomy to expose the L1/L2 spinal level (Patel et al 2012). Isolated tGFP mitochondria were injected into the mediolateral gray matter at 4 circumferential sites of the spinal cord separated by 2mM in the rostral caudal direction using a glass micropipette needle (World Precision Instruments, Sarasota, FL cat no. 4878) pulled and beveled to a 20-30 µm inner diameter pore opening. One cohort of naïve animals was used to determine tGFP co-localization with other mitochondrial markers (n=2). Each injection site consisted of 750 nL of 12.5µg tGFP mitochondria suspended in vehicle (isolation buffer with 5mM pyruvate, 2.5 mM malate and 10mM succinate); hence a total of 50µg tGFP mitochondria in 3µL vehicle was injected per cord. Animals survived 24 hours after injections and then spinal cords were processed for histological assessment. A separate cohort of animals was used to determine cell-type co-localization after SCI (n=11). Each injection site consisted of 750 nL of either vehicle (n=3) (isolation buffer with 5mM pyruvate, 2.5 mM malate and 10mM succinate) or 25µg tGFP mitochondria (n=8) suspended in vehicle; hence a total of 100µg tGFP mitochondria in 3µL vehicle was injected per cord. Animals survived 24 (n=6) or 48 (n=5) hours after injections and then spinal cords were processed for histological assessments.

4.2.10 Immunohistochemistry and Image Analysis

At 24 hours after injections animals were overdosed with 0.2 mL Fatal-Plus solution (Vortech Pharma Ltd., Dearborn, MI) followed by transcardial perfusion first with 0.1M phosphate buffered saline (PBS), then 4% paraformaldehyde in PBS. A 1.5cm segment of spinal cord centered on theL1/L2 injection sites was dissected, cryoprotected in 20% sucrose/PBS, embedded in gum tragacanth, cryopreserved, and serially cryosectioned coronally at 25μM, keeping every section as we have reported (Patel et al 2010, Rabchevsky et al 2002). Antibodies used for fluorescent imaging and co-localization comparisons included rabbit anti-tGFP (0.13μg/mL, Evrogen # Ab513), mouse anti-COXIV (2μL/mL, Cell Signal #11967), mouse anti-TOMM20 (5μg/mL, abcam # ab56783), mouse anti-RECA1 (5μg/mL, abcam # ab9774), mouse anti-Ox42 (5μg/mL, abcam # ab78457), goat anti-rabbit 488 (4μg/mL, Invitrogen # A11008), goat anti-mouse Biotin (7.5μg/mL, Vector # BA-9200), and Streptavidin Texas red (3.3μg/mL, Vector # SA-5006). Images were obtained using Nikon Eclipse Ti Confocal microscope and NIS elements software (Nikon Instruments).

4.2.11 Statistical Analyses

Mander's overlap analyses were carried out using NIS software (Nikon Instruments), in which the percentage of overlap between pixels which were both TRITC + and FITC + was calculated within the injection site ROI in tissue sections. Changes in OCR and respiratory control ratio (RCR) were analyzed using a one-way analysis of variance (ANOVA) for each respiration state. For passage OCR comparisons, we first found no differences within the groups of the passage OCR using one-way ANOVA. Because there were no differences, the passages were combined to do a broad comparison between treatment groups. The treatment groups (naïve vs tGFP) were then compared using Student's T test. Dose-response incorporation studies *in vitro* were analyzed using a one-way ANOVA with Tukey's multiple comparisons. All analyses were performed using Graphpad Prism 6 (Graphpad Software, Inc., La Jolla, CA). Significance was set to $p < 0.05$.

4.3 Results

4.3.1 Transgenic Labeling with pTurboGFP-mito Vector

The pTurboGFP-mito vector encodes tGFP as a fusion protein with the mitochondrial targeting sequence of subunit VIII of cytochrome c oxidase complex. When transfected into PC-12 cells, this plasmid targets the protein to the inner mitochondrial membrane (Matz et al 1999, Rizzuto et al 1995, Rizzuto et al 1989). By exploiting the puromycin resistance cassette of the vector, puromycin was used to select for and amplify cells that expressed tGFP (**Figure 4.1**).

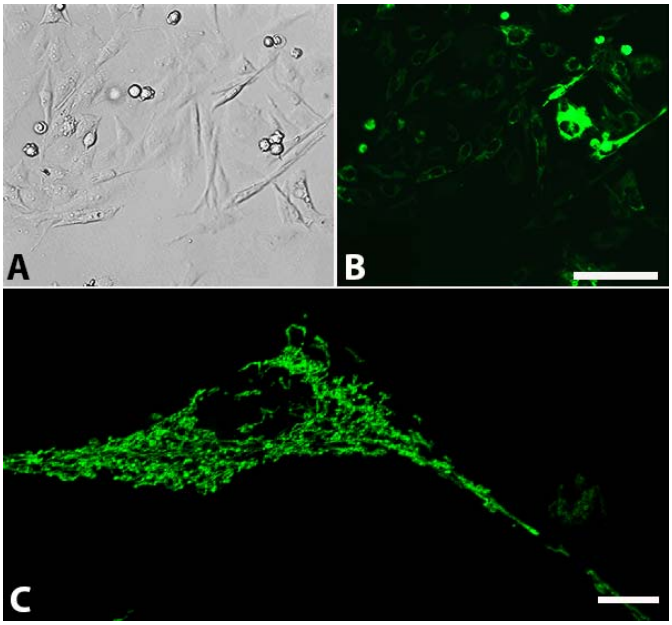

Figure 4.1. tGFP transfected PC-12 Adh cells. Representative images show PC-12 cells expressing tGFP fluorescent protein under **A.** bright-field or **B.** Green Fluorescent Protein filters. Cells were under constant selection using puromycin (passage 19). High transfection efficiency is evident, though it should be noted that there are varying degrees of signal intensity. **C.** High magnification of a tGFP transfected cell showing perinuclear mitochondrial networks throughout the cytoplasm. **A** and **B** taken on AMG scope, scale bar = 50μM. Image **C** taken on Nikon confocal Ti-e microscope, 488nm excitation laser, scale bar= 10μM.

4.3.2 Transmission Electron Microscopy

The morphological features of tGFP-labeled mitochondria under TEM showed typical healthy structures such as prominent cristae and intact outer and inner mitochondrial membranes (**Figure 4.2**), as we have reported (Patel et al 2009a). Verifying the structural integrity of the labeled mitochondria to be transplanted is important, but to ensure that isolated tGFP mitochondria were functioning properly we assessed their respiration rates to confirm the integrity of the electron transport system; notably in comparison to mitochondria labeled with a fluorescent dye.

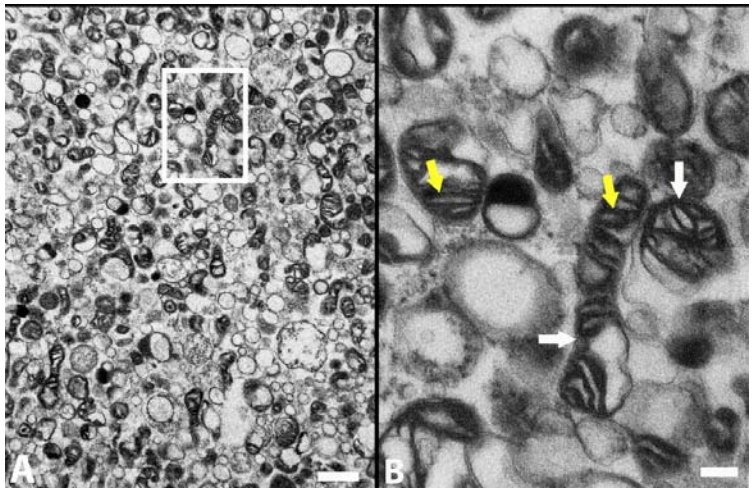

Figure 4.2. TEM images of tGFP mitochondria. TEM shows that the tGFP-labeled mitochondria have dense cristae (yellow arrows) and intact membranes (white arrows), indicative of healthy mitochondria. **B.** is a higher magnification of boxed insert shown in **A**. Scale bars = 1 um (A), 200 nm (B).

4.3.3 Comparing Fidelity of Mitochondrial Labels

There are concerns about both the fidelity of MTG to irreversibly label targeted mitochondria and the potential to affect the function of isolated mitochondria (Buckman et al 2001). To compare the fidelity of the MTG label versus the transgenic tGFP label, we performed an experiment in which labeled, isolated mitochondria were gently pushed through a 0.2 µM filter which does not allow the mitochondria (0.4 – 1 µM) to pass through, but does allow for unbound MTG or tGFP to pass through. We found that while the filtered MTG/mitochondria

solution resulted in positive green fluorescence labeling of naive cells (**Figure 4.3A**), there was no fluorescent labeling with the filtered tGFP/mitochondria solution (**Figure 4.3B**). This indicates that using MTG in mitochondria transplantation experiments may render ambiguous results since the dye can label endogenous mitochondria as well. Therefore, transgenic labeling of mitochondria in cultured cells affords an alternative method of labeling mitochondria in an indelible manner.

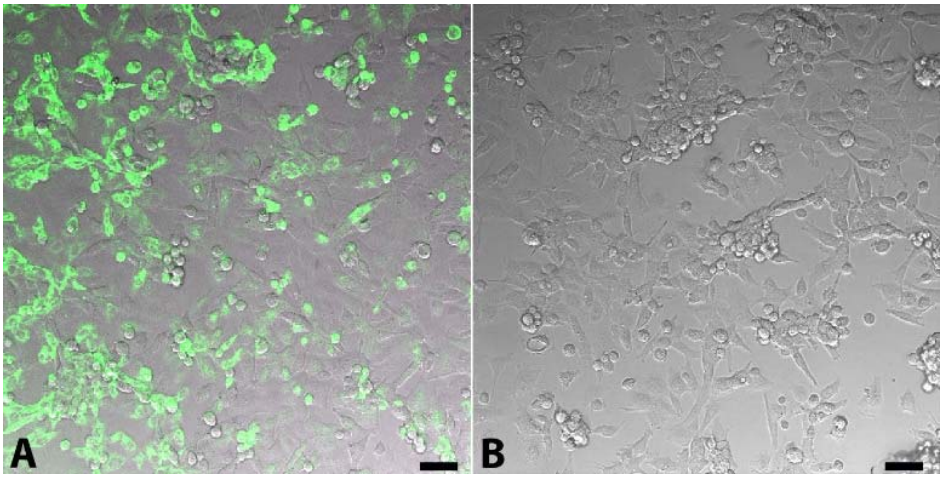

Figure 4.3. MTG label dissociates from mitochondria, leading to non-specific labeling. A. MTG labeling (green) of PC-12 cells after MTG mitochondria solution passage through 0.02 um filter. **B**. Absence of tGFP fluorescence after passing the tGFP mitochondria solution through 0.02um filter, indicating no leakage of the label. Scale bars= 50μM.

4.3.4 Testing Respiration of Isolated, Transgenically-Labeled Mitochondria

Prior to comparing transgenic versus MTG labeling of mitochondria on bioenergetic integrity, we tested transgenically labeled tGFP mitochondria for functionality to ensure the integrity of the electron transport chain. Isolated mitochondria were assayed using the Seahorse Bioscience Flux Analyzer to determine the OCR and RCR, as described in section **4.2.5**. Mitochondrial respiration rates at the different states gives insight into the function of different complexes of the mitochondrial electron transport system. The following methods

are published in our lab (Patel et al., 2014). For further reference, Brand and Nicholls have published a review of mitochondrial assessment techniques and theories (Brand & Nicholls 2011). Briefly- addition of pyruvate, malate, and ADP creates movement of electrons through the electron transport system, creating ATP and consuming oxygen in the process. OCR at this point is referred to as state III respiration- it includes the flow of electrons through the electron transport chain from complex I through complex IV, including coupling to the ATP synthase complex to give a complete picture of the electron transport system integrity. This is a measurement of oxygen consumption that corresponds to ATP production. Oligomycin is then added, resulting in state IV respiration- where the ATP synthase complex is inhibited so that any oxygen consumption is caused by leakage of electrons from the electron transport chain. Subsequent addition of FCCP, a protonophore, causes collapse of the membrane potential across the inner mitochondrial membrane, and uncouples the ATP synthase complex from the electron transport chain. Referred to as state V.1 respiration, proton pumping across the membrane is at a maximal rate, and is reflected by a high rate of oxygen consumption. Final addition of rotenone (a complex I inhibitor) and succinate (feeding electrons into complex II) elicits state V.2 respiration. Oxygen consumption in this state is caused by electrons entering the electron transport chain through complex II. The ratio of state III divided by state IV respiration gives the RCR- a ratiometric measurement that is indicative of mitochondrial integrity as it incorporates respiration from both the entirety of the electron transport chain as well as leakage of electrons. For example, respiratory competent mitochondria with low leakage will have a high OCR after pyruvate, malate, and ADP addition, but a very low OCR following addition of oligomycin, thus resulting in a higher RCR value.

We first compared mitochondria isolated from cells at various passage numbers to ensure that there were no alterations in mitochondrial functionality with age or cell passage numbers. Simultaneously, respiration rates of tGFP-labeled mitochondria were also compared to respiration rates of naïve, unlabeled PC-12 mitochondria (**Figure 4.4**).

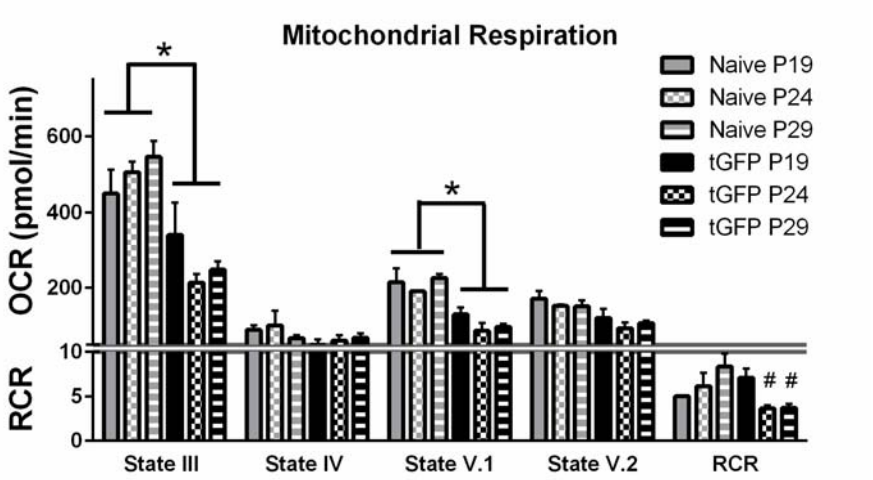

Figure 4.4. OCR of isolated tGFP-labeled mitochondria or naïve non-labeled mitochondria at different passage generations. One-way ANOVA was performed for each state of respiration within treatment groups. With no significant differences among passage number OCR values using a one-way ANOVA, the groups were collapsed (indicated by the horizontal bars) and compared using Student's T tests to determine overall group effects. RCR were analyzed using a one-way ANOVA for each cell group, with Tukey's multiple comparisons. Bars are means ± SEM. *p<0.0001 tGFP vs Naïve; #p<0.05 vs tGFP P19. n= 3/group performed in triplicate.

There were no passage-dependent differences in respiration rates within cell lines, indicating that the passage generation of the cells did not significantly affect respiration; though there was a trend for decreased state III and V.1 OCR with increased passages of the tGFP mitochondria group. Therefore, group passage OCR values were collapsed to compare differences between naïve and tGFP mitochondria at each state. Results showed significant differences in respiration when comparing tGFP to naive groups (State III- $P < 0.0001$; State V.1- $P < 0.0001$) (**Figure 4.4**), indicating that tGFP mitochondria respire at lower rates than naïve mitochondria, perhaps producing less ATP. Additionally, there were significant differences in RCR values [$F(2, 6) = 8.388$, $P=0.0183$]; post hoc analyses showed tGFP mitochondria from lower passage numbers had significantly higher RCR values. While this is important to note, it is not yet

known what optimal respiration rates are for mitochondria to be transplanted since ATP production may be different among cell types. Therefore, in subsequent experiments we utilized tGFP mitochondria from low passage numbers.

Respiration rates of tGFP-labeled mitochondria were then compared to MTG-labeled mitochondria. Results show that regardless of the label, there were no significant differences in OCR at any state (State III- [F (2, 6) = 3.652, P= 0.0917]; State IV- [F (2, 6) = 3.098, P= 0.1190]; State V.1- [F (2, 6) = 2.010, P= 0.2147]; State V.2- [F (2, 6) = 1.277, P= 0.3450]), or RCR values among groups [F (2, 6) = 0.1853, P= 0.8355] (**Figure 4.5**). The electron transport system does not appear hindered by either the MTG or tGFP label as the RCR for each group was above 5. While tGFP mitochondria were found again to respire at overall lower rates, they remained well-coupled. It should be noted that, per manufacturer's protocol, MTG is reconstituted in Dimethyl sulfoxide (DMSO) to a final concentration of 1% DMSO in solution, which may have effects on the lipid membrane of mitochondria causing partial mitochondrial ETS uncoupling and increased OCR.

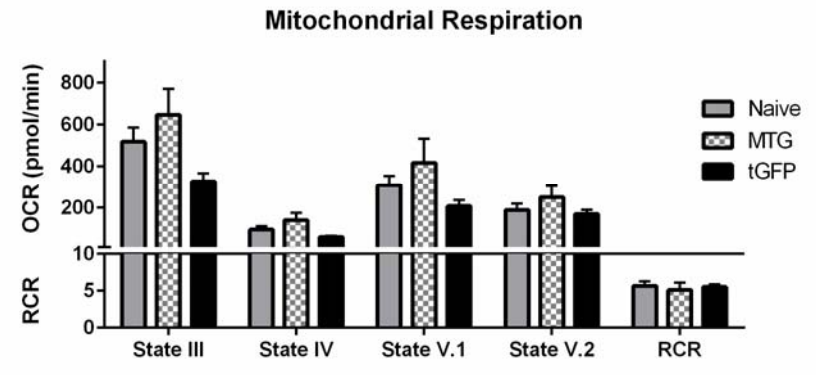

Figure 4.5. tGFP vs MTG mitochondrial respiration. Mitochondria were isolated from either transgenic tGFP PC-12 cells or naïve PC-12 cells that were then labeled using MTG, then assayed for respiration using the Seahorse Flux Analyzer. Bars are means ± SEM. (One-way ANOVA for each state) n=3/group, performed in triplicate.

After isolating well-coupled transgenically-labeled mitochondria from cell culture, we optimized techniques for increasing both bioenergetics and mitochondrial yield. In order to perform *in vivo* transplantation experiments, a sufficient yield of respiratory-competent mitochondria is needed to elicit responses following their supplementation. Using isolation methods with or without ficoll, we have found that we can obtain a higher yield of crude mitochondria versus purified mitochondria. However, when the health of cell culture-derived mitochondria in the crude vs purified fractions was tested, we found that purified mitochondria give much higher respiration rates (data not shown). Our initial use of trypsin as a means to permeabilize the cell membranes and release mitochondria resulted in a higher yield of mitochondria. Importantly, however, we found in preliminary studies that intraspinal transplantation of mitochondria isolated with trypsin caused tissue damage due to residual trypsin remaining in the pellet (data not shown), even after washing and centrifugation. Therefore, while the isolated mitochondria appear well-coupled, trace amounts of trypsin in the suspension can be detrimental to tissues *in vivo*. Therefore, subsequent studies using mitochondria derived from cell culture were isolated using manual scraping with the ficoll purification step.

During *in vivo* transplantation experiments, isolated mitochondria may be exposed to room temperature (RT) for up to 30 minutes while in the microinjection needle. An experiment was performed on tGFP mitochondria to test the effects of temperature and substrate supplementation on respiration (**Figure 4.6**). The mitochondria were resuspended in isolation buffer and either left at RT or on ice for 30 minutes, and either with or without substrate supplementation (5mM pyruvate/malate and 10mM succinate).

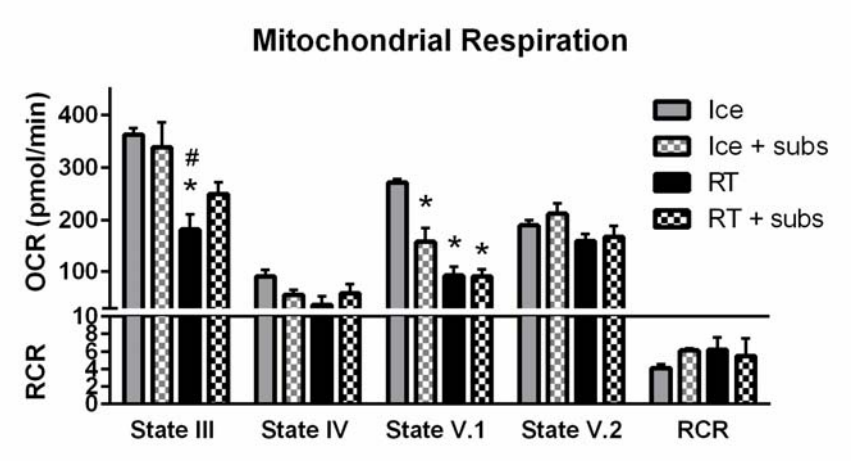

Figure 4.6. Mitochondrial respiration changes with temperature and substrate addition. Mitochondrial respiration was highest when left on ice, with state III and V.1 decreasing significantly at RT. Addition of substrates (subs) at RT helped maintain state III respiration. Bars are means ± SEM. *p<0.05 vs Ice; #p<0.05 vs Ice + subs (One-way ANOVA for each state, Tukey's multiple comparison) n=3/group in triplicate.

Mitochondria that were kept on ice in centrifuge tubes had higher respiration rates compared to mitochondria left at RT. State III OCR changed significantly [F (3, 8) = 7.407, P= 0.0107] and post hoc analysis revealed significantly decreased OCR in samples that were left at room temperature without substrates compared to those on ice, with or without substrates. Addition of 5mM pyruvate malate and 10mM succinate substrates to mitochondria held at RT partially restored state III OCR towards the respiration of mitochondria held on ice. This indicates that substrate addition helps to maintain mitochondrial bioenergetics in our injection paradigm.

State V.1 respiration was significantly different among groups [F (3, 8) = 22.79, P= 0.0003]; post hoc analyses showed lower respiration in all samples compared to the naive sample on ice. There were no differences in State IV [F (3, 8) = 2.561, P= 0.1279], State V.2 [F (3, 8) = 2.059, P= 0.1842], or RCR [F (3, 8) = 0.5777, P= 0.6458] among the groups.

4.3.5 tGFP Mitochondrial Transplantation in vitro

We tested whether isolated transgenically-labeled tGFP mitochondria could be incorporated into PC-12 cells by co-incubation. The tGFP mitochondria were isolated from cell culture and 10µg was mixed with 2mL fresh complete media and added to 35 mm culture dishes that were 80% confluent with naïve PC-12 cells. After one hour, cells were live-imaged and showed positive tGFP labeling within somas (**Figure 4.7**).

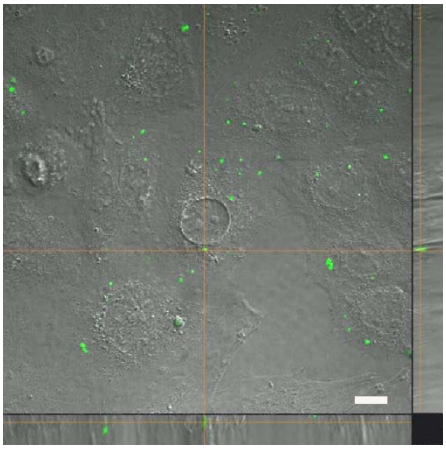

Figure 4.7. Transplanted tGFP mitochondria are taken into naïve PC-12 Adh cells. After 10 µg tGFP mitochondria were incubated with unlabeled PC-12 cells for one hour, live-imaging showed positive tGFP labeling within soma. The bottom panel shows the X plane, and the right panel shows the Y plane. Cross hairs indicate one instance of punctate tGFP mitochondria within a cell. Image was taken using Nikon Ti confocal microscope. Scale bar = 25 µm.

We next applied increasing concentrations of tGFP mitochondria to naïve PC-12 cells. After two hours of co-incubation, the cells were washed of any remaining extracellular mitochondria and live-imaged (**Figure 4.8A**). Upon visualization, there appeared to be much more instances of tGFP labeling in the higher dosage groups, with no labeling in the control group (**Figure 4.8A**). These differences in fluorescence were compared to assess the dose-dependent incorporation of tGFP mitochondria. Images of the ROIs (**Figure 4.8B**) were captured and thresholded to a non-transplanted plate to remove non-specific background fluorescence for quantification. Our results showed that there was a

significant dose-dependent difference between different groups [F (3, 8) = 5.430, P= 0.0248]; post-hoc analysis showed a significantly higher amount of tGFP immunofluorescence within PC-12 Adh cells administered 20µg tGFP mitochondria compared to naive with decreasing amounts of fluorescence in the lower dosage groups (**Figure 4.8C**).

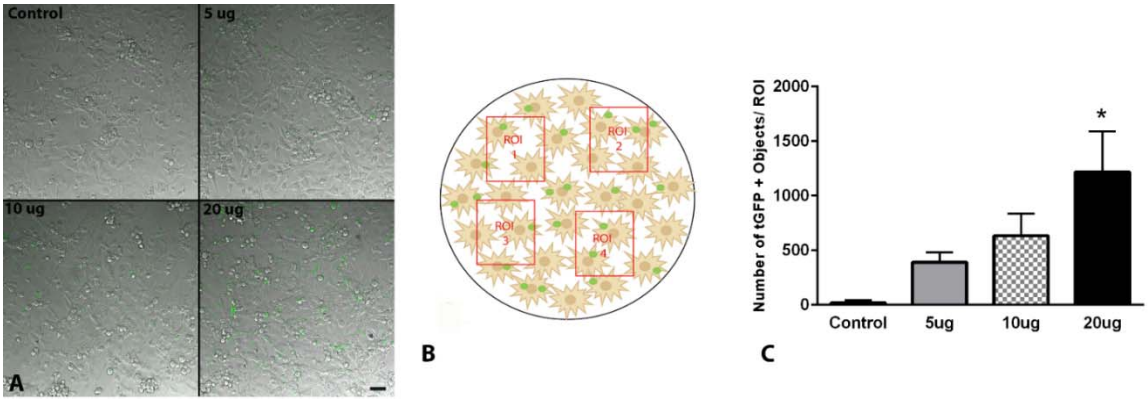

Figure 4.8. tGFP mitochondria are taken up by PC-12 Adh cells in a dose-dependent manner. A. Representative DIC/FITC images of individual ROI in cell cultures from each dosage showing varying amounts of tGFP mitochondria within cells. **B.** Schematic depiction of four random non-overlapping ROIs chosen per plate analyzed for each dosage, replicated in three plates. **C.** Quantification of ROI densities of tGFP for each dosage administered showed that the 20µg transplant group had the highest number of mitochondria taken up. Bars are means ± SEM. *p <0.05 vs control group using one-way ANOVA with Tukey's multiple comparisons. n=3/dosage performed in triplicate, scale bar = 50µM, applies to all images.

To further confirm that mitochondria were successfully incorporated into cultured cells, time-lapse experiments were performed. After 10 µg of isolated tGFP-labeled mitochondria were incubated with naïve PC-12 cells for 2 hours as described earlier, the cells were imaged over a 12 hour period during which positive intracellular tGFP fluorescence was evident (**Figure 4.9**). Remarkably, cells could be seen replicating during this time, segregating transplanted mitochondria between daughter cells.

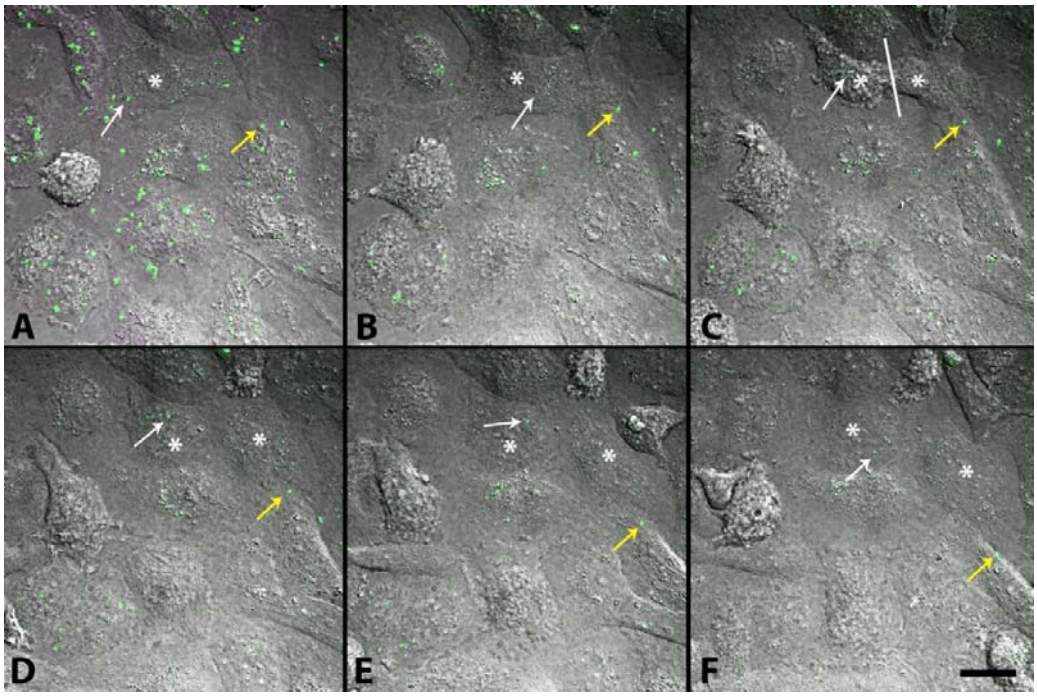

Figure 4.9. Movement of exogenous tGFP mitochondria within PC-12 cells. After 10 µg tGFP mitochondria was added to naïve PC-12 cells and incubated at 37°C on a gently rolling platform for 2 hours, they were washed off and replaced with complete media before time lapse images were taken over a 12-hour period. Images represent beginning of imaging **A** separated by 100 minutes for each time frame (**B-F**). Mitochondria can be visualized moving within cells (yellow arrow). As a cell divides (white asterisk on mother cell in **A** and **B**, then on each daughter cell in **C-F**, with division occurring at white line in **C**), transplanted mitochondria can be seen throughout the division process, and are retained in the daughter cells (white arrow). Images were taken using Nikon Ti confocal microscope. Scale bar = 20µM.

4.3.6 In vivo Transplantation

Using the optimal isolation methods, mitochondrial transplantation was performed *in vivo* to determine if transgenically-labeled, cell culture-derived exogenous mitochondria can be incorporated into living spinal cord tissues. tGFP mitochondria were isolated and injected into the medial lateral gray matter of the rat spinal cord at the L1/L2 spinal level. 24 hours after transplantation animals

were euthanized and spinal cords processed for histology. An anti-tGFP antibody was used in tandem with antibodies specific to mitochondrial proteins to determine cell type co-localization (**Figure 4.10**).

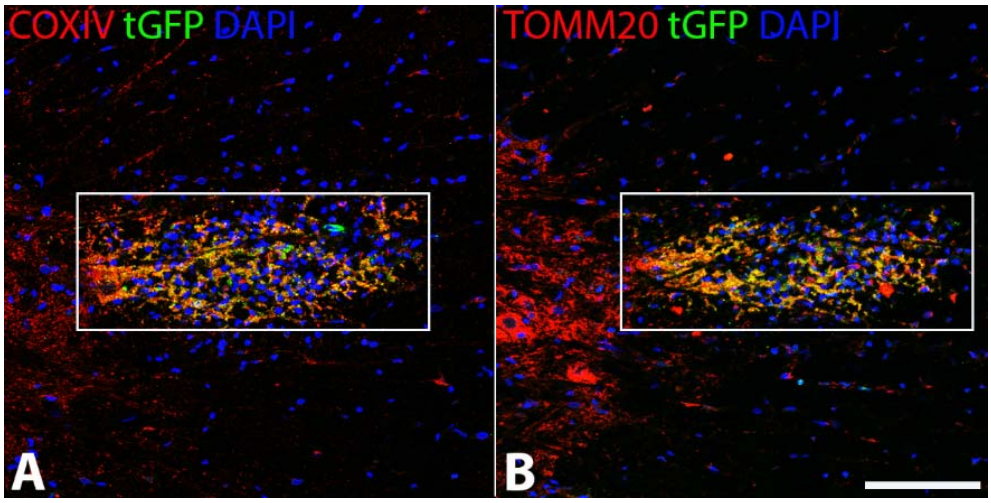

Figure 4.10. tGFP labeled mitochondria injected into the spinal cord co-localize with mitochondrial markers. tGFP mitochondria were isolated from PC-12 cells and injected into the rat spinal cord. Antibodies against tGFP and the inner (**A**) (COXIV) and outer (**B**) (TOMM20) mitochondrial membranes show that the injected green fluorescence is intact mitochondria. Images taken on Nikon Ti confocal microscope. White boxes indicate region of injection and co-localization analyses. Scale bar= 100μM.

COXIV antibody targets the inner mitochondrial membrane, while TOMM20 antibody targets the outer mitochondrial membrane. When visualized with tGFP which also localizes to the inner membrane, COX IV co-localization indicates that the tGFP signal is indeed mitochondria. Further, the exogenous mitochondria appear intact as the tGFP tag localizes to the inner membrane and TOMM20 labels the outer membrane; positive co-localization indicates grafted mitochondria with both inner and outer membranes intact (**Figure 4.10**). When quantifying the co-localization of the tGFP positive and Texas Red positive pixels in the injection region (indicated by white boxes), the Mander's overlap value for tGFP and COXIV was 0.843 and for tGFP and TOMM20 was 0.855. This

indicates that within the region of injection, the tGFP mitochondria are co-localized with mitochondrial markers.

Cell type co-localization was evident within macrophages and endothelial cells at both 24 and 48 hours after injection (**Figure 4.11**). Positive signal overlap (yellow) of green (tGFP) signal within cell membranes (red) indicate co-localization. Exogenous tGFP mitochondria were found to be within both microglia/macrophages and endothelial cells of the spinal cord at both 24 and 48 hours after injection (**Figure 4.11**). There may be a cell-specific mode for mitochondrial incorporation. For example, there is much evidence of punctate tGFP+ signal within the cell membrane of macrophages (**Fig. 4.11 A** and **B**), though it is not known if the mitochondria underwent phagocytosis or whether they were passively incorporated into the cytoplasm. Additionally, tGFP mitochondria were found within endothelial cells at both time points (**Fig. 4.11 C** and **D**). There was positive tGFP signal directly associated with the membranes of some endothelial cells that appeared perinuclear, which may indicate the mitochondria are being taken into perivascular pericytes (**Figure 4.11 C,** tGFP+ signal closely associated with endothelial membrane). Further studies will utilize markers for pericytes to determine if exogenous mitochondria are being taken into these cells, and we will comprehensively characterize cell-type incorporation over time.

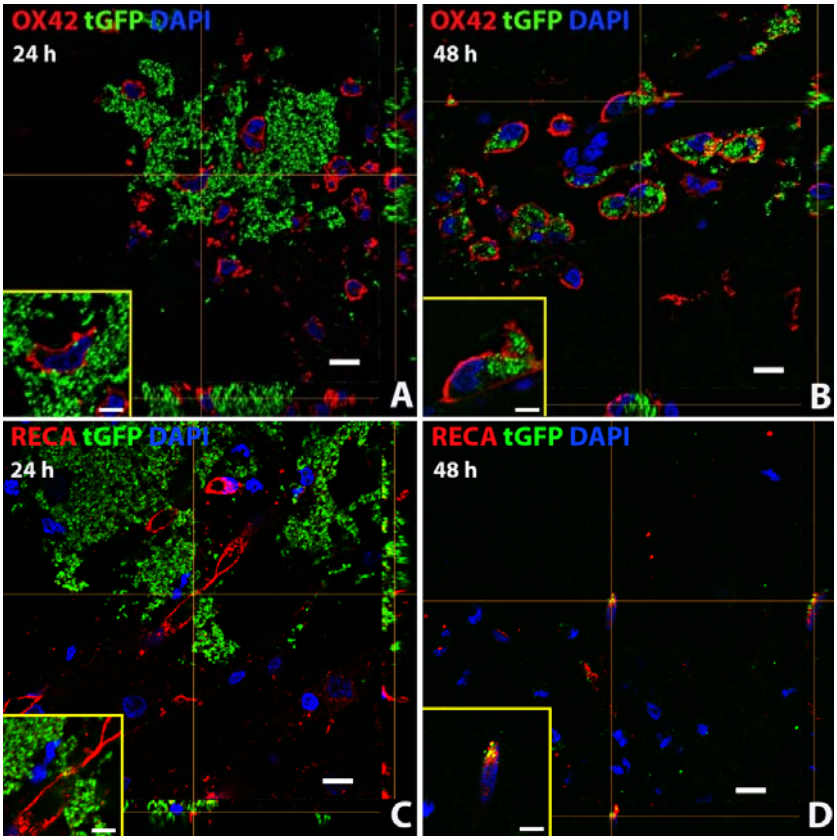

Figure 4.11. Exogenous tGFP mitochondria are incorporated into different cell types *in situ*. tGFP mitochondria were injected into the naïve spinal cord. Representative z-stack images were taken from spinal cords at the 24 (**A, C**) or 48 hour (**B,D**) time points after injection. OX42 = microglia/macrophages, RECA = endothelial cells. Scale bars = 10μM. Images were taken with Nikon Ti confocal microscope.

4.4 Discussion

The results of our feasibility study demonstrate that transgenically-labeled tGFP mitochondria are a viable option for visually tracking transplanted mitochondria both *in vitro* and *in situ*. It is possible to label the inner mitochondrial membrane of cultured cells with tGFP with high transfection efficiency and isolated mitochondria have intact inner and outer mitochondrial membranes, as well as dense cristae as seen in TEM images. We also found that supplementation of isolated mitochondria with pyruvate malate and succinate is beneficial for maintaining state III respiration at room temperature for prolonged

periods of time often required for transplantation procedures *in vivo*. Further, we demonstrate that the transgenic tGFP label is an indelible marker of transplanted mitochondria, and contrary to previous studies (Katrangi et al 2007), we found that MTG did not stay irreversibly bound to exogenous mitochondria; this may result in host labeling and inaccurate conclusions of successful transplantation. Others have also found MTG fluorescence intensity to be at least partially dependent upon membrane potential (Keij et al 2000).

The bioenergetics of mitochondria isolated from cultured cells did not change across multiple passages, but there was an overall decreased respiration rate of transgenically-labeled mitochondria when compared to unlabeled mitochondria. This may be partially contributed to the stable transfection attained by puromycin selection. While the transgenic cells have a puromycin resistance sequence, they grew more slowly than naive cells at the same passage numbers. We noted that the cell doubling time for unlabeled cells is about 24 hours, whereas the doubling time for transgenic cells was closer to 72 hours. We did not note any higher levels of die-off or cell death while the transgenic cells were under selection. At lower cell passage generations, the isolated mitochondria remained well-coupled with comparable RCR to naïve mitochondria. In contrast, MTG-labeled mitochondria showed higher respiration than tGFP-labeled mitochondria, although this increase was not significant. Importantly, naïve, MTG-labeled and tGFP-labeled mitochondria had healthy RCRs indicating that the electron transport chain is well coupled to the ATP synthase complex. Differences in respiration of MTG labeled mitochondria vs naive unlabeled mitochondria has been documented (Buckman et al 2001), where it was concluded that MTG alters ETC activity such as uncoupling the ETC from ATP synthesis.

Use of transgenically-labeled mitochondria opens the possibilities for cell type co-localization/double labeling and tracking experiments to evaluate incorporation of exogenous mitochondria distinguishable from host cells. Transgenic labeling of mitochondria *in vitro* can supply a pool of stably transfected mitochondria that affords the opportunity to visualize the movement

and integration of exogenous mitochondria within host cells and/or tissues. This can be especially important in future studies to determine the fusion and fission properties of exogenous mitochondria in the context of their successful integration into the host mitochondrial networks after transplantation. Further, this labeling strategy could be useful for visualizing mitochondria in paradigms of transplantation after cytotoxic insult to cultured cells to determine beneficial effects afforded by mitochondrial supplementation.

Upon co-incubation of tGFP mitochondria with naïve PC-12 cells, we showed that exogenous mitochondria were taken into cells within hours and could be seen moving within cells. This reflects previous reports that supplemented mitochondria, labeled in various manners, are taken into cultured cells upon co-incubation (Chang et al 2013a, Clark & Shay 1982, Katrangi et al 2007, Kitani et al 2014b). Our results showed concentration-dependent tGFP mitochondria incorporation into naïve cells, and time lapse imaging over 12 hours after co-incubation showed tGFP mitochondria moving within cells. We also performed *in vivo* transplantation to test incorporation in spinal cord tissues *in situ*. Co-labeling of TOMM20 and COXIV showed that the tGFP+ signals represent exogenous mitochondria, and subsequent immunohistochemistry indicated that transplanted tGFP mitochondria were co-localized predominantly with both microglia/macrophages and endothelial cells. Further analyses are quantifying the incorporation propensity into these cells, as well as other cell types of the spinal cord including neurons, oligodendrocytes, and astrocytes. Mitochondrial uptake into cells similar to our results has been reported, but it is yet unknown what the mechanism of incorporation is- whether the process is passive or active, as multiple studies have found evidence for different mechanisms not always supporting each other. For instance, some have shown that different cell lines are more likely than others to incorporate exogenous mitochondria upon co-incubation, which was theorized to be due to differential endocytic properties of cell types (Clark & Shay 1982). Others have shown xenogenic transfer of exogenous mitochondria in culture upon co-incubation (Katrangi et al 2007). It has been posited alternatively that mitochondria cannot

be taken into recipient cells via passive endocytosis (Pacak et al 2015). This group utilized chemicals to block different methods of internalization and found that only cytochalasin D, which blocks actin polymerization, inhibited mitochondrial uptake. They also blocked clathrin-dependent endocytosis, tunneling nanotubes, and macropinocytosis, but found none of these inhibited mitochondrial uptake. However, others reports that macropinocytosis is necessary for mitochondrial internalization utilizing the same blocker of macropinocytosis the Pacak study used (Kitani et al 2014b). Different cell types were used in the two studies, which may support the findings of Clark and Shay (1982) that cell types can behave differently. While these studies all support that exogenous mitochondria can be taken into host cells in culture, there is not yet consensus on mechanisms by which this happens.

In summary, by using transgenic mitochondrial labeling and time-lapse imaging, it is possible to visualize mitochondrial uptake into cells in real time *in vitro*, allowing further investigation into the exact mechanisms of incorporation. Importantly, we present data showing that transgenic labeling is indelible without affecting mitochondrial integrity so that they may be effectively tracked and visualized after transplantation in both cultured cells and tissues *in situ.* We found the transgenic tGFP tag 1) permanently labels mitochondria with no evidence of dissociation, 2) does not affect mitochondrial integrity, and 3) is easily identified using both fluorescent microscopy alone or with enhanced antibody labeling. Our transgenically-labelled mitochondria did have lower overall respiration rates compared to unlabeled mitochondria, which is a caveat that must be considered for future transplantation experiments. Depending upon the purpose of the experiment, there is a caveat that using tGFP mitochondria may respire more slowly, but they have a reliable marker for visualization.

Our next set of experiments utilized these isolation protocols for transplantation of exogenous mitochondria into the injured spinal cord to determine the effects mitochondria transplantation have on tissues *in vivo* where there is a complex environment including different cell types, potential immune responses, as well as further technical hurdles to consider.

Note:

Portions of this chapter were adapted and reprinted by permission from Elsevier: Gollihue J.L., Patel S.P., Mashburn C., Eldahan K.C., Sullivan P.G. and Rabchevsky A.G. (2017) Optimization of mitochondrial isolation techniques for intraspinal transplantation procedures. *Journal of Neuroscience Methods* Epub 2017 May 23 DOI: 10.1016/j.jneumeth.2017.05.023

CHAPTER 5

Mitochondrial Transplantation *in vivo:* Bioenergetics, Incorporation, and Functional Recovery

5.1 Introduction

Contusion spinal cord injury can result in lifelong debilitation and has a profound impact on day to day activities of individuals living with SCI. In the event of an injury, the primary injury site comprises necrotic tissue that can cause secondary injury cascades, including glutamate excitotoxicity, decreased ATP production, increased lipid and protein oxidation, and resulting apoptosis and necrosis (see **Chapter 1.2** for details). It is widely accepted that mitochondrial dysfunction is intimately related to detrimental secondary pathophysiology resulting from SCI. Similar to SCI, mitochondrial dysfunction has been found to be pivotal to disease and injury progression in other injury models including traumatic brain injury, cardiac ischemia, stroke, Parkinson's disease, and Alzheimer's disease (Aygok et al 2008, Bolanos et al 2009, Ide et al 2001, Krajewski et al 1999, Lin & Beal 2006, McCully et al 2009, Mizuno et al 1989, Sullivan et al 2007, Swerdlow & Khan 2004, Winklhofer & Haass 2010, Xiong et al 1997).

As such, mitochondrial medicine is a developing field of therapeutics aimed at improving mitochondrial health and function for a variety of physiological disease and injury states. Several groups have shown that using different methods of targeting mitochondria dysfunction results in neuroprotection, tissue sparing, and functional recovery. Antioxidants are used to decrease ROS and RNS damage caused by dysfunctional mitochondria in models of nephrotoxicity, TBI, SCI, PD, neurodegeneration, and oxidative stress (Ahmed et al 2014, Bains & Hall 2012, Hall et al 2010, Jin et al 2014, Patel et al 2014, Robb et al 2008, Sheu et al 2006, Smith et al 2008, Ungvari et al 2009, Xiong & Hall 2009). Mild uncoupling of the ETS resulting in increased ATP production has also been shown to be a potential therapy for mitochondrial

dysfunction after SCI, quinolinic acid neurological injury, and models of neurological insult *in vitro* (Brand & Esteves 2005, Jin et al 2004, Maragos et al 2003, Patel et al 2009b, Rodriguez-Jimnez et al 2012, Sullivan et al 2004). Mitochondrial substrate precursors such as acetyl L-carnitine (ALC) and N-acetylcysteine amide (NACA) have been used to improve mitochondrial function after TBI, SCI, age-related cognitive function, and PD (Carta & Calvani 1991, Laird et al 2013, Liu et al 2002, Patel et al 2012, Patel et al 2010, Petruzzella et al 1992, Puca et al 1990). All of these therapies attempt to increase functional neuroprotection by intervening in mitochondrial dysfunction in one form of another.

Gaining credence is a new therapy of mitochondrial transplantation that has emerged as a possible treatment option to restore mitochondrial function after injury, consequently improving long term functional outcome (McCully et al 2017). Transplanted mitochondria may exert beneficial effects by increasing ATP production and calcium buffering capacity, decreasing overall ROS production, providing more antioxidants, and providing a new pool of mtDNA-see **Chapter 2**. Though this therapy is relatively new, transplantation has been shown to be an important player in recovery after ischemic injury to cardiac tissue (Cowan et al 2016, Masuzawa et al 2013, McCully et al 2009, Pacak et al 2015). It has also been shown recently that astrocytes inherently donate their mitochondria to nearby neurons after stroke injury *in vivo*, and that astrocytes can be induced to release mitochondria after injury resulting in neuroprotection (Hayakawa et al 2016). Further, they showed that blocking astrocyte donation of mitochondria using CD38 siRNA inhibited mitochondrial transfer and resulted in neuronal cell death. This shows both the importance and possibility of mitochondrial transfer into damaged cells resulting in cell survival. Intravenous injections of isolated fluorescently-labeled mitochondria in a mouse model of Parkinson's Disease resulted in increased ATP production, increased Complex I activity, decreased ROS, and increased behavioral rotarod scores compared to vehicle injected animals (Shi et al 2017). In a rat model of Parkinson's Disease, injections of Pep-1 conjugated isolated mitochondria into the medial forebrain bundle increased

locomotor scores and dopaminergic neuronal sparing (Chang et al 2016). We have previously shown that exogenous transgenically-labeled mitochondria can be taken into cells of the injured rat spinal cord and are visible at 24 and 48 hours post injury (Gollihue et al 2017).

In the current studies, we investigated the therapeutic effects of immediate mitochondrial transplantation after traumatic SCI. We hypothesized that supplementing the injured spinal cord with a pool of healthy, well-coupled mitochondria could provide a new source of increased energy production, decreased oxidation, and dampened effects of glutamate excitotoxicity resulting in increased tissue bioenergetics. Further, we theorized that exogenous mitochondria would be successfully incorporated into a variety of cell types. Lastly, we posited that these beneficial effects in the short term would result in long term benefits, such as hindlimb functional recovery and tissue sparing.

5.2 Methods

5.2.1 Transgenic Labeling of PC-12 Cells

PC-12 cells were transgenically labeled with a mitochondrial-targeting tGFP, as detailed in **Chapter 4.2.1**. Following transfection, cells were kept under constant selection using media containing 3 µg/mL puromycin in complete media.

5.2.2 Mitochondrial Isolation from Cell Culture

Purified mitochondria were isolated from transfected tGFP-PC-12 cells as described in detail in **Chapter 4.2.2**. Briefly, when cells were 95% confluent they were manually removed from culture plates using a cell scraper. Mitochondria were isolated using multiple centrifugation and resuspension steps to yield purified mitochondria. Importantly, after ficoll purification the non-mitochondrial layer was gently aspirated off the final pellet, ensuring the sample did not have contamination that would make it difficult to pull into the injection needle (see **Chapter 3.7**).

5.2.3 Mitochondrial Isolation from Soleus Muscle

Immediately following CO_2 asphyxiation and decapitation, the soleus muscle was dissected from naïve Sprague Dawley rats (n=6, see **Table 5.1**). The animal was placed on its stomach, with the hindlimb stretched backwards. 70% EtOH was sprayed on the hindlimb, and scissors were used to blunt dissect the skin away from the underlying calf muscle. The skin was then cut away from the muscle on the lateral sides, followed by cutting the Achille's tendon. The muscle was pulled up and away from the leg, exposing the underlying soleus muscle. The tendons were cut at both insertion sites, and the soleus muscle was removed and placed in 2mL of isolation buffer (215 mM mannitol, 75 mM sucrose, 0.1% BSA, 20 mM HEPES, and pH adjusted to 7.2 with KOH) containing 1 mM EGTA and trypsin. The muscle was chopped into smaller pieces using scissors to increase surface area exposed to the isolation buffer and trypsin. The sample was then mechanically homogenized taking care not to introduce air bubbles. Protease inhibitor was added to halt trypsin activity, followed by centrifugation at 1500 rcf, 4°C, 5min. The supernatant was removed and spun at 13,000 rcf for 10min, 4°C after which the pellet was resuspended in isolation buffer and purified using ficoll gradient (7.5%/10%) centrifugation at 32,000 rpm for 30 min, 4°C.The pellet was removed and resuspended in 0.6 mL isolation buffer without EGTA, and spun at 10,000 rcf for 10min, 4°C.The resulting pellet contain purified mitochondria, which was resuspended in isolation buffer without EGTA for Pierce BCA protein assay and microinjection into spinal cord.

5.2.4 Spinal Cord Injury and Microinjection Surgical Procedures

Adult (12 weeks old, 225-250g) female naïve Sprague Dawley rats (Harlan) underwent intraperitoneal injections of anesthesia (80mg/kg ketamine and 10mg/kg xylazine, Butler Animal Health Supply) followed by lacrilube opthalmic ointment applied to both eyes before surgery to prevent drying. The surgical site along the dorsal spine is shaven with an electric hair trimmer and cleaned with both 70% ethanol and betadine solutions. Animals then had a T12

laminectomy to expose the L1/L2 spinal level (Patel et al 2012). Sham animals received a laminectomy only, whereas injured animals received a severe 250 kDyn contusion injury using a force controlled Infinite Horizon impactor computerized injury device (Precision Systems and Instrumentation, LLL, Lexington KY (Scheff et al 2003)). Injured animals were split into three cohorts- the first cohort received vehicle injection, the second received cell-derived tGFP mitochondria, and the third received muscle-derived mitochondria. Injections were made immediately after injury into the mediolateral gray matter at 4 circumferential sites of the injured cord separated by 2mM in the rostral caudal direction (see **Figure 3.1**) using a glass micropipette needle (World Precision Instruments, Sarasota, FL cat no. 4878) pulled and beveled to a 20-30 μm inner diameter pore opening. Each injection consisted of 750 nL of either vehicle (isolation buffer with 5mM pyruvate, 2.5 mM malate and 10mM succinate) or mitochondria suspended in vehicle (for a total of 50, 100 or 150 μg); hence a total of 3μL volume was injected per spinal cord. Muscle incisions were closed using silk sutures and skin incisions were closed using wound clips, followed by application of hydrogen peroxide and betadine. Immediately following surgery, animals were single housed in a clean cage on top of a towel on a 37°C heating pad, and monitored until recovery from anesthesia. Yohimbine 1−2 mg/kg s.c. (Lloyd Laboratories) was used to counteract the effects of xylazine. Buprenorphine HCl (0.02−0.05 mg/kg s.c, Butler Animal Health Supply) was administered subcutaneously immediately after surgery to alleviate pain, and then every 8 hours for 3 days following operation. The antibiotic cefazolin (33.3 mg/kg, s.c, Butler Animal Health Supply) was given twice daily for 5 days post−operatively to decrease incidence of infection. The animals were housed individually until staple removal, with the addition of aspen chew sticks and plastic toys for environmental stimulation. Cages were lined with absorbent pads for the duration of buprenorphine use, as pica has been observed in these animals. After discontinuation of buprenorphine, pine bedding was used. Additional parenteral fluids (Lactated Ringer's solution) were provided as needed for 24−72 h post-surgery to compensate for dehydration brought on by

anesthesia. Bladder expression was performed 2 times per day until adequate spontaneous voiding returned to avoid urinary tract infections. Skin wound clips were removed 10−14 days post−injury under isoflurane anesthesia. Animals survived either 1) 24 hours for mitochondrial respiration analyses (n=45), 2) 24h, 48h, or 7 days for histological analyses (n=15), or 3) 6 weeks for long term behavioral and tissue sparing analyses (n=36)- see **Table 5.1** for division of animal cohorts.

Table 5.1. Separation of animal cohorts by outcome measure. Animals were separated into cohorts for different timepoints and different outcome measures. Depending on the outcome measure, cell derived tGFP or muscle derived mitochondria were transplanted. It should be noted that in addition to these animals, 6 rats were used as donors for leg muscle-derived mitochondria, and 7 animals from long term studies were removed from the study for various reasons (see **Section 5.3.3**).

Table 5.1				
Outcome Measure	**Group**	**Dosage of Mitochondria (µg)**	**Terminal Time Point**	**n=**
Acute Bioenergetics- OCR Complex I Assay	Sham	N/A	24 hr	9
	Vehicle Injection	N/A	24 hr	10
	tGFP Mito	50	24 hr	6
		100	24 hr	7
		150	24 hr	6
	Muscle Mito	50	24 hr	3
		100	24 hr	4
Immunohistochemistry- tGFP Spread and Cell-type Colocalization	Vehicle	N/A	24 hr	1
			48 hr	1
			7 days	1
	tGFP Mito	100	24 hr	4
			48 hr	4
			7 days	4
Long Term Studies- Behavior, Tissue Sparing, Neuronal cell counts	Vehicle	N/A	6 weeks	10
	tGFP Mito	100	6 weeks	11
	Muscle Mito	100	6 weeks	8

5.2.5 Behavioral Analyses

5.2.5.1 Overground Locomotor Rating Scale (BBB)

The BBB locomotor rating scale was used to analyze the hindlimb functional recovery of animals after contusion SCI. Assessments were performed according to published protocol (Basso et al 1995). Animals underwent contusion injury, followed by BBB assessment at 2, 7, 14, 21, 28, 35, and 42 days post injury. Testing was performed at the same time in the same room on each testing day to reduce variation. The scores for the right and left leg were averaged for each time point.

5.2.5.2 von Frey Filament

Mechanical tactile sensitivity and allodynia was measured using von Frey filament (Stoelting, Inc, Wood Dale, IL). Briefly, eight monofilaments increasing in logarithmic stiffness were used to incrementally stimulate the plantar hindpaw. As described previously, a modified up-down method was used to determine the 50% withdrawal threshold (Chaplan et al 1994). An intermediate force von Frey filament (#4.31, 2.0g force) was first applied to the glabrous skin until the filament was slightly bent. If the animal immediately withdrew the hindpaw in response, this was designated a positive response and the next filament tested was of a lesser force. When there was not an immediate withdrawal of the hindpaw, the next filament applied was of a greater force. The thresholds for both hindpaws were averaged and reported.

5.2.6 Mitochondrial Isolation from Spinal Cords

For bioenergetics assays, animals were CO_2 asphyxiated and decapitated 24 hours after injury and injections. A 1cm segment of spinal cord surrounding the injury site and including all of the injection sites was quickly dissected and total mitochondria were isolated as described previously (Patel et al 2012, Sullivan et al 2007). Briefly, the spinal cord was placed in a homogenization tube with 2mL isolation buffer containing EGTA ((215 mM mannitol, 75 mM sucrose, 0.1% BSA, 20 mM HEPES, and pH adjusted to 7.2 with KOH) containing 1 mM EGTA), and physically homogenized with 6 quick rotations of the pestle, without

introducing bubbles into the solution. The sample was poured into a 2mL Eppendorf tube and centrifuged at 1400 rcf for 3 min, 4°C. The supernatants containing mitochondria were poured into a separate Eppendorf tube which was filled up to 2mL with isolation buffer containing EGTA. To increase yield, the pellet was resuspended in 500uL isolation buffer containing EGTA and again centrifuged at 1400 rcf for 3 min 4°C. The supernatants containing mitochondria were again poured into separate tubes and filled to 2mL with isolation buffer containing EGTA. The supernatant tubes were centrifuged at 13000 rcf for 10 min at 4°C. The resulting supernatant was discarded, and 350 uL isolation buffer containing EGTA was used to resuspend each pellet containing mitochondria. The samples underwent nitrogen bombing at 1200 PSI for 10 min at 4°C. The samples were placed on top of a ficoll gradient (7.5%/10%) and centrifuged at 32000 rpm for 30 min 4°C. The supernatant was removed leaving a purified mitochondrial pellet. The pellet was resuspended in 450 uL isolation buffer without EGTA and centrifuged 10,000 rcf for 10 min 4°C to remove remaining EGTA from the sample. The pellet was resuspended in isolation buffer without EGTA. BCA protein assay was performed to determine protein content.

5.2.7 Assaying Respiration of Isolated Mitochondria

Mitochondria were assayed for OCR immediately after isolation using the Seahorse Bioscience XF^e Flux Analyzer as described previously (Patel et al 2014, Sauerbeck et al 2011) and described in detail in **Chapter 4.2.5**. Briefly, mitochondrial respiration was assessed using Seahorse Bioscience eXF24 Flux Analyzer at 37°C using respiration buffer: 215 mM mannitol, 75 mM sucrose, 2 mM $MgCl_2$, 2.5 mM inorganic phosphates, 0.1% BSA, 20 mM HEPES, pH 7.2. After isolation, purified mitochondria were added to the respiration buffer and centrifuged in cell plate cartridges to concentrate mitochondria to the bottom of each well. Then, 5mM pyruvate/ 2.5 mM malate/ 1mM ADP, 1µg/uL oligomycin, 3 µM FCCP, and 100nM rotenone/10mM succinate were sequentially added to each well. Oxygen levels were measured after each substrate/inhibitor addition to calculate each state of mitochondrial respiration.

5.2.8 Mitochondrial Complex I Assay

Function of the ETC complex I was assayed as we have previously described (Patel et al 2009b). Immediately after mitochondria were isolated, 20 µL was stored at -80C. At the time of the assay, the samples were thawed at room temperature, then diluted to 1 µg/µL using 10 mM phosphate buffer (pH 7.4) and vortexed to mix. The samples then underwent three cycles of freeze/thawing. This was followed by 3 cycles of sonication consisting of 0.5 seconds sonication/0.5 seconds of rest for 10 seconds total/cycle. The samples were placed on ice between cycles to prevent overheating. 6 µg protein was added to buffer containing 45.45mM phosphate buffer, 1mM KCN, and 150uM NADH so that the total amount/well was 100uL. Each sample was run in wells both with and without 10uM Rotenone. 50uM CoQ10 was added using the BioTek Synergy HT plate reader (Vinooski, VT) and changes in NADH fluorescence (excitation 360nm/emission 460nm) were measured at 1 min intervals and reported as nmol/min/mg protein. The reduced form of NADH emits light at these wavelengths, while the oxidized form does not.

5.2.9 Spinal Cord Processing for Histological Analyses

Rats survived to their terminal time point after injection (24 hours, 48 hours, 7 days, or 6 weeks). They were overdosed with 0.2 mL Fatal-Plus containing sodium pentobarbital (Vortech Pharma Ltd., Dearborn, MI) followed by transcardial perfusion with150 mL of 0.1M PBS, then with 250mL 4% paraformaldehyde (PFA) in phosphate buffered saline. A 3cm segment of spinal cord centered on the L1/L2 injury site was dissected, and post-fixed up to 4 hours with 4% PFA followed by washing overnight in 2M phosphate buffer. The cords were cryoprotected in 20% sucrose/PBS at 4°C until the cords sank in the solution, then embedded in tragacanth blocks and serially cryosectioned coronally at 20µM (Rabchevsky et al 2001). For the 24 hour, 48 hour, and 7 day cohorts in which more sections were necessary for planned histological analyses, every other section was mounted. Ten slide series were collected so that adjacent spinal cord sections on any given slide were spaced equally 400 µM

apart. For long term studies with a 6 week time point in which lesion volume analysis was performed, every 5th section was mounted onto a slide. Ten slide series were collected with adjacent sections on a slide separated by 1000 μM.

5.2.10 Immunohistochemistry and Fluorescent Imaging

Antibodies used for fluorescent imaging and co-localization studies included rabbit anti-tGFP (0.13μg/mL, Evrogen # Ab513), mouse anti-RECA1 (5μg/mL, abcam # ab9774), mouse anti-GFAP (2μg/mL, abcam # ab10062), mouse anti-CC1 (0.5μg/mL, Cal Biochem #OP80), mouse anti-NeuN (5μg/mL, Millipore # MAB377), mouse anti-Ox42 (5μg/mL, abcam # ab78457), phosphor-PDGF Receptor β (5uL/mL Cell Signaling mAb #3166), goat anti-rabbit 488 (4μg/mL, Invitrogen # A11008), goat anti-mouse Biotin (7.5μg/mL, Vector # BA-9200), and Streptavidin Texas red (3.3μg/mL, Vector # SA-5006). Images were obtained using Nikon Eclipse Ti Confocal microscope and NIS elements software (Nikon Instruments).

5.2.11 Quantification of tGFP Volume and Spread Over Time

A set of tissue section slides for each time point were used to analyze the tGFP mitochondria volume and spread over time after injection. Anti-tGFP antibody was used to label injected mitochondria, as described above. Each spinal tissue section was then analyzed under the Nikon confocal microscope for the presence of distinct tGFP labeling. When a discreet tGFP injection bolus was present, ND2 software was used to measure the area of the bolus. Each of the four injection epicenters per spinal cord was verified by finding the largest area of discreet bolus. Every section both rostral and caudal of the injection epicenter that contained a discreet tGFP bolus was measured for bolus area. After defining the boundaries of the injection bolus, the tissue thickness and periodicity of the sectioning paradigm was used to calculate the total bolus volume of each cord that included all four injections. The rostral-caudal length through the cord that punctate tGFP labeling was evident, regardless of an apparent discreet injection bolus, was also calculated.

5.2.12 Quantification of Brain Macrophage Response

For the 24 hour, 48 hour, and 7 day animal cohorts, we analyzed the macrophage density at each injection epicenter. Once the injection site was located, a score of 0-3 was assigned for each injection epicenter. 0 indicates no abnormal density in macrophages, similar to staining evident in naïve tissues. A score of 1 indicated there was some increased infiltration/activation of brain macrophages. This included a change in morphology of the macrophages from the inactivated state with long cellular processes to an activated state in which processes were withdrawn and the shape of the macrophage was larger and more spherical. A score of 2 represented an increase in activated brain macrophages within the confines of the injection site, usually within a dense bolus. 3 was the highest score, and represented an injection site in which there was a brain macrophage response with a high density that exceeded the original injection bolus size.

5.2.13 Cell-type Co-localization Over Time

Cell-type co-localization of tGFP mitochondria was quantified for different cell types in the 24 and 48 hours and 7 day cords. Separate sets of slides were labeled for either microglia, endothelial cells, oligodendrocytes, astrocytes, pericytes or neurons, and co-labeled with antibodies against tGFP as described above in **5.2.11**. Eight sections total per spinal cord were quantified using the left side injections of each spinal cord including the injection epicenter, one section (400um) from the injection epicenter towards the injury, one section (400um) from the injection epicenter away from the injury site, and the first section away from the injection epicenter that no longer contained a visible bolus (see **Figure 5.8A** for counting schematic). The region of interest counted for each section was the left dorsal quadrant of the cord, drawing a vertical line from the central canal to the dorsal surface, and a horizontal line from the central canal to the lateral surface (see **Figure 5.8B** for depiction of ROI). Slides were visualized under an Olympus BX51 microscope at 100X magnification (10x eye piece) using a FITC/TRITC combination filter to simultaneously visualize the green and red

channels. Positive co-localization was defined by the yellow overlap of signal, or the green punctate signal contained within the cell membrane of the cell-type marker. Cells were verified using the DAPI filter to ensure that the nucleus was within the focal plane. Counts were performed within the ROI of a total of 8 spinal cord sections of each animal for 1) each time a specific cell was co-localized with the tGFP signal and 2) total cell counts for the specific cell type. Quantification of co-localization was reported as a percentage of the total number of a specific cell type within the ROI divided by the number of that specific cell type within the ROI that also stained positive for tGFP.

5.2.14 Tissue Sparing Analyses

Tissue sections were stained for eriochrome cyanine-cresyl violet (ECCV) to differentiate white matter and gray matter as previously described (Rabchevsky et al 2002, Rabchevsky et al 2001). Sections were imaged using a Nikon microscope (Nikon Corporation, Tokyo,Japan) and Scion Imaging analysis software (Scion Corporation, Frederick,MD, USA) was used to delineate injured versus spared tissue in each section. ROIs were manually drawn around the entire cord, spared gray matter, and injured tissue which allowed extrapolation of the spared white matter area. Eleven sections equally spaced apart by 1000 μm and centered on the injury epicenter were analyzed to get the volume of damaged versus spared tissue using the Cavalieri method (Michel & Cruz-Orive 1988).

5.2.15 Stereology

Analysis was performed to determine sparing of the neurons in the medial portion of lamina VII and lamina X of the L1/L2 spinal cord in the 6 week injured cohorts. Stereological counts of neurons were performed using a method previously published (Patel et al 2012). We used an Olympus BX51 microscope to image sections and the Bioquant image analysis program to analyze our tissues (Nova Prime, V6.70.10, Bioquant Image Analysis Corp., Nashville, TN). Briefly, a region of interest was drawn over lamina VII and X, containing putative

CPG interneurons. A counting grid was placed over this region, with each counting frame measuring 125 X 125 μm. Disectors were set to 50 X 50 μm, and section thickness was set at 10μm, with a 2μm guard zone on both the top and bottom of the tissue to keep from double-counting cells across sections. NeuN positive cells were then counted under 40X magnification (10x eyepiece). The criteria for being counted required the neuron cell body to be contained within the disector and the nucleus was in focus within the set 10μm counting thickness, as verified by Hoechst staining (Hou et al 2008). The coefficient of error (CE) was calculated for each group (vehicle- 0.116, tGFP mitochondria- 0.1126, and muscle mitochondria – 0.1456) to determine intra-animal variation. The inter-animal variation, or coefficient of variance (CV), was also calculated (vehicle- 0.7007, tGFP mitochondria- 0.6506, and muscle mitochondria- 0.5145). The number of neurons in each section was extrapolated using a previously published equation (McCullers et al 2002).

5.2.16 Statistical Analyses

Changes in OCR and RCR for acute bioenergetic studies were analyzed using a one-way ANOVA for each respiration state or RCR, with Tukey's multiple comparisons post hoc test. Complex I functional assays, injected tGFP bolus volume and rostral-caudal length, and tissue sparing analyses were analyzed using one-way ANOVA with Tukey's multiple comparisons test when appropriate. Cell type incorporation was analyzed using a one-way ANOVA for each cell type, number of co-localization instances, and for percentage co-localization within each time point, with Tukey's multiple comparison test. Brain macrophage density analyses were performed using Mann-Whitney U test for each time point analyzed. Rostral-caudal location of cell-type colocalization, von Frey tests, BBB scoring and neuronal stereology counts were analyzed using a repeated measures two-way ANOVA with Tukey's multiple comparisons when warranted. All analyses were carried out using Graphpad Prism 6 (Graphpad Software, Inc., La Jolla, CA). Significance was set to $p < 0.05$.

5.3 Results

5.3.1 Acute Mitochondrial Bioenergetics

We transplanted mitochondria into the injured spinal cord in a dose-dependent manner. Vehicle or one of three dosages of transgenically-labeled tGFP-mitochondria were microinjected into the injured spinal cord at 50, 100, or 150 µg and 24 hours later the spinal cord was dissected and assessed for mitochondrial bioenergetics. Mitochondria isolated from this portion of spinal cord includes both endogenous mitochondria and exogenous transplanted mitochondria. When assayed for mitochondrial bioenergetics in terms of OCR, there were significant differences in state III [F (4, 27) = 6.269, P= .0011] and state V.1 [F (4, 27) = 11.80, P= <0.0001] respiration. Post hoc analyses indicated significantly maintained state III (89% of sham) and state V.I (73% of sham) OCR in the 100µg tGFP-injected group compared to significantly impaired rates in vehicle injected groups (**Figure 5.1**). There were no significant differences in RCR among tGFP mitochondria injected, vehicle injected, or sham laminectomy animals indicating that mitochondria in each group are well-coupled.

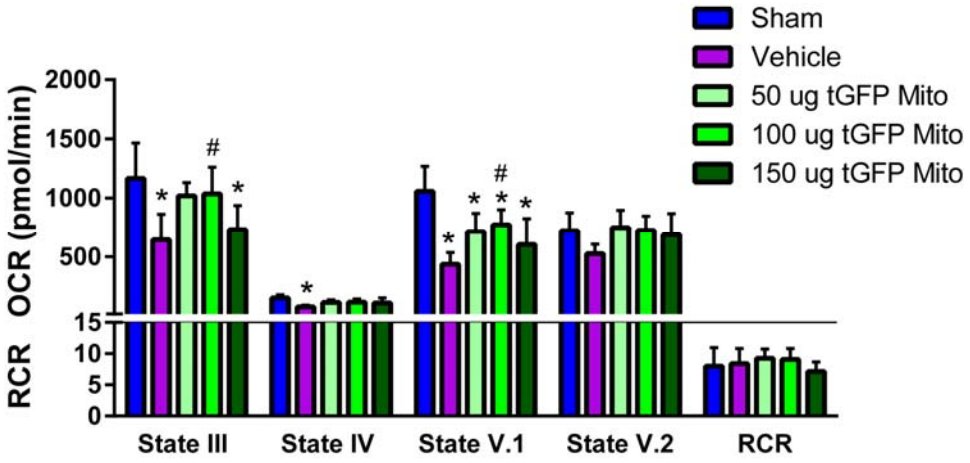

Figure 5.1. Culture-derived tGFP mitochondrial transplantation after SCI maintains OCR. SCI caused significant decreases in mitochondrial respiration at state III, IV, and V.1, which was partially maintained with mitochondrial transplantation. State III and V.1 OCR were maintained near sham levels after 100µg tGFP mitochondrial transplantation. Bars are means ± SEM. *p<0.05 vs

Sham; #p<0.05 vs Vehicle. (One-way ANOVA for each state, Tukey's multiple comparison) n=6-7/group.

The use of tGFP-labeled mitochondria allows for visualization and tracking of transplanted mitochondria *in situ*, which is important for determining cell-type incorporation and temporal uptake of exogenous mitochondria. However, cultured cells can have a lower energy demand, resulting in mitochondria that are well coupled but respire at lower rates (see **Chapter 4.3.4**). We were concerned that these lower respiring mitochondria may not have enough energy producing capability to be optimally beneficial to the injured cord, so we also tested the injection of muscle-derived mitochondria. We chose to inject muscle mitochondria at the 100 µg dosage to compare to the optimal dosage found in our tGFP mitochondrial transplant study (see **Figure 5.1**). Further, we hypothesized that because muscle mitochondria respire at higher rates than tGFP mitochondria, a lower dosage of 50 µg muscle mitochondria could possibly give the same OCR increases as tGFP mitochondria.

Muscle mitochondria were isolated from the soleus muscle of a separate naïve rat and injected into the injured spinal cord. Following transplantation, we found significant differences in state III OCR [$F(3, 8) = 12.23$, $P= 0.0023$] and post hoc analyses revealed significant increases with either 50 µg (83% of sham levels) or 100 µg (88% sham levels) mitochondria injection compared to vehicle injected groups (**Figure 5.2**). There were also significant differences in state IV [$F(3, 8) = 8.940$, $P= 0.0062$] and state V.1 respiration [$F(3, 8) = 12.64$, $P= 0.0021$]. Post hoc analyses showed significantly increased state IV OCR with 100 µg muscle mitochondria compared to vehicle and significant decreases in state V.1 respiration after injury compared to sham levels which was not rescued through mitochondrial transplantation. There were no significant differences in RCR among muscle injected, vehicle injected, or sham laminectomy animals indicating that the mitochondria in each group are well coupled.

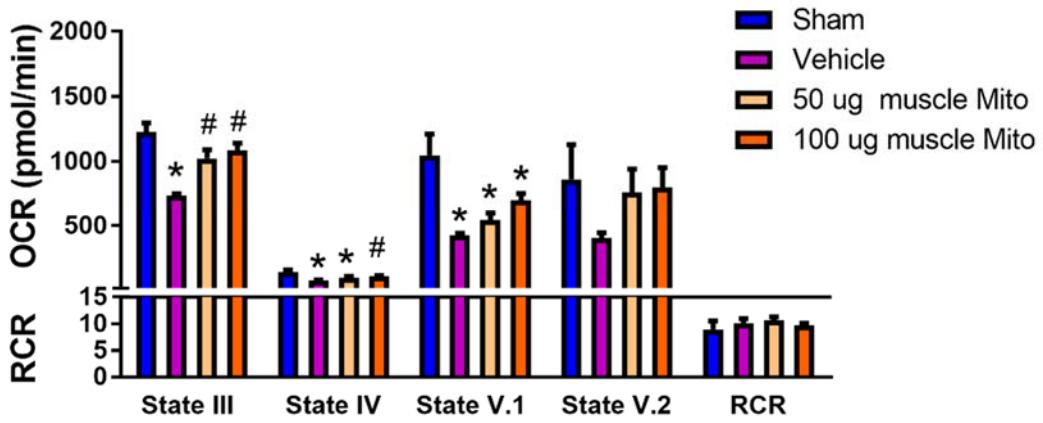

Figure 5.2. Muscle-derived mitochondrial transplantation after SCI maintains OCR. State III and IV OCR were maintained with 100 µg muscle-derived mitochondrial transplantation. State V.1 OCR deficits after injury were not rescued with transplantation. Bars are means ± SEM. *p<0.05 vs Sham; #p<0.05 vs Vehicle. (one-way ANOVA for each state, Tukey's multiple comparison). n=2-4/group in triplicate.

Using isolated mitochondrial samples obtained from the same animal cohorts used in acute OCR studies we assessed the function of complex I, the NADH Coenzyme Q oxidoreductase enzyme of the ETS (**Figure 5.3**).

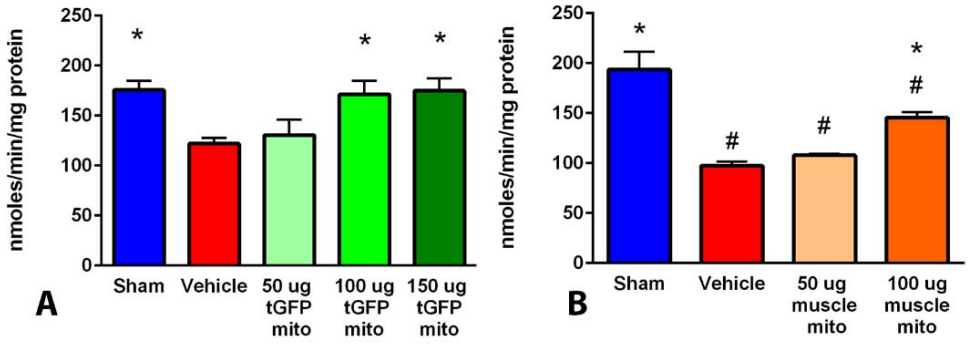

Figure 5.3. Complex I function following SCI and mitochondrial transplantation. Using the same mitochondrial samples used in OCR studies, we analyzed the function of mitochondrial ETC complex I. **A**. Complex I function was maintained near sham levels with 100 µg and 150 µg tGFP mitochondria compared to vehicle injection. n= 6-7/group. **B**. Complex I function significantly

increases after 100 µg muscle mitochondria transplantation compared to vehicle injections. n= 2-4/group. Bars are means ± SEM. #p<0.05 vs Sham Laminectomy; *p<0.05 vs Vehicle. (One-way ANOVA, Tukey's multiple comparison).

Mitochondrial transplantation maintained complex I function near sham levels. Similar to our OCR outcome measures, there were significant differences in complex I function in tGFP mitochondria injected experiments [F (4, 26) = 5.432, P= 0.0026] and muscle mitochondria injected experiments [F (3, 9) = 21.51, P= 0.0002]. Post hoc analyses showed that transplantation of 100 µg tGFP or muscle mitochondrial significantly maintains complex I function compared to vehicle. Interestingly, 150 µg tGFP mitochondria also significantly increased complex I function, though it did not significantly increase state III OCR compared to vehicle.

Our results show the state III OCR of the 100 µg mitochondria injected animals of either mitochondrial origin was comparable to sham indicating rescue of oxidative phosphorylation function in the injured spinal cord to almost 90% of sham levels. We have shown historically that maintaining state III respiration towards sham levels corresponds to maintained long term behavioral recovery (Patel et al 2012). Thus, we chose to use the 100 µg dosage to investigate the effects of mitochondrial transplantation on both cell-type incorporation and long term recovery.

5.3.2 Characterization of Transplanted tGFP Mitochondria in situ

We characterized the uptake of exogenous tGFP mitochondria into resident cells of the injured spinal cord. Analysis of multiple time points after injury gave a time course picture of exogenous mitochondrial incorporation within tissues after 24 hours, 48 hours, and 7 days post injection. Injection sites contained a bolus at the injection epicenter, with scattered punctate labeling further from the injection site (**Figure 5.4A**). Earlier time points had a very discreet injection bolus (**Figure 5.4B,C**) in addition to scattered punctate tGFP

mitochondria (**Figure 5.4D**) within the cord. By the 7 day time point, these discreet injection boluses had almost completely disappeared, save for a few instances, and only dispersed tGFP mitochondrial stippling was present. We analyzed the spread of 100 µg dosage injected tGFP mitochondria in two ways. The first was a measure of the rostral-caudal distribution of all 4 injection boluses. There were significant differences in bolus length among time points [$F(2, 9) = 22.46$, $P= 0.0003$] (**Figure 5.4E**); post hoc analyses revealed a significant decrease in bolus length of the 7 day group compared to 24 and 48 hour time points. The measured length of the bolus had insignificantly increased length in the 48 hour group compared to 24 hour group. We further measured the rostral-caudal length that instances of punctate mitochondria were visible, and found that there were no significant differences among groups [$F(2, 9) = 2.996$, $P=0.1006$] (**Figure 5.4F**). Interestingly, this may indicate that tGFP mitochondrial dispersal is quite uniform across time points, and the bolus disappears at a different rate than the punctate instances of tGFP mitochondria. The second analysis was a measure of total volume of the injection boluses throughout the spinal cord (**Figure 5.4G**). The tGFP mitochondria injection bolus volume was significantly different among time points [$F(2, 9) = 15.61$, $P= 0.0012$]; post hoc analysis indicated the volume was similar for 24 hour and 48 hour time points but was significantly different at the 7 day time point.

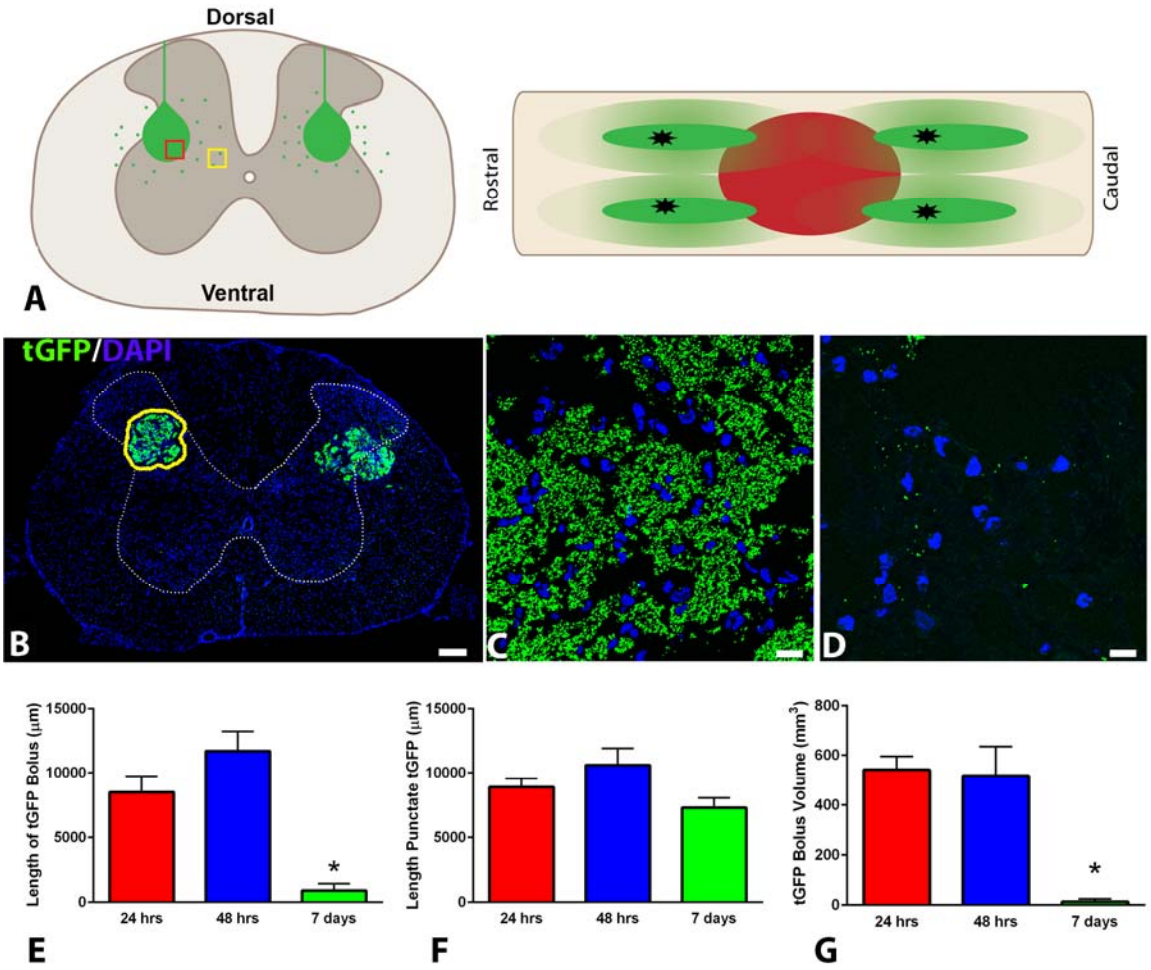

Figure 5.4. Quantification of transplanted tGFP mitochondria volume and spread. A. Injection schematics depicting bilateral injections into the spinal cord. Cross section shows a portion of the injection bolus is boxed in red, and representation of the punctate area analyzed is boxed in yellow. Longitudinal section indicates four peri-contusion injection sites (black stars) with injection bolus as solid green oval. Punctate tGFP labeling is represented by the shaded green oval. **B.** Representative image of bilateral tGFP injections. For volumetric measurements, the discreet bolus was circled (yellow) to give an area for each section which was used to calculate the subvolume of each section measured. **C.** High magnification image of tGFP located within the bolus of (B) as delineated in red box in (A). **D**. High magnification image of punctate tGFP-labeled mitochondria in (B) that were not part of the discreet bolus, as delineated in yellow box in (A). **E.** Rostral-caudal length of tGFP bolus was significantly

decreased at 7 days compared to 24 hour and 48 hour groups. **F.** Length in the rostral-caudal direction that any visible evidence of punctate mitochondria was apparent. **G**. Analysis of bolus volume was achieved by measuring the area of each bolus (circled in yellow in image B) and multiplying the subvolume by the total thickness of all sections with a bolus present to get total volume of bolus/cord. tGFP injection bolus was similar at the 24 and 48 hour time points, and significantly decreased at 7 days post injection. Scale Bars- B= 200μm, C and D =10μm. Bars are means ± SEM. *p<0.05 vs 24 hrs; #p<0.05 vs 48 hrs. (One-way ANOVA, Tukey's multiple comparison) n=4/group.

All of the tGFP injection sites (4/animal) for the 24 and 48 hour groups were visible using fluorescent microscopy. By 7 days post injection, the injection sites had almost disappeared so that only 3 total injections across all four animals in the group could be visually verified. Some instances of a remaining injection bolus were still evident and the rostral-caudal spread of punctate tGFP stippling was similar to 24 and 48 hour time points.

We set out to characterize the cell-type co-localization with tGFP mitochondria. We looked at multiple different resident spinal cord cell types when performing our analyses, including neurons, macrophages, endothelial cells, astrocytes, pericytes, and oligodendrocytes (**Figure 5.5**).

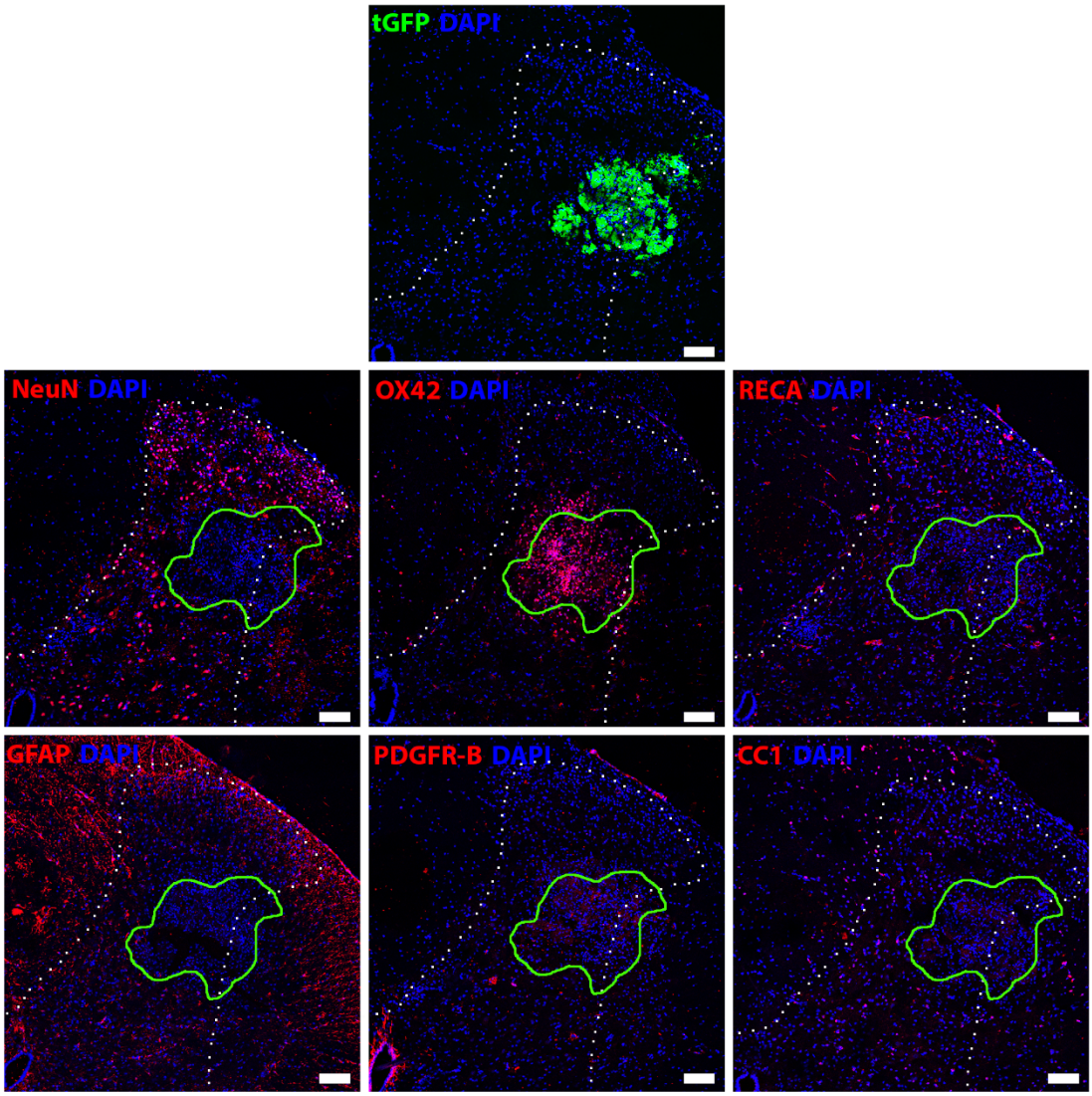

Figure 5.5. Resident cell types of the spinal cord within the tGFP mitochondria injection bolus. The top box shows an injection bolus into the dorsal horn of the spinal cord at 24 hours post injection. Adjacent slide series (separated by 40uM) were stained with specific cell type markers and images represent different cell types within the same injection site. Green lines delineate the margins of the injection bolus, the white dotted lines outline the dorsal horn gray matter. Within the injection bolus, there appeared to be a loss of neurons and oligodendrocytes. There was a noticeably increased density of brain macrophages in the area of the injection bolus. Additionally, there were endothelial cells and pericytes evident within the injection bolus. While there

were not astrocytes within the bolus, they were prevalent in the area surrounding the injection. NeuN= neurons, OX42 = macrophages, RECA = endothelial cells, GFAP = astrocytes, PDGFR-B= pericytes, CC1 = oligodendrocytes, tGFP = exogenous tGFP mitochondria, DAPI = cell nucleus. Scale bars= 100um.

When examining the different cell types within the injection epicenter bolus, we noted an almost complete absence of neurons within the bolus, while there was an influx and high density of macrophages. The concentration of mitochondria or volume of the injections could be inherently damaging the spinal cord tissue. When comparing vehicle injected and tGFP mitochondria injected animals, we typically saw that there was increased density of brain macrophages at the mitochondria injection sites compared to vehicle (**Figure 5.6A**), indicating the tGFP mitochondria could be causing an inflammatory response more so than vehicle injection alone. Semi-quantitative analyses were performed to evaluate the brain macrophage densities within the injection epicenters at different time points (**Figure 5.6B**). Mann-Whitney U test showed a significant effect between vehicle injected and tGFP mitochondria injected groups at 24 hours [P= 0.0012], 48 hours [P= 0.0002], and 7 days post injection [P= 0.0196].

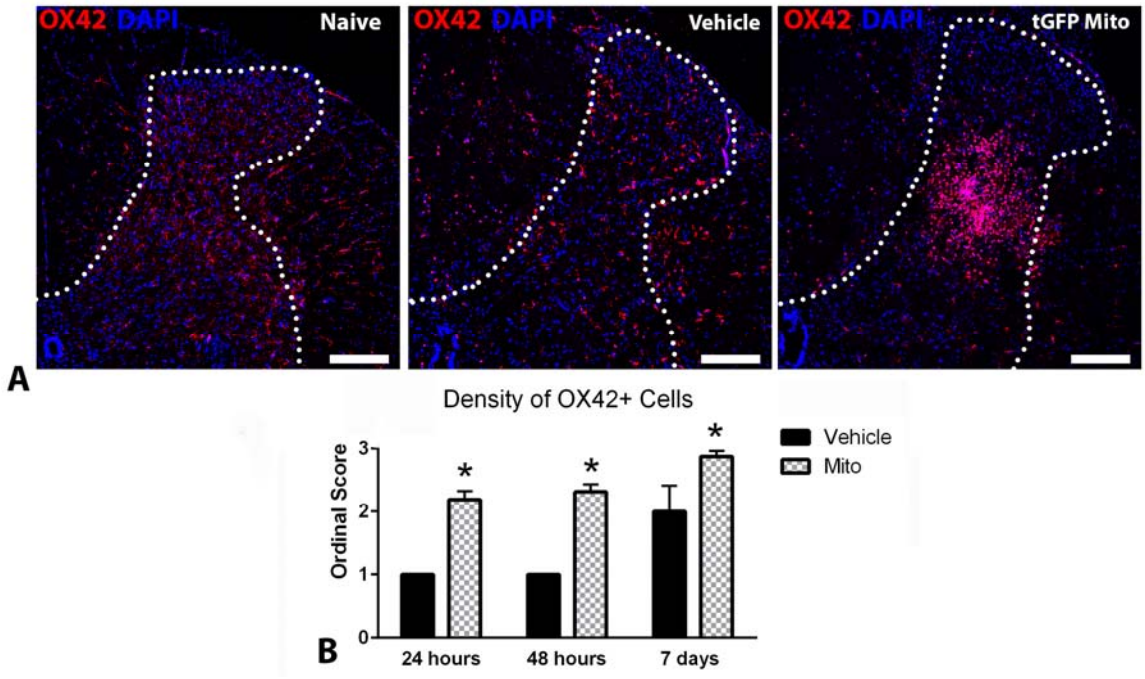

Figure 5.6. Brain macrophage activation at the mitochondria injection sites. **A.** Brain macrophage infiltration was compared between naïve, injured/vehicle injected, and injured/tGFP mitochondria injected animals at 24 hours post injection. There is an obvious high density of brain macrophages within the tGFP injection site compared to a vehicle injection site. **B**. At each of the injection epicenters, the macrophage density was given a semi-quantitative score of 0-3. For 0, there was no abnormal response (similar to **A** naïve), while a score of 3 indicated extensive activation of brain macrophages. There was a significant increase in the macrophage response when tGFP mitochondria were injected compared to vehicle injections at all time points. Bars are for visual representation of means ± SEM. *$p<0.05$ vs vehicle; (Mann-Whitney U test for each time point) n=4 vehicle injection sites per time point, n=16 tGFP injection sites per time point. OX42 = macrophages, DAPI = cell nucleus. Scale bars= 200um.

One of our goals was to discern which cell types of the spinal cord had higher propensities to incorporating exogenous mitochondria, so we first characterized positive co-localization. Representative images show positive co-

localization of various cell types both away from and within the bolus of tGFP injection (**Figure 5.7**). The left column represents instances of co-localization within the dense tGFP bolus, while the right column represents instances of co-localization that were seen away from the bolus where only stippling was present. For our purposes, co-localization was defined in two different ways. The first criterion of positive incorporation was when tGFP labeling was present within the cytoplasm of the cell, as evident by green tGFP labeling within the confines of the red cell membrane marker juxtapositioned to the nucleus (DAPI). This was most often the case when using OX42 staining for macrophages, which labels the cell membrane of macrophages. The second criterion of positive incorporation was when the tGFP labeling was present and overlapped with the cell specific marker. GFAP labels the cytoplasm of astrocytes, thus both the incorporated tGFP signal and GFAP signal overlapped. If either of these definitions was met, this was counted as a positive instance of co-localization.

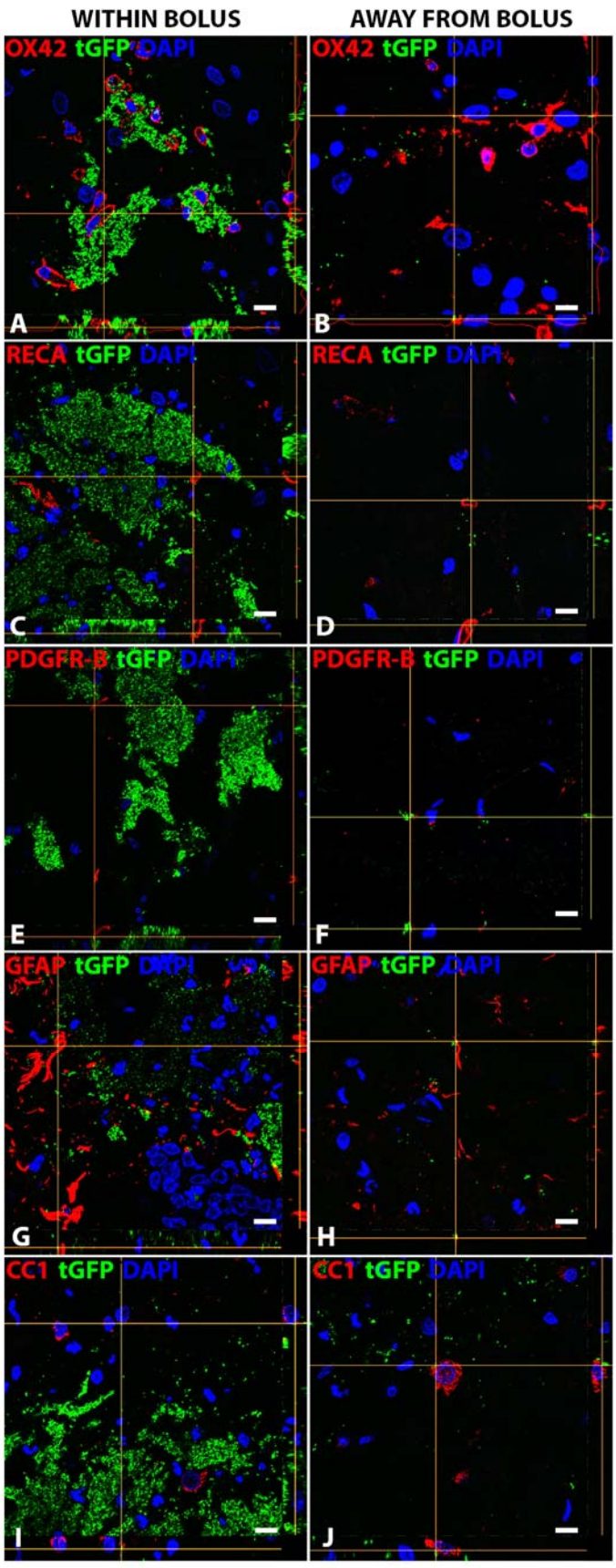
WITHIN BOLUS
AWAY FROM BOLUS
OX42 tGFP DAPI
A
OX42 tGFP DAPI
B
RECA tGFP DAPI
C
RECA tGFP DAPI
D
PDGFR-B tGFP DAPI
E
PDGFR-B tGFP DAPI
F
GFAP tGFP DAPI
G
GFAP tGFP DAPI
H
CC1 tGFP DAPI
I
CC1 tGFP DAPI
J

Figure 5.7. Representative images of cell type-specific tGFP co-localization. Images show instances of positive co-localization with different cell types at 24 hours post injury. Z-stack images were captured, with the bottom panel of each image representing the x plane and the right panel of each image representing the y plane. 'Within Bolus' (left column) indicates images that were taken in the area of dense tGFP mitochondria, while 'Away from Bolus' (right column) indicates images that were taken in areas of more sparse punctate tGFP mitochondria. Crosshairs in each picture are placed over an instance of tGFP colocalization with that specific cell type. OX42 = macrophages, RECA = endothelial cells, PDGFR-B= pericytes, GFAP = astrocytes, CC1 = oligodendrocytes, tGFP = exogenous tGFP mitochondria, DAPI = cell nucleus. Scale bars= 10um.

We found instances of cell-type specific colocalization with tGFP mitochondria for various cell types including brain macrophages, endothelial cells, pericytes, astrocytes, and oligodendrocytes at 24 hours post transplantation. Colocalization was evident for all cell types both within the injection bolus site as well as more distal from the injection epicenter, where sparse punctate tGFP was present. However, no colocalization of tGFP mitochondria within neurons was evident when we looked either within the bolus or distal to the bolus site. For better visualization purposes, representative high magnification images were taken to show instances of colocalization 24 hours after transplantation (**Figure 5.8**).

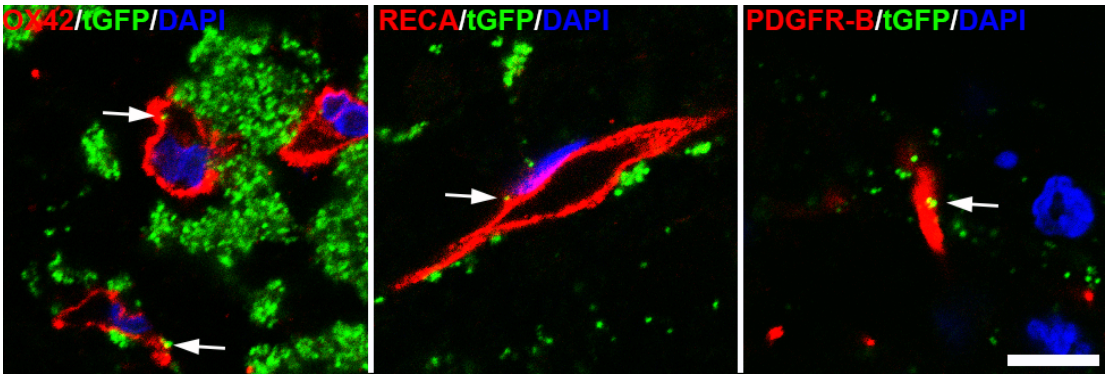

Figure 5.8. High magnification images showing positive colocalization. Images show instances of cell-type specific colocalization of tGFP mitochondria either macrophages (Ox42), endothelial cells (RECA), or pericytes (PDGFR-B). White arrows point to instances of tGFP mitochondria colocalization within the cell. Tissues were processed 24 hours post tGFP mitochondria transplantation. OX42 = macrophages, RECA = endothelial cells, PDGFR-B= pericytes, tGFP = exogenous tGFP mitochondria, DAPI = cell nucleus. Scale bar = 10um.

We quantified the propensity of tGFP mitochondria to be incorporated into different cell types across time. Tissue sections were analyzed per hemi cord as depicted in the schematic (**Figure 5.9A**) including the 2 injection epicenters, one section both rostral and caudal of the injection epicenters, and the first section distal to the injection epicenter that did not have a bolus present, but had punctate tGFP signal present. From each of these sections we quantified the percentage of a specific labeled cell type within the dorsolateral cross section ROI (**Figure 5.9B**) that were co-localized with tGFP mitochondria to compare their affinities for exogenous mitochondrial uptake.

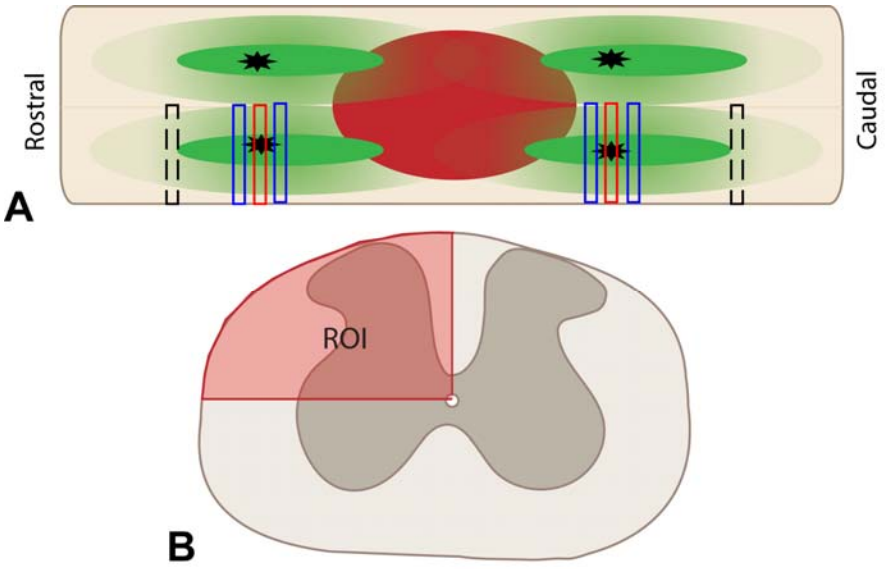

Figure 5.9. Counting schematic for cell-type co-localization with tGFP mitochondria. **A.** 8 sections were analyzed for the left side of each injected cord. This includes both injection epicenters (red box), the next section 400 um rostral and 400 um caudal of the injection epicenters (blue box), and the first section distal from the injection epicenter that no longer has an injection bolus but punctate tGFP mitochondria were present (dashed black box). Injection epicenters are denoted by the black stars, injection boluses are depicted as solid green ovals, and punctate tGFP stippling is represented by faded light green shading. We found the caudal injection sites to be closer to the injury epicenter than the rostral injections sites. This is due to the location of the T12 laminectomy, which reveals the L1/L2 spinal level at the caudal side of the laminectomy. The location of the injury epicenter is therefore at the caudal side of the laminectomy window, and closer to the subsequent caudal injection sites. **B.** For each section analyzed, the ROI for cell counts was defined by drawing a horizontal line from the central canal to the lateral side and a vertical line from the central canal to the dorsal surface (red). Both the total labeled specific cell types and instances of co-localization were counted within this left dorsolateral quadrant.

Comparisons were made to determine which cell type was overall more likely to incorporate mitochondria. The cell type counts for each of the 8 sections (analyzed as described in **Figure 5.9**) were summed to give a total number of that cell type per spinal cord (**Figure 5.10A**, red). Likewise, the co-localization instances from each of the 8 sections analyzed were totaled (**Figure 5.10A**, green). One-way ANOVAs were performed to evaluate differences among total cells counted of a specific type, and showed significant differences at 24 hours [$F(4, 15) = 72.59$, $P<0.0001$], 48 hours [$F(4, 15) = 87.46$, $P<0.0001$], and 7 days [$F(4, 15) = 37.32$, $P<0.0001$]. Post hoc analyses revealed that total macrophages counted were significantly higher than all other cell types at each time point. One-way ANOVA showed significant differences among the number of co-localized cells among cell types at 24 hours [$F(4, 15) = 10.62$, $P=0.0003$], 48 hours [$F(4, 15) = 45.55$, $P<0.0001$], and 7 days [$F(4, 15) = 5.159$, $P=0.0081$]. Post hoc analyses showed that co-localization numbers were significantly higher in macrophages than other cell types. It should be noted that brain macrophages infiltrate the injury site and therefore there is a higher number of total macrophages in the ROI compared to other cell types (**Figure 5.10A**). This potentially puts the macrophages at an optimal location for interactions with the tGFP mitochondria. Consequently, we additionally report the percentage of cells that are also co-localized with tGFP (**Figure 5.10B**). One-way ANOVA revealed significant differences among cell type co-localization percentages at 24 hours [$F(4, 15) = 6.384$, $P=0.0033$] and 48 hours [$F(4, 15) = 5.854$, $P=0.0048$]. Tukey's multiple comparisons showed both macrophages and pericytes co-localized with tGFP at a significantly higher rate than oligodendrocytes at 24 and 48 hours post injection, which had the lowest colocalization percentages at any time point. There was also colocalization of tGFP mitochondria with endothelial cells and astrocytes at each time point.

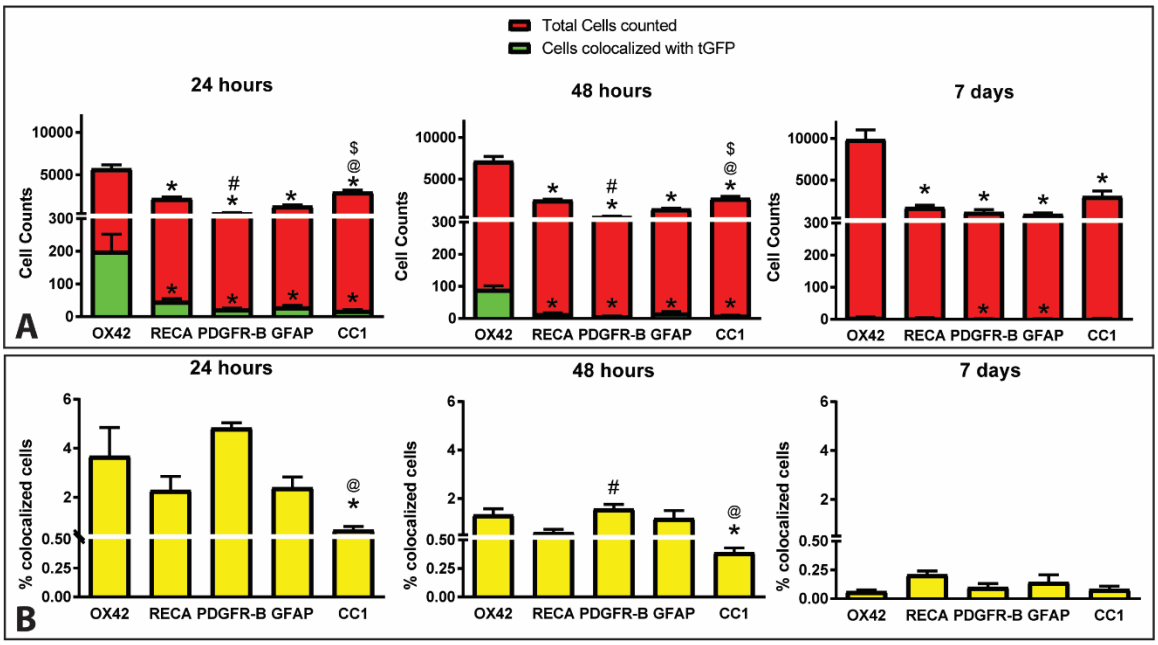

Figure 5.10. Cell-type co-localization of tGFP mitochondria across three time points. A. Cell type incorporation was compared for each cell type at a given time point. Total numbers of a given cell type were counted (red), as well as the number of cells co-localized with tGFP (green) per ROI. **B.** Co-localization was calculated as a percentage of total cells. Macrophages and pericytes had significantly higher co-localization percentages compared to oligodendrocytes at 24 and 48 hours. There were no differences in percentage of co-localization among the cell types at 7 days. OX42 = macrophages, RECA = endothelial cells, PDGFR-B= pericytes, GFAP = astrocytes, CC1 = oligodendrocytes, tGFP = exogenous tGFP mitochondria. *p<0.05 vs macrophages, # p<0.05 vs endothelial cells, @ p<0.05 vs pericytes, $ p<0.05 vs astrocytes; (One-way ANOVA, Tukey's multiple comparison) n=4/group. Bars are means ± SEM.

The differences in cell type incorporation may be due to the different endocytic and phagocytic properties of each cell type. Additionally, we did not see any evidence of incorporation in neurons, though there was evidence of uptake in all other cell types examined in the injury penumbra. In fact, there was a profound loss of neurons in the gray matter where the injection epicenter was located (**Figure 5.5**). This may be due to many factors, including the

mitochondrial concentration and volume of injection into this area. Disturbance of the tissue by the injection compounded by the activated brain macrophages may be responsible for neuronal death at the injection site. However, if other cell types in the injury penumbra can be rescued using mitochondrial transplantation, the injury environment may be more favorable for overall cell survival, including neurons. Macrophages can be either pro inflammatory or anti-inflammatory, and are responsible for phagocytosing debris and foreign substances as well as having a part in mediating immune response. Astrocytes are important support cells for neurons, help maintain the blood brain barrier, and carry out functions in ion homeostasis of the extracellular space. Oligodendrocytes play an imperative role in insulating axons to increase signal transmission efficiency. Endothelial cells supply blood and oxygen to tissues, and pericytes wrap around endothelial cells for contraction of vessels and regulation of blood flow. Each of these cell types have important functions in maintaining homeostasis within the spinal cord tissue, and salvaging these cells could be as beneficial for functional recovery as neuronal cell survival after SCI.

The injection epicenter contained a dense bolus of tGFP mitochondria, and based on the high concentration in this area it may be difficult for mitochondria to have access to various cells for incorporation. Alternatively, sections that are further from the injection epicenter showed dispersed tGFP mitochondria and may have differential uptake as higher concentrations of mitochondria have been shown to aggregate with less extensive distribution into nearby tissues (Chang et al 2013a). We therefore mapped the propensity of co-localization in relation to the injection epicenters where there is a higher possibility for aggregation. We quantified the cell-type incorporation, as described above, and analyzed this across the rostral-caudal distribution of the 8 sections analyzed for each spinal cord (**Figure 5.11**). Two-way ANOVAs were performed and showed differences in cell-type colocalization for macrophages [$F(2, 9) = 8.123$, $P = 0.0096$], endothelial cells [$F(2, 9) = 10.69$, $P = 0.0042$], oligodendrocytes [$F(2, 9) = 9.575$, $P = 0.0059$], astrocytes [$F(2, 9) = 22.54$, $P = 0.0003$], and pericytes [$F(2, 9) = 928.3$, $P < 0.0001$]. We found that there were

differences in colocalization percentages dependent upon the location in relation to the injection epicenter, especially at the 24 hour time point. At 24 hours, macrophages had higher incorporation percentages one section rostral of each injection site compared to the most caudal section analyzed. Endothelial cells had higher co-localization percentages closer to the injection epicenters compared to the distal sections. This indicates there could be spatial-dependent incorporation in addition to cell-type dependent incorporation.

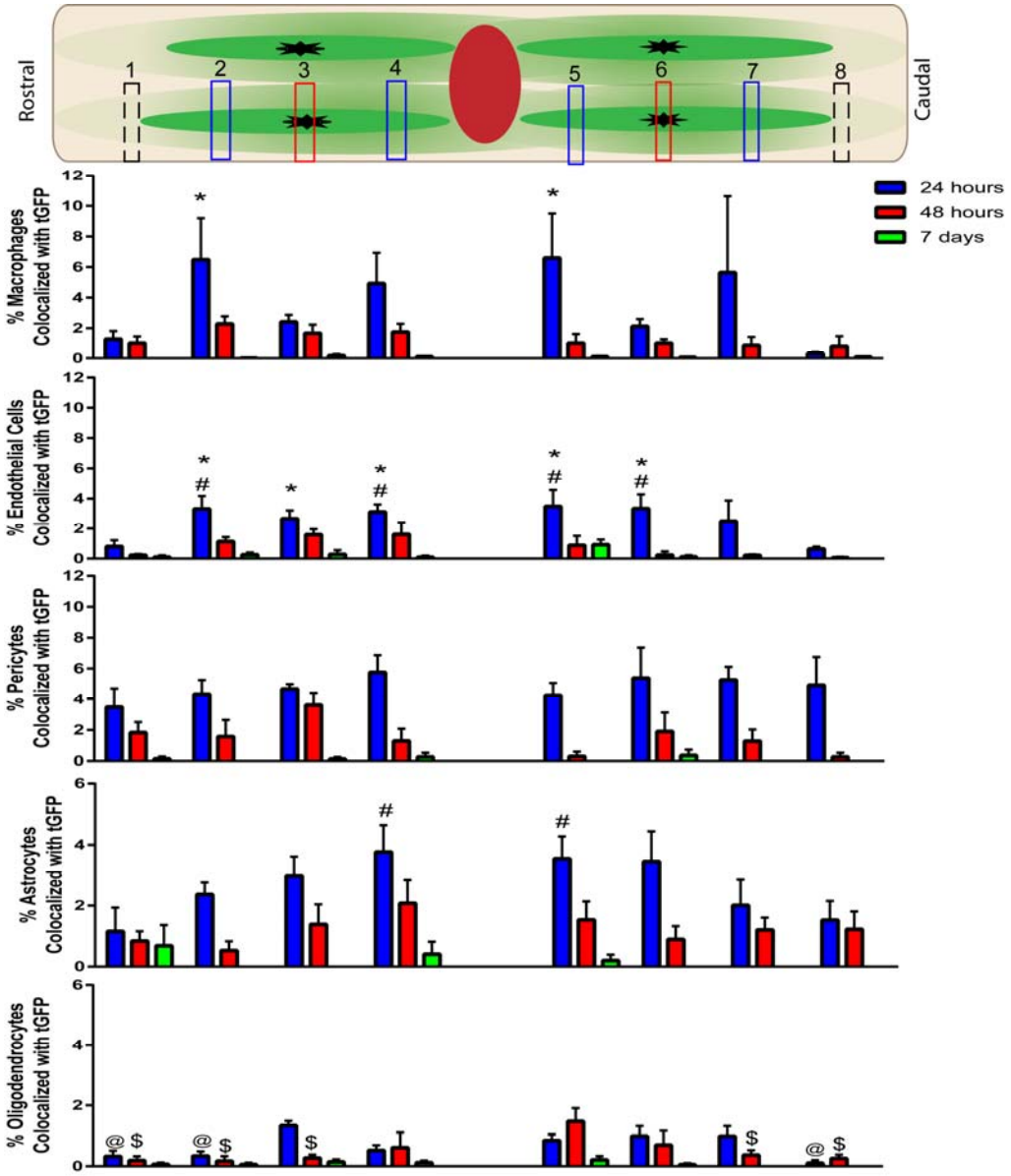

Figure 5.11. Rostral-caudal cell-type incorporation of tGFP mitochondria over time. Co-localization was quantified within ROIs across 8 different sections (numbered 1-8) in relation to injection epicenters. Top panel schematic of counted sections corresponds to the rostral-caudal counts of co-localization percentages. There were differences in colocalization percentages among location sites when analyzed within cell types. *p<0.05 vs section 8, #p<0.05 vs section 1, @p<0.05 vs section 3, $ p<0.05 vs section 5; (Two-way repeated measures ANOVA, Tukey's multiple comparison) n=4/group. Bars= mean ± SEM.

5.3.3 Behavioral Recovery and Tissue Sparing after Mitochondrial Transplantation

We tested the effects of mitochondrial transplantation after SCI on hindlimb functional recovery and tissue sparing. Anesthetized animals underwent a severe contusion injury at the L1/L2 spinal level, followed immediately by 4 injections for a total of 100 µg tGFP-labeled or muscle-derived mitochondria into the injury penumbra (see **Figure 3.1** for injection schematic).

The starting numbers per experimental group was n=12 per group. Throughout the course of the 6 week long study, there was an attrition of animals due to various causes. As animals were randomly assigned to groups, and we were blinded to the groups throughout the study, this resulted in uneven numbers per group at the terminal timepoint. 3 animals died from anesthesia during surgical procedures, 3 animals were removed from the study and euthanized due to extensive autophagia of the hindlimbs, and one animal was removed from the study due to its high 2-day BBB score (more than 2 SD from the mean, indicating a bad contusion injury). This resulted in final groups of Vehicle injection n= 10, tGFP mitochondria injection n=11, muscle mitochondria injection n=8.

Animals were tested for mechanical sensitivity of hindpaws using the von Frey hair test, and hindlimb motor recovery using the overground locomotor BBB scale. Results show that 3 weeks after injury, mechanical hypersensitivity was increased in each group, as filaments with less force elicited responses in the

hindpaws (**Figure 5.12**). At 6 weeks post injury, hindpaw sensitivity approached baseline levels in all groups, but was somewhat decreased in the mitochondria transplant groups. Two-way ANOVAs showed no differences among treatment groups [F (2, 26) = 1.370, P= P = 0.2718]. However, there were significant differences among time points [F (2, 52) = 17.64, P<0.0001]. Post hoc analyses showed each treatment group was significantly decreased at 3 weeks compared to their baseline levels. Vehicle injected animals scored closer to their baseline levels at 6 weeks, but both mitochondrial transplant groups were still more hypersensitive at 6 weeks compared to their baseline levels.

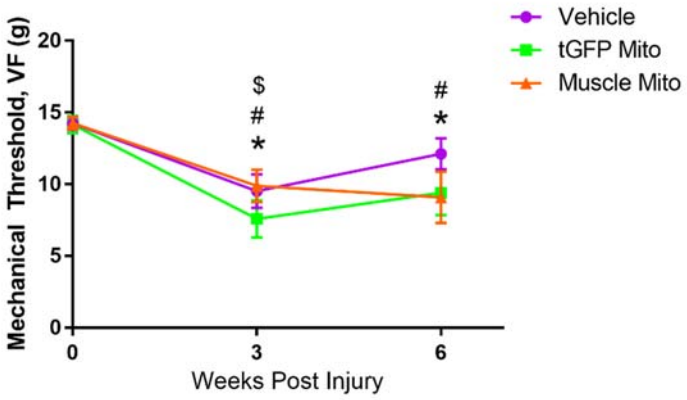

Figure 5.12. Mechanical hypersensitivity following SCI and mitochondrial transplantation. At three weeks post injury, each group had significantly decreased mechanical thresholds compared to baseline levels, though there were no differences among groups. At 6 weeks post injury, the vehicle injected and tGFP mitochondria injected animals began to return towards baseline levels, while the muscle mitochondria transplanted group remained significantly lower than baseline. Two-way ANOVA showed no significant treatment effect differences between groups at any given time point, though there were significant time-dependent differences across groups. Bars are means ± SEM. $ p<0.05 vehicle vs baseline vehicle; *p<0.05 tGFP mito vs baseline tGFP mito; #p<0.05 muscle mito vs baseline muscle mito (Two-way repeated measures ANOVA, Tukey's multiple comparison) n=8-11/group.

Two-way ANOVAs revealed that there were no significant differences in the BBB analysis among treatment groups [F (2, 26) = 0.01894, P = 0.9812] (**Figure 5.13A**). All animals recovered some functional recovery compared to scores at 2 day post injury, which is consistent with vehicle recovery scores we have reported with this injury type (Patel et al 2012). The BBB scale can be separated into three categories- the first third of the scale (score 0-7) evaluates movements of the three joints of the hindlimbs, the next part of the scale (score 8-13) evaluates stepping and coordination, and the highest part of the scale (14-21) evaluates fine movements of the paw during coordinated stepping. A score of 7 indicates extensive movements of all joints in the hindlimb, 8 indicates plantar placement of the hindpaw, and a score of 9 indicates the animal is beginning to make weight supported plantar placements of the paw or is stepping on the dorsal face of the hindpaw. A score of 10 indicates the animal is making weight supported plantar steps. The animals in these studies plateaued at an average score of ~8, which is indicative of plantar placing of the hindlimb that is not weight bearing (Basso et al 1995). This level of recovery correlates to historical data using this injury severity and spinal level, indicating there was no overt damage/ effect of volumes of injections. We further performed a post hoc analyses on the BBB scores that transforms the scale to make it more ordinal and translational (Ferguson et al 2004) and again found no differences among groups [F (2, 26) = 0.01319, P = 0.9869] (**Figure 5.13B**). It is important to note that while we did not see improvements in functional recovery with either type of mitochondrial transplantation, there was no loss of function.

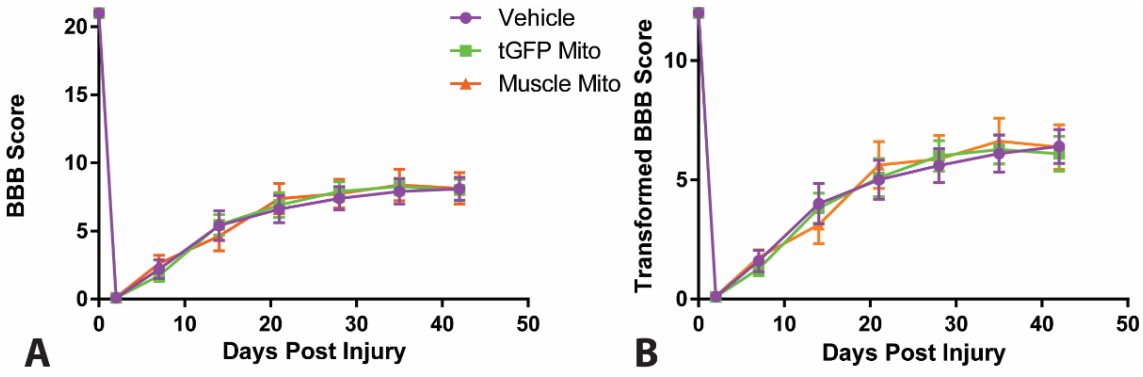

Figure 5.13. Functional hindlimb recovery following SCI and mitochondrial transplantation. A. BBB scores for all animals was decreased after SCI, with gradual increases over time after injury. **B.** Transformed scores of original BBB scores. There were no significant differences among animal groups at any time point using either analysis. Bars are means ± SEM. (Two-way ANOVA, Tukey's multiple comparison) n=8-11/group.

Following terminal behavioral analyses, animals were euthanized and spinal cords were processed for tissue sparing analysis. Total lesion volume, percent sparing at the injury epicenter, and gray and white matter sparing were similar between both treatment groups, supporting our behavioral findings (**Figure 5.14**). There were no significant differences between groups of lesion volume [F (2, 26) = 1.913, P=0.1679] (**Figure 5.14A**) or percent sparing at injury epicenter [F (2, 26) = 0.8532, P=0.4376] (**Figure 5.14B**). Mitochondria injections were targeted to the medial lateral gray matter, allowing for possible mitochondrial integration into either gray matter or white matter. We therefore compared tissue sparing of either gray or white matter volume to determine if transplanted mitochondria differentially spare different tissue types (**Figure 5.14C** and **D respectively**). Again, we saw no treatment effects among groups in either gray matter tissue sparing [F (2, 26) = 1.586, P=0.2240] or white matter tissue sparing [F (2, 26) = 0.03762, P=0.9631].

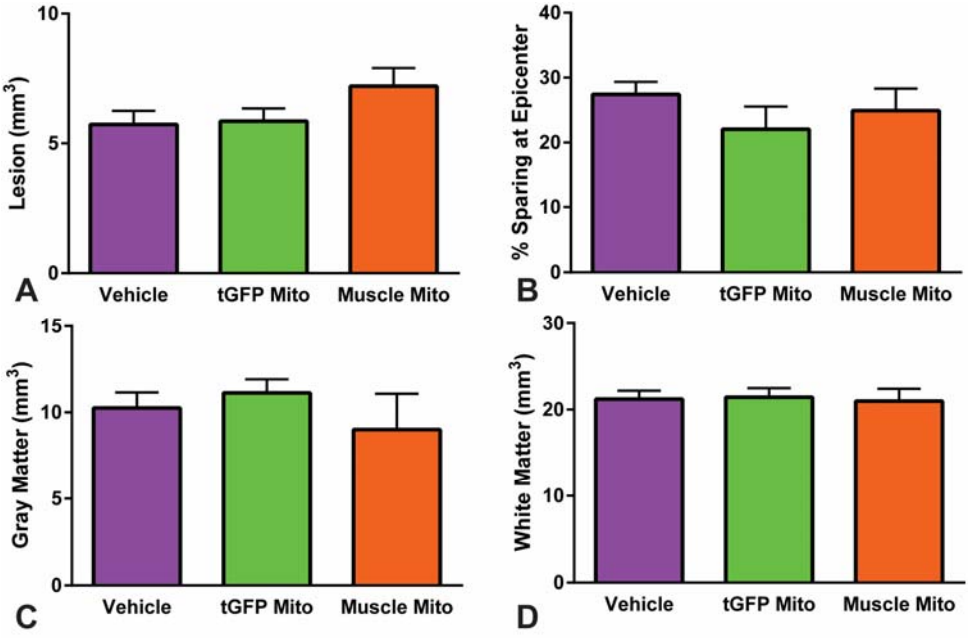

Figure 5.14. Tissue sparing analyses 6 weeks after injury and mitochondrial transplantation. Tissue sparing and lesion volumes were compared among vehicle, tGFP Mito injected, and Muscle Mito injected injured rats. At 6 weeks post injury and injection, total lesion volume and percentage sparing at the injury epicenter was assessed. Additionally, tissue sparing was analyzed for gray matter and for white matter to determine if there were tissue-type differences in sparing. There were no differences among groups in any of the measures assessed. Bars are means ± SEM. (One-way ANOVA, Tukey's multiple comparison) n=8-11/group.

There were no differences in tissue sparing among groups and this reflects what we might expect given the functional BBB scores after severe injury at L1/L2 (Magnuson et al 2005). We were also interested in determining if mitochondrial transplantation resulted in sparing of putative CPG interneurons, which represent only a portion of the gray matter sparing analyses. To more specifically investigate if mitochondrial transplantation salvaged these interneurons, we performed stereology of putative CPG neurons after injury and transplantation (**Figure 5.15**). We defined the ROI for neuronal counts to include lamina X and the central portion of lamina VII (**Figure 5.15A**).

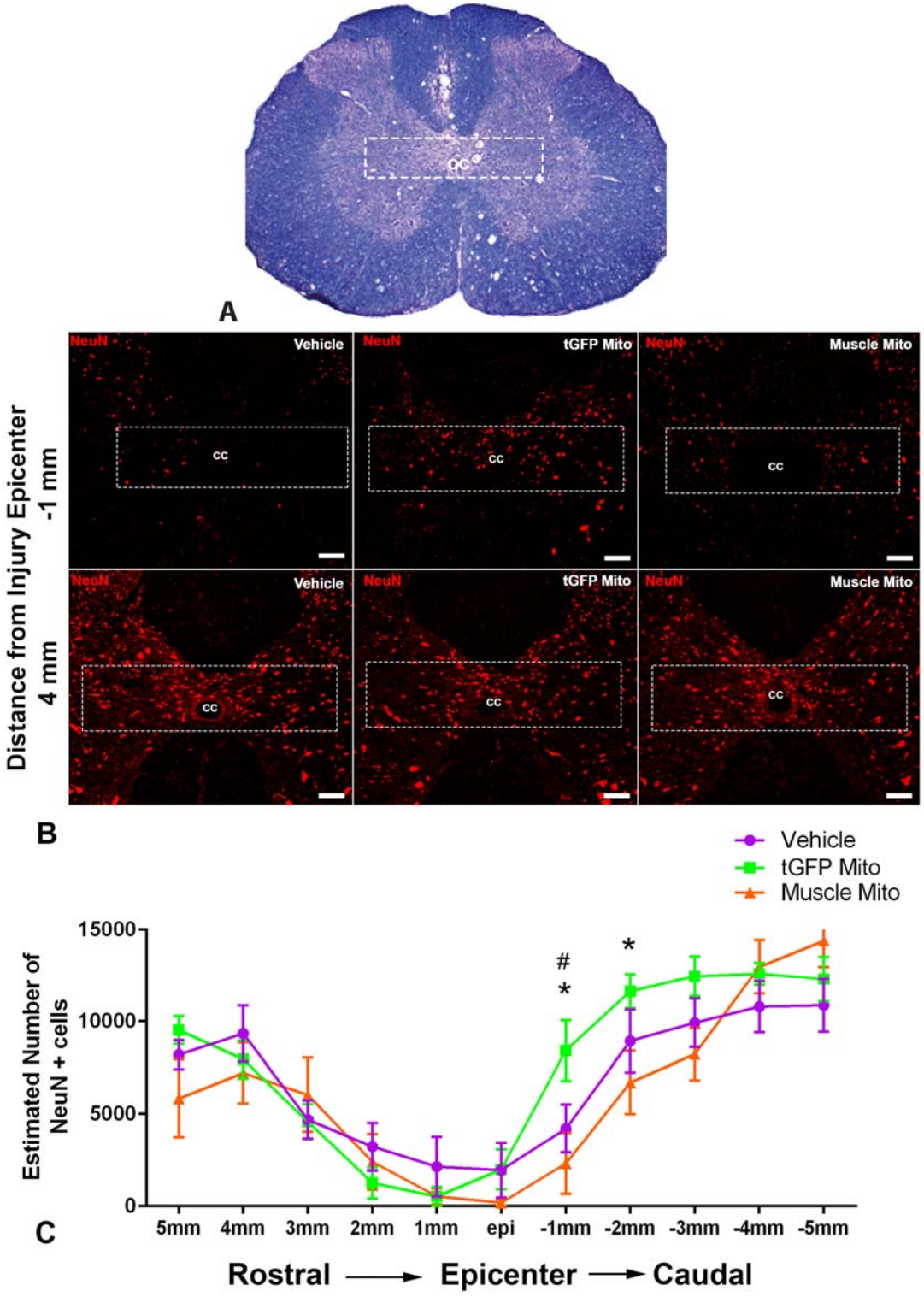

Figure 5.15. Neuronal counts in the upper lumbar spinal cord after injury. A. ECCV stained section of the spinal cord representing the ROI analyzed including Lamina X and part of Lamina VII, which include putative CPG neurons. **B.**

Representative images showing neurons in the ROI (dashed box) at 4mm rostral and -1mm caudal of the injury epicenter. There appeared to be more NeuN staining within the ROI of the mitochondria injected animals at 1mm caudal to the injury compared to either vehicle or muscle mitochondria injected groups. **C.** Stereological counts were performed across 11 equally spaced spinal cord sections, centered on the injury epicenter (epi). Each point on the graph is then an extrapolated estimate of the number of NeuN positive cells per 1mm length of spinal cord section analyzed. NeuN positive cells were significantly higher in tGFP mitochondria injected groups compared to the other cohorts at 1mm caudal of injury epicenter, and significantly higher in tGFP mitochondria groups compared to muscle mitochondria groups at 2 mm caudal of the injury epicenter. Bars are means ± SEM. cc= central canal. * $p<0.05$ tGFP mito vs muscle mito; # $p<0.05$ tGFP mito vs vehicle, (2-way ANOVA, Tukey's multiple comparison) n=8-11/group.

There were significant differences in neuronal sparing among groups [$F(2, 286) = 3.658$, $P=0.0270$]. Post hoc analyses showed that there were significantly more neurons in the ROI of tGFP mitochondria injected groups compared to vehicle or muscle mitochondria injected groups at 1 mm caudal of the injury epicenter. While there was more neuronal sparing at these regions, there was no corresponding functional recovery. This may be due to the fact that the putative CPG interneurons were not spared with mitochondrial treatment (**Figure 5.15C**, epicenter). Without these neurons there is a loss of rhythmic output to rhythmic elements which project on ventral motor neurons of the lumbar enlargement. If neuronal sparing of putative CPG interneurons had occurred rostral of the injury in the T13 spinal level, there may have been BBB improvements as was seen in previous publications (Magnuson et al 2005, Patel et al 2012). However, our studies showed neuronal sparing in levels caudal of the injury in the absence of putative CPG interneuron sparing. Our results are in agreement with Magnuson et al (2005) who showed that a kainic acid depletion

of putative CPGs in gray matter with concurrent caudal gray matter sparing did not result in improved BBB scores.

5.4 Discussion and Future Directions

We showed for the first time that mitochondrial transplantation into the injured spinal cord results in increased bioenergetics at 24 hours post transplantation using either cell culture-derived tGFP-labeled mitochondria or muscle-derived mitochondria. Cell culture derived mitochondria are optimal for post-transplant visualization; however, we have shown that these mitochondria respire at a lower rate than naïve spinal cord-derived mitochondria. To assess whether different sources of isolated mitochondria with inherent differences in respiration rates alter the effects of transplantation on acute bioenergetics, we compared culture derived to muscle derived mitochondria. When comparing the two sources of mitochondria on acute bioenergetics 24 hours after SCI, we found both to significantly maintain state III respiration at the 100 µg dosage compared to vehicle. As we have shown previously that maintaining state III respiration near sham levels corresponds to improved long term tissue sparing and functional recovery (Patel et al 2012), we used both sources of mitochondria at the 100 µg dosage to evaluate the effects of mitochondrial transplantation on long term histological and behavioral outcome measures.

We evaluated the time course of exogenous tGFP mitochondrial incorporation into host cells and saw evidence as early as 24 hours post injection. Discreet tGFP mitochondria boluses were evident, though these decreased significantly in volume and rostral-caudal spread by 7 days post injection, and completely disappeared by 6 weeks. By 7 days post injury, the injection sites were barely evident as the exogenous tGFP mitochondria had dissipated within the tissues. A discreet bolus injection was not always visible in the 7 day cohort, but instances of small, punctate tGFP signal were visualized and calculated to have similar rostral-caudal distribution to earlier time points.

We also evaluated the propensity of different cell types to incorporate exogenous mitochondria and found that brain macrophages and pericytes had

the highest propensity to colocalize with tGFP mitochondria, with lowest amount of incorporation into oligodendrocytes. We cannot at this time discern if the tGFP mitochondria were functionally incorporated within the macrophages or if they were phagocytosed. While mitochondria were incorporated into a variety of cell types, it is important to note that they were conspicuously absent in neurons.

When the same transplantation paradigm was used in long term studies, we did not see a restoration of functional recovery, tactile sensation, or tissue sparing. Von Frey testing showed a significantly decreased hindlimb mechanical sensitivity thresholds in each group after injury, with some recovery towards baseline at later stages. The vehicle injected group recovered closer to baseline (pre-injury) levels, which may indicate slight hypersensitivity in the transplantation groups. BBB hindlimb locomotor scores for each group showed functional loss 2 days after contusion SCI, with some recovery that plateaued at day 35 post injury. This is consistent with spontaneous recovery with this injury severity at the L1/L2 spinal level that we have reported (Patel et al 2012). Lesion volume analyses were consistent with the behavioral outcome measures showing no group differences between lesion volume or percent tissue sparing at the injury epicenter. We further analyzed sparing of the spinal cord white matter or the gray matter and again found no differences. Stereological counts showed significantly higher numbers of NeuN positive cells when tGFP mitochondria were injected compared to vehicle or muscle derived mitochondria, though this was only evident 1 to 2mm caudal to the injury epicenter. While these differences were significant, they were not so different that they resulted in changes in behavioral recovery. The injury was performed at the L1/L2 spinal level, whereas the neuronal sparing differences were seen more caudal. This spinal level may not contain the putative CPG interneurons, so functional locomotor differences may be more dependent upon ventral horn motor neurons at these spinal levels, which were not targeted by our mitochondrial injections. This data is intriguing as it shows that neuronal sparing may be possible through mitochondrial transplantation, though there may be a threshold of neuronal sparing needed to achieve measurable functional recovery. Additionally, caudal injection sites that

target the ventral motor neurons, in addition to the CPGs may provide more potential locomotor recovery. Potential means for increasing the efficiency of mitochondrial transplant are discussed in **Chapter 6**. Importantly, these findings show that acute bioenergetic recovery may not be the best criteria for advancing experiments to long term functional recovery in mitochondrial transplant paradigms. Instead, exploration of other markers of recovery at the acute time points of 24 and 48 hours that do correlate into functional hindlimb recovery is necessary. One such outcome measure could be tissue sparing analyses at more acute time points such as 48 hours and 7 days post injury. These would be expected to correlate to long term tissue sparing analyses.

Our findings indicate the feasibility of mitochondrial transplantation into injured tissue with restored acute bioenergetics. There are multiple caveats to consider when trying to interpret why our short term outcome measures did not correspond to long term functional outcome measures. First, we noted an increased density of brain macrophages in the injection and injury sites. The volume of vehicle or mitochondria injected may disturb the intact spinal cord tissue causing injury and subsequent infiltration of brain macrophages. Further, mitochondria are a source of DAMPS (see **Chapter 1.2.1.3**) that may elicit a stronger immune response compared to vehicle alone. Thus, mitochondria injection could cause an influx of macrophages, increasing the overall number of healthy cells in that area. The mitochondria assayed for bioenergetic analyses includes both endogenous host mitochondria as well as injected mitochondria. If macrophage infiltration resulted in a higher density of healthy cells, then mitochondria from these macrophages would also be included in our OCR assays. However, if there truly was an overt immune response, we would expect this to be reflected in our long term studies. There was no decrease in functional recovery when mitochondria were injected, which means if there was an immune response it did not exacerbate long term functional deficits.

There was evidence for more mitochondrial integration at shorter time points of 24 or 48 hours compared to 7 days post injury. If mitochondria are being taken into cells but not successfully incorporated as part of the endogenous

mitochondrial network, they may only exert beneficial effects at acute time points correlating to our OCR assays. As the exogenous mitochondria undergo mitophagy, a mitochondrial-specific form of autophagy, the OCR increases and benefits may disappear. This can be evaluated in future studies by measuring mitochondrial respiration at different time points after injury to determine exactly how long the improved bioenergetics effects are present.

There may be a possibility that mitochondria are exerting their effects extracellularly. The McCully lab noted functional benefits of cardiac tissue mechanics after ischemia/reperfusion injury was followed by direct mitochondrial injection (Masuzawa et al 2013, McCully et al 2009). Similar to our studies, they noted a low incorporation rate and theorized that the benefits seen could possibly be contributed by extracellular functions of the transplanted mitochondria. If mitochondria can function extracellularly, it can be hypothesized that this would be short lived before the immune response and debris-clearing mechanisms are enacted to remove the mitochondria. This may explain short-term effects in the absence of long term effects.

There are probably various reasons for the scarcity of tGFP label at 7 days and 6 weeks after injection- 1) It is likely that a certain amount of the injected mitochondria that are not taken into cells will be phagocytosed, especially at the injection site bolus as the density of mitochondria may be too high to be incorporated into the surrounding host cells; 2) tGFP mitochondria within the extracellular spaces will diffuse through the tissue away from the injection site with time, especially in the white matter where there is greater longitudinal diffusion; 3) When tGFP mitochondria are successfully incorporated within cells, they may fuse and divide with host cell mitochondria leading to a wider dispersal of fluorescent tGFP indicator within the cell. However, others reported evidence of fluorescently-labeled mitochondria at chronic time points. Using direct injection technique of mitochondria transplantation, one group showed the presence of exogenous mitochondria using fluorescent microscopy as late as 4 weeks after injection of human mitochondria into a porcine model of cardiac ischemia using an antibody against human mitochondria (Kaza et al

2016). Another group directly injected GFP-labeled mitochondria conjugated with the peptide carrier protein Pep-1 into the rat brain of a Parkinson's Disease model, and found instances of GFP as long as 12 weeks after injection (Chang et al 2013a).

While advances have been made in mitochondrial transplantation therapies, many caveats need to be addressed to make this therapeutic technique beneficial in models of SCI. Similar to previously published studies, we show that mitochondrial transplantation has beneficial short term effects. Increasing incorporation efficiency is the first step we can take to make our transplantation approach more successful in achieving our recovery goals after SCI. Alternative transplantation techniques for increasing incorporation rates or functionality of exogenous mitochondria are discussed in detail in **Chapter 6**.

CHAPTER 6

Overall Conclusions, Discussions, and Future Directions

6.1 Conclusions

We have learned much in our studies to aid in the progression of mitochondrial transplantation as a therapy after a rat model of SCI. We characterized transgenic labeling of mitochondria in culture to serve as a donor of exogenous mitochondria both *in vitro* and *in vivo* for easy visualization. We saw similar acute bioenergetic results *in vivo* when performing either allogeneic transplantation of transgenically-labeled mitochondria or syngeneic muscle-derived mitochondrial transplantation (**Figure 5.1 and 5.2**). This opens the possibility to transplant from either source depending on the needs of the study.

Transgenic mitochondria may serve an important purpose for tracking studies, while muscle mitochondria transplantation may have importance in dose response studies as higher mitochondrial yields can be obtained from muscle tissue and higher concentrations can be successfully injected after SCI. Tracking tGFP-labeled mitochondria incorporation into host tissues of the injured spinal cord showed integration into specific cell types occurred at different percentages. Discreet injection boluses were evident at 24 and 48 hours post injection, though they significantly decreased by 7 days and were completely gone by 6 weeks.

There was a cell-type dependent incorporation efficiency. At 24 and 48 hours post injection, macrophages and pericytes had the highest percentage of tGFP mitochondria incorporation (**Figure 5.10**). Macrophages may be taking mitochondria into their cytoplasm, but it is also possible that these tGFP mitochondria are in the process of being phagocytosed. Different measures can be taken to determine whether this is a functional incorporation, which are discussed in **section 6.3.5**. Pericytes are found within the vascular basement membrane and are closely associated with endothelial cells. They have many similarities to macrophages, including originating from the mesoderm, possessing lysosomes, similar cell surface markers, and prostaglandin secretion-

for review on CNS tissue pericytes (see (McCully et al 2017). Perhaps unsurprisingly then is that pericytes are also known to be inherently phagocytic which may explain their higher tendency to pick up exogenous mitochondria. Other cell types incorporated tGFP mitochondria, though at lower rates. Oligodendrocytes took in the least amount of mitochondria, though this could possibly be due to the location of the injection sites which were more targeted to the gray matter. Injections targeted to the white matter may give oligodendrocytes more opportunities for interacting with tGFP mitochondria, and thus possibly more incorporation. There was no evidence of tGFP incorporation within neurons at any time point.

There were no differences among treatment groups in lesion volume at the 6 week time point, and both gray matter and white matter tissue sparing were similar across the groups. Long term behavioral recovery was not apparent using our transplantation paradigm, though possible explanations and counteractive measures are presented later in this chapter. Some differences in neuron sparing in the CPGs were apparent, though this occurred caudal of the injury site and did not result in hindlimb recovery. Similar to our findings, changes in tissue bioenergetics, cell survival, and cellular mechanics have been reported in other studies, though it should be noted that few behavioral outcome measures have been either tested or reported after mitochondrial transplantation *in vivo* (Hayakawa et al 2016, Kaza et al 2016, Pacak et al 2015). However, one group has examined mitochondrial transplantation in a rat model of Parkinson's disease and saw significantly improved locomotion behavior (Chang et al 2013a, Chang et al 2016) see **Chapter 2.1.2** for details. Alternative approaches that may increase mitochondrial incorporation to promote further behavioral and functional recovery are discussed in detail later in this chapter.

6.2 Discussion

Great strides have been made in the field of mitochondrial replacement and transplantation therapies, and many techniques have proven to be beneficial, although there are still very important questions that must be

addressed before such therapies can be used widely and safely. There is discordance among labs as to the mechanisms of mitochondrial incorporation into host cells. While some argue that it may be endocytosis, others indicate the mechanism is much more complicated. Is the formation of nanotubes between cells necessary or is it the connection supplied by gap junctions or connexin pores? Are the connections seen *in vitro* formed *in vivo*? Some reported mitochondrial uptake upon co-incubation with cells *in vitro* (Clark & Shay 1982, Katrangi et al 2007) or into host cells after direct injection *in vivo* (Kaza et al 2016, McCully et al 2009), while others found no such incorporation after co-incubation *in vitro* (Spees et al 2006). One group showed conjugation of mitochondria with Pep-1, a cell penetrating peptide that increases incorporation, was necessary to incite mitochondrial uptake (Chang et al 2013a, Chang et al 2013b, Chang et al 2016). Still others found connexins or gap junctions necessary for cells to take in extracellular mitochondria (Islam et al 2012, Koyanagi et al 2005, Wang & Gerdes 2015). One group proposed an actin-dependent cellular incorporation of injected mitochondria (Pacak et al 2015). One possible incorporation method for these organelles could be massive endocytosis (MEND) (Lariccia et al 2011), which is a rapid internalization of large amounts of the plasma membrane. We found that coincubation alone *in vitro* was sufficient for mitochondria uptake into cultured cells. Similarly, we found direct injection of isolated mitochondria into spinal cord tissue *in vivo* results in uptake, though there is a relatively low incorporation rate (around 6% or lower of any specific cell type within the ROI analyzed, **Figure 5.10**). If the incorporation mechanism were revealed, then development of targeted techniques that take advantage of this mechanism could increase uptake efficiency into host cells. Further, it may be possible to exploit the uptake mechanism to specifically target certain cell types such as neurons so that they take in mitochondria at higher rates, which would be desirable in neuroprotection studies.

Whether there are major technical differences among the studies that contributed to conflicting results or if there are other confounding factors remains unclear. Contradictory findings may be due to various cell types having different

metabolic needs or capacities for endocytosis. Additionally, the type of damage to the host cells may be a crucial factor. Whether the cell undergoes stress, depleted mtDNA, or damage to the ETC may dictate whether the cell can endocytose mitochondria as multiple studies have reported that only compromised cells can take in exogenous mitochondria (Cho et al 2012, Katrangi et al 2007); still others have noted the incorporation in healthy cells (Clark & Shay 1982). We found that healthy cells in culture are capable of taking in mitochondria upon co-culture, and injured tissues *in vivo* can take in exogenous mitochondria resulting in maintained bioenergetics. Importantly, a seminal finding is that mitochondrial transplantation from healthy cells to injured neurons *in vivo* occurs naturally, which can be further enhanced by direct injection of exogenous mitochondrial particles into injured tissues (Hayakawa et al 2016). This innate ability of damaged neurons to incorporate extracellular mitochondria after traumatic injury may open a new avenue for neuroprotective strategies.

The origin of donated mitochondria may also be essential to uncovering optimal transplantation benefits. We delivered mitochondria from two different sources- cultured cells or muscle tissue, though isolating mitochondria from cell types commonly found in the spinal cord should also be compared. When targeting neuronal delivery, it may be better to use mitochondria from neurons, in the case that there are different inherent properties of mitochondria to be taken into like cell types. Astrocytes release mitochondrial particles into the extracellular matrix and are proven to be taken into neurons (Hayakawa et al 2016), as such we may also choose to utilize mitochondria from this source. Future studies may compare mitochondria isolated from neurons and astrocyte-derived mitochondrial particles in an effort to increase incorporation efficiency into spinal cord tissue with an emphasis on neuronal uptake. However, the McCully group noted that using different sources of mitochondria does not alter cardioprotection after transplantation (Kaza et al 2016, McCully et al 2009). Additionally, we observed maintained bioenergetics at 24 hours post transplantation of either cell culture- or leg muscle-derived mitochondria, so we may not see differences with neuronal mitochondria transplantation.

Furthermore, while neurons may be spared directly through targeted mitochondrial transplantation, it may be possible to protect neurons more indirectly by increasing the overall health of the injury environment. Sparing other resident cell types of the spinal cord could provide a more hospitable environment and decrease overall necrosis and apoptotic factors, thereby decreasing extracellular-induced damage to neurons.

6.3 Alternative Approaches and Future Directions

6.3.1 Mitochondrial Delivery Methods

We used direct injection techniques for mitochondrial delivery as others have shown it to be a feasible option (Chang et al 2013a, Masuzawa et al 2013, McCully et al 2009). Initial proposals considered cell-mediated delivery and liposome delivery methods as well. One pitfall of direct injection is that mitochondria are relatively unprotected from the extracellular matrix environment prior to cellular uptake compared to cell- or liposome- mediated delivery. As our early experiments showed increased OCR at 24 hours when using the direct injection method, this delivery method was used for the immunohistological and long term studies. However, we saw a higher density of macrophages with a concurrent loss of visible neurons in the injection epicenters that may be due to aggregation of the injected mitochondria. To counteract this possible damage, changing injection parameters to include more injections of lower volumes and concentrations may increase total numbers of mitochondrial incorporation into host cells. The same amount of mitochondria can be injected per spinal cord, though more spread out with potentially less aggregation. Increasing the number of injection sites could also allow for differentially targeted injections such as the CPGs at L1/L/2, and the ventral gray matter in more caudal regions. Additionally, based on our relatively low incorporation numbers and lack of behavioral recovery, other delivery methods should be investigated.

There are multiple methods that may be refined to increase incorporation after transplantation. Some have used cell-mediated delivery methods to donate mitochondria from transplanted cells into injured cells both *in vitro* (Cselenyak et

al 2010, Plotnikov et al 2008, Spees et al 2006) and *in vivo* (Islam et al 2012). Using cell-delivery systems would protect mitochondria from extracellular matrix molecules. However, the mechanism of transfer, whether it be nanotube formation, connexin pore mediated, or gap junctions needs to be better understood (**Chapter 2.4**). For instance, donor cells need to be chosen that are compatible with targeted cells to successfully make these types of functional connections. This may allow for targeted delivery to specific cell types, depending on the docking and delivery mechanisms of the donor and host cells.

Another delivery method to be considered is the encapsulation of mitochondria within liposomes. Liposomes have been used for targeted delivery to cells, though they have been used to carry small molecules such as RNA and not usually something as large as a mitochondrion organelle. Liposome delivery systems have been investigated to target macromolecules to the mitochondria (Weissig et al 2006, Yamada et al 2008, Yamada et al 2007). Modified liposomes with surface-linked polyethylene glycol and transactivating-transduction protein were delivered through caudal tail vein injections and found to cross the blood-spinal cord barrier to accumulate within cells at the injury site in a rat model of contusion SCI (Gollihue & Rabchevsky 2017). Though delivering intact mitochondria themselves to a cell is not widely published, liposomal delivery methods of mitochondria are being investigated (Brzezinska 2012). One consideration to make before pursuing this avenue of delivery is that liposomes may be digested by macrophages before they can fuse with targeted cells to deliver the mitochondria (see Ahsan et al 2002).

Vascular perfusion delivery methods of isolated mitochondria showed beneficial effects similar to using direct mitochondrial injections into injured heart tissue (Cowan et al 2016). This study used the coronary arteries to deliver mitochondria to ischemic heart tissue *in vivo*, eliminating the need for surgical implantation of isolated mitochondria. Cowan et al (2016) also noted that the mitochondrial incorporation efficiency was less when using perfusion delivery methods compared to direct injection into the heart tissue. To use a similar approach after SCI, one could perform intrathecal injections circumventing the

blood-spinal cord barrier to perfuse mitochondria over the pia of the injured spinal cord. However, this would not likely target mitochondrial delivery to neurons in the gray matter, but instead to resident cell types of the spinal white matter.

Concentrating isolated mitochondria for injections can result in aggregation, making cellular incorporation more difficult. If delivery efficiency can be increased, then lower concentrations may be injected with the same endpoint number of mitochondria being taken into cells. Pep-1 is a cell penetrating peptide that allows for fast translocation of peptides across lipid bilayers with a hydrophobic core (Henriques et al 2010). This fast transfer could mean that mitochondria will be exposed to the extracellular matrix for a shorter amount of time. In a dose response study of Pep-1 conjugated mitochondrial transplant, lower dosage groups were found to have more mitochondrial dispersion within tissues compared to higher concentrations, which had the tendency to aggregate (Chang et al 2013a). Future studies could use Pep-1 conjugation with different dosages of mitochondria to evaluate changes in incorporation compared to our data for non-conjugated mitochondria.

6.3.2 Inflammatory Response

Previously published studies investigating mitochondrial transplantation tested for inflammatory markers and did not find increases. Masuzawa et al (2013) did not report inflammation after direct autologous mitochondria injection, instead they found that mitochondria transplantation resulted in significantly decreased tumor necrosis factor alpha (TNFa), interleukin 6 (IL-6), and high-sensitivity C-reactive protein (hsCRP) (Masuzawa et al 2013). Further, they showed anti-mitochondrial antibodies were not present in blood serum samples 28 days after injections. However, there could be differences when allogeneic mitochondria are transplanted, as was used in our studies (**Chapters 4 and 5**), compared to a syngeneic or autologous mitochondrial transplant.

Mitochondrial transplantation after injury resulted in increased OCR acutely, which is thought to be due to exogenous mitochondria supplementing or replacing those damaged after the injury. However, this did not correspond to

increased functional recovery. One theory to explain increased OCR at the 24 hour time point that does not correspond to long term outcome measures is that activation and recruitment of brain macrophages to the injection site may increase the density of healthy cells in otherwise damaged tissue. To determine if macrophage influx is responsible for increased OCR at the acute time point, we could assay different mitochondrial populations. After injury and transplantation, mitochondria will be isolated from the spinal cord. Unlike our experiments performed in **Chapter 5** we will separate out the different populations of synaptic and non-synaptic mitochondria. The non-synaptic mitochondrial population contains mitochondria from all different cell types, including neurons, oligodendrocytes, astrocytes, endothelial cells, resident microglia, and infiltrating macrophages. The synaptic population, however, contains mitochondria only from neuronal cells. This allows distinction between increases in OCR that may be attributed to infiltrating brain macrophages (within the non-synaptic population), and what may be attributed to increased health due to transplantation (synaptic population). One major caveat, however, is that we did not see any mitochondrial incorporation into neuronal cells, and thus we may not see increases in synaptic OCR. Further, we have previously shown that synaptic mitochondria respire at lower rates than non-synaptic mitochondria when isolated from naïve spinal cord tissue (Patel et al 2014). Another way to test if macrophage infiltration may be the cause of increased respiration is to use different drugs such as a CCR2 antibody to block infiltration (see Ren & Young 2013). This will result in the same resident spinal cord cells to be assayed across treatment groups with the aim of revealing whether increased respiration was peripheral macrophage-dependent.

Another potential approach is to separate out the macrophages from our spinal cord homogenate before isolation of mitochondria. For instance, macrophage markers can be applied to the homogenate followed by fluorescence-activated cell sorting (FACS) to remove the macrophages, leaving behind homogenate containing the other resident cell types of the spinal cord. Mitochondria is isolated from the remaining homogenate, and increases in OCR

will reflect that of the resident spinal cord tissue. One caveat to this approach is that this will also remove endogenous macrophages that were already in our injury/injection sites, which were shown to have the highest mitochondrial incorporation efficiency.

6.3.3 Mechanisms of Action

It was recently shown that daily intraperitoneal injections of ATP after contusion SCI in rats significantly increased BBB scores above injury only groups (Sun et al 2013). However, prolonged high amounts of extracellular ATP after SCI activates P2X7 purine receptors on neurons, resulting in increased intracellular calcium and neuronal cell death (Wang et al 2004); antagonistic drugs that inhibit this receptor following SCI significantly improve BBB locomotor scores (Peng et al 2009). These studies indicate that there may be functional recovery following ATP supplementation, though extended or excessive amounts appears to be detrimental. Mitochondria transplantation may provide an additional source of ATP, though the benefits of transplantation seem to be dependent upon more than just energy alone. McCully at al found that injections of ATP or ADP did not give the same cardioprotection as mitochondria injections (McCully et al 2009). Similarly, delivery of ATP in liposomes to damaged neurons did not result in the same increase in cell survival when astrocyte-derived mitochondrial particles were delivered in a mouse model of stroke (Hayakawa et al 2016), concluding that benefits afforded by mitochondrial transplantation are multifaceted and not just as an extra energy source. Future studies that determine the exact mechanisms by which mitochondrial transplantation may benefit damaged cells can immensely extend our knowledge in this novel treatment field.

6.3.4 Time Points of Injections

The environment of the injured spinal cord may be too harsh at the acute timepoint for transplantation. Our mitochondria injections occurred within 30 minutes of SCI. Hayakawa et al (2016) transplanted mitochondria into the mouse

brain 3 days after stroke; given the complex inflammatory response acutely after SCI this delayed time point may be more agreeable to mitochondrial survival and incorporation. Confounding this further, our tGFP mitochondria may be experiencing “donor rejection” as was seen in other transplantation paradigms involving bone marrow stromal cells injected into the naïve brain (Coyne et al 2006). Others have shown that transplantation of fetal spinal cord tissue and neurotrophic factors into the transected adult rat spinal cord showed axonal regeneration and motor function recovery; this was only evident when transplantation occurred two or four weeks after transection, but was not apparent with acute transplantation (Coumans et al 2001). Neural precursor cell transplantation in a rat model of compression SCI was successful in improving hindlimb BBB scores when transplants occurred 2 weeks but not 8 weeks after injury, indicating there may be an optimal time window for transplantation paradigms (Gollihue & Rabchevsky 2017). Similar to (Okano et al 2003), who found that neural stem cell transplantation at the acute time point after SCI may not be optimal as the inflammatory response is in full swing, we propose transplanting at later time points. For transplantation to be clinically relevant, therapies administered 3.2 hours after injury should be investigated, as this is the average time after SCI a patient is admitted and diagnosed (Bracken et al 1997). Future transplantation studies may attempt this clinically relevant time point, as well as a later time point of 3 days post SCI to correspond to published studies using stroke injury models (Hayakawa et al 2016).

6.3.5 Quantifying Incorporation

One major hurdle in these studies is quantifying the amount of tGFP mitochondria that are successfully taken into host cells. First, we must define what is considered successful incorporation- are the mitochondria simply taken into the cytoplasm, do they need to maintain their membrane potential, and do they have to incorporate into the endogenous mitochondrial network? For our tracking purposes, we define successful incorporation as co-localizing with the labeled cell which was verified using confocal fluorescent microscopy. However,

as the tGFP tag is coded for by nuclear DNA and not the mitochondrial DNA, the tag will not be propagated after transplantation. This means that the tag will most likely dissipate over time, making the exogenous mitochondria hard to track as time progresses. Further, the tag will be progressively degraded as different portions of the mitochondrial network are mitophagocytosed, a natural occurrence that works to maintain an overall healthy membrane potential (Twig et al 2008b). Together, these make fluorescent tracking of mitochondria difficult at later time points.

We attempted to measure the tGFP mitochondrial presence in injured spinal cords after 6 weeks, but only one instance of dispersed punctate tGFP mitochondria was evident and could only be visualized at high magnification. These studies attempt to discern the tGFP label for identification of exogenous mitochondria, though the presence of exogenous mitochondria could be established by utilizing a xenogenic transplantation model. Not only could we use species-specific mitochondrial antibodies that will not dissipate over time (Kaza et al 2016), but we could also perform quantitative real-time PCR (qRTPCR) on the mtDNA to quantify exogenous mitochondria.

Others have measured mtDNA to demonstrate transfer *in vitro*. We used PC-12-Adh cells originating from the rat *Rattus norvegicus* as our source of donor mitochondria and transplanted into the Sprague Dawley strain of *Rattus norvegicus* rats. We transplanted mitochondria between like-species based on previous published studies suggesting mitochondrial uptake occurs more prevalently when like-species are used (Clark & Shay 1982, Yang & Koob 2012). However, the differences in the mtDNA may not be enough to discern between host and exogenous mitochondria. Alternatively, other studies have performed xenogenic transfer with successful incorporation. Future studies may employ xenogenic transplant after SCI so that the host and donor mtDNA can be differentiated and quantified using real time qRTPCR. This will allow quantification at chronic time points that is more dependable than tGFP immunolabeling, possibly giving more insight into the time-dependent uptake and maintenance of transplanted mitochondria.

Additional metrics of successful incorporation need to be investigated. Evaluating the health of exogenous mitochondria after they have been incorporated into cells is an important measure, such as maintenance of membrane potential. One possible way of testing this immunohistologically is by co-labeling the tGFP mitochondria before transplantation with MitoTrackerRed CMXRos, a membrane-potential mitochondrial marker. Utilizing fluorescent microscopy, the proportion of mitochondria *in situ* that have both the tGFP tag and MitoTracker Red fluorescence, indicating transplanted mitochondria that maintained membrane potential, can be evaluated. Additionally, we can define successful incorporation as exogenous mitochondrial integration into the host cell mitochondrial network. *in vitro* studies can utilize transgenic labeling of host cell mitochondria with DsRed, then co-incubation with isolated tGFP mitochondria. Live time-lapse imaging allows tracking of tGFP mitochondria movement within the cell, and fusion events that result in co-localization with DsRed host mitochondria. To test this *in vivo*, a transgenic rat line that has DsRed-labeled mitochondria could be created. Upon transplantation of tGFP mitochondria after SCI, we will be able to track the fusion, or co-localization, of tGFP mitochondria with the endogenous DsRed-labeled mitochondrial network. Alternatively, there is a mouse line currently available that has a yellow fluorescent protein that targets mitochondria of neuronal cells that can be used in the same manner (JAX Labs, Bar Harbor, ME). Using a mouse line as the recipient of PC-12 tGFP mitochondria would further allow for qRTPCR (see previous paragraph) to corroborate our findings of exogenous mtDNA with fluorescent microscopy indicating the presence of exogenous tGFP mitochondria.

One method that could be extremely helpful in our characterization studies is FACS flow cytometry. At a timepoint after transplantation, the spinal cord will be dissected and homogenized as the first step of mitochondrial isolation. This homogenate includes all different cell types of the spinal cord. Fluorescently labeling one cell type at a time will allow measurement of the proportion of that cell with and without tGFP mitochondria, thus quantifying uptake propensity. When homogenate samples undergo mitochondrial isolation procedures, the final

sample includes both endogenous mitochondria and tGFP mitochondria. These mitochondria can be sorted based on whether or not they have the fluorescent tag, and their OCR values can be compared. Comparisons can be made between the bioenergetics within the endogenous mitochondria population of vehicle-injected animals to mitochondria-injected animals. This allows evaluation of whether mitochondrial transplantation benefits the health and survival of host mitochondria. The two mitochondrial populations can be further assayed for membrane potential, calcium buffering capacity, and fusion and fission proteins.

Once methods have been further refined to quantify incorporation of exogenous mitochondria both *in vitro* and *in vivo*, studies can be performed to discern possible mechanisms of isolated mitochondrial uptake. Multiple mechanisms of incorporation have been proposed, though there is currently not a consensus on the matter (see **Chapter 2.4**). It is widely accepted that mitochondria are of bacterial origin. Moreover, there are many types of bacteria up to 5um in size that can successfully enter into a cell where they can reside and replicate. Therefore, we theorize that it may be possible that the mechanism used by bacteria for host cellular infiltration is similar to that used by isolated mitochondria for incorporation. Like bacteria, mitochondria may have proteins on their surface that bind to receptors on host cell surfaces, initiating a zipper-like actin-mediated phagocytosis. This zipper-like mechanism of incorporation can utilize different receptors such as integrin for binding and signaling (for review of bacterial invasion methods see Cossart & Sansonetti 2004). Interestingly, it was found that neuronal internalization of mitochondria-containing particles *in vivo* is dependent upon integrin-mediated Src/Syk signaling pathways (Hayakawa et al 2016). Further comparisons must be made between bacteria and mitochondria to determine if they share a conserved cell surface protein that interacts with host cell receptors.

6.4 Summary of Thesis

The data and conclusions derived from the studies of this dissertation investigate different facets of mitochondrial transplantation after traumatic SCI. We have described the importance of healthy mitochondrial function, as well as the involvement of dysfunctional mitochondria in the pathophysiology of SCI. This was followed by a thorough discussion of the current state of the mitochondrial transplantation field. Importantly, we are the first to transplant exogenous mitochondria in a model of spinal cord injury. Different experimental techniques were explored to best test the effects of mitochondrial transplant. Transgenically-labeled cell culture-derived mitochondria were characterized for their use as the exogenous mitochondrial source and were found to possess an indelible fluorescent marker that could be tracked both *in vitro* and *in situ*. *In vivo* studies showed that transplanting either culture or leg muscle-derived mitochondria acutely maintained bioenergetics of the injured spinal cord. tGFP mitochondria co-localized within a multitude of cell types, though at various percentages indicating that incorporation is cell-type dependent. Co-localization was also time-dependent, as evidence of tGFP mitochondria significantly declined at 7 days, and was all but absent at 6 weeks post injection. Hindlimb functional recovery and tissue sparing were not improved with mitochondrial transplantation, though multiple alternative approaches are addressed that may increase the efficiency of incorporation and thus benefits of mitochondrial transplantation.

While optimization of therapeutic techniques can be further refined, we have shown feasibility for transplantation after SCI. Further systematic characterization is necessary to fully understand the intricacies of transplantation paradigms, but I believe that mitochondrial transplantation can be developed into a viable option for treatment after SCI as well as other injury and disease states in which dysfunctional mitochondria are implicated.

Appendix 1. Abbreviations

ADP	Adenosine diphosphate
AIF	Apoptosis inducing factor
ALC	Acetyl-L-carnitine
AMPA	α-amino-3-hydroxy-5-methyl-4-isoxazolepropionic acid
ANOVA	Analysis of variance
ATP	Adenosine triphosphate
BBB	Basso, Beattie, Bresnahan overground locomotor scale
CAP	Chloramphenicol
CNS	Central nervous system
CPG	Central pattern generator
CTVT	Canine transmissible venereal tumor
DAMPs	Damage-associated molecular patterns
DMSO	Dimethyl sulfoxide
ECCV	Eriochrome Cyanine-Cresyl Violet
EGTA	Ethylene glycol tetraacetic acid
ETC	Electron transport chain
EtOH	Ethyl alcohol
ETS	Electron transport system
FACS	Fluorescence-activated cell sorter
FADH	Flavin adenine dinucleotide
FCCP	Carbonilcyanide *p*-trifluoromethoxyphenylhydrazone
hsCRP	High-sensitivity C-reactive protein
IL-6	Interleukin 6
IMM	Inner mitochondrial membrane
MEND	Massive endocytosis
MERFF	Myoclonic epilepsy with ragged-red fibers
mBMSC	Mouse bone marrow derived stromal cells
MnSOD	Manganese superoxide dismutase
MPTP	Mitochondrial membrane permeability transition pore
mtDNA	Mitochondrial DNA

MTG	MitoTracker Green FM
NACA	N-acetylcysteine amide
NADH	Reduced nicotinamide adenine dinucleotide
NMDA	N-methyl-D-aspartate
NSAIDs	Non-steroidal anti-inflammatory drugs
OCR	Oxygen consumption rate
OGD	Oxygen glucose deprivation
OH^-	Hydroxyl radicals
PBS	Phosphate buffered saline
PCR	Polymerase chain reaction
PD	Parkinson's Disease
PFA	Paraformaldehyde
PPARγ	Peroxisome proliferator-activated receptor gamma
qRTPCR	Quantitative real-time PCR
RCR	Respiratory control ratio
RNS	Reactive nitrogen species
ROI	Region of interest
ROS	Reactive oxygen species
RT	Room temperature
SCI	Spinal cord injury
TBARS	Thiobarbituric acid-reactive substances
TEM	Transmission electron microscopy
tGFP	Turbo green fluorescent protein
TMRE	Tetramethylrhodamine Ethyl Ester
TNF-α	Tumor necrosis factor alpha
TUNEL	TdT-mediated dUTP nick-end labeling

REFERENCES

Agrawal SK, Fehlings MG. 1996. Mechanisms of secondary injury to spinal cord axons in vitro: role of Na+, Na(+)-K(+)-ATPase, the Na(+)-H+ exchanger, and the Na(+)-Ca2+ exchanger. *The Journal of neuroscience : the official journal of the Society for Neuroscience* 16: 545-52

Ahmed LA, Shehata NI, Abdelkader NF, Khattab MM. 2014. Tempol, a superoxide dismutase mimetic agent, ameliorates cisplatin-induced nephrotoxicity through alleviation of mitochondrial dysfunction in mice. *PloS one* 9: e108889

Ahsan F, Rivas IP, Khan MA, Torres Suarez AI. 2002. Targeting to macrophages: role of physicochemical properties of particulate carriers--liposomes and microspheres--on the phagocytosis by macrophages. *Journal of controlled release : official journal of the Controlled Release Society* 79: 29-40

Allen R, Alfred. 1914. Remarks on the Histopathological Changes in the PSinal Cord due to Impact: An Experimental Study. *The Journal of Nervous and Mental Disease* 41: 141-47

Ankarcrona M, Dypbukt JM, Bonfoco E, Zhivotovsky B, Orrenius S, et al. 1995. Glutamate-induced neuronal death: a succession of necrosis or apoptosis depending on mitochondrial function. *Neuron* 15: 961-73

Arai M, Imai H, Koumura T, Yoshida M, Emoto K, et al. 1999. Mitochondrial phospholipid hydroperoxide glutathione peroxidase plays a major role in preventing oxidative injury to cells. *J Biol Chem* 274: 4924-33

Arimura S, Yamamoto J, Aida GP, Nakazono M, Tsutsumi N. 2004. Frequent fusion and fission of plant mitochondria with unequal nucleoid distribution. *Proceedings of the National Academy of Sciences of the United States of America* 101: 7805-8

Armstrong JS. 2007. Mitochondrial medicine: pharmacological targeting of mitochondria in disease. *Br J Pharmacol* 151: 1154-65

Aygok GA, Marmarou A, Fatouros P, Kettenmann B, Bullock RM. 2008. Assessment of mitochondrial impairment and cerebral blood flow in severe brain injured patients. *Acta Neurochir Suppl* 102: 57-61

Azbill RD, Mu X, Bruce-Keller AJ, Mattson MP, Springer JE. 1997. Impaired mitochondrial function, oxidative stress and altered antioxidant enzyme activities following traumatic spinal cord injury. *Brain research* 765: 283-90

Bains M, Hall ED. 2012. Antioxidant therapies in traumatic brain and spinal cord injury. *Biochimica et biophysica acta* 1822: 675-84

Baptiste DC, Fehlings MG. 2006. Pharmacological approaches to repair the injured spinal cord. *J Neurotrauma* 23: 318-34

Basso DM, Beattie MS, Bresnahan JC. 1995. A sensitive and reliable locomotor rating scale for open field testing in rats. *J Neurotrauma* 12: 1-21

Basso DM, Beattie MS, Bresnahan JC. 1996. Graded histological and locomotor outcomes after spinal cord contusion using the NYU weight-drop device versus transection. *Experimental neurology* 139: 244-56

Beckman JS, Beckman TW, Chen J, Marshall PA, Freeman BA. 1990. Apparent hydroxyl radical production by peroxynitrite: implications for endothelial

injury from nitric oxide and superoxide. *Proceedings of the National Academy of Sciences of the United States of America* 87: 1620-4
Berry M, Riches AC. 1974. An immunological approach to regeneration in the central nervous system. *British medical bulletin* 30: 135-40
Bethea JR, Nagashima H, Acosta MC, Briceno C, Gomez F, et al. 1999. Systemically administered interleukin-10 reduces tumor necrosis factor-alpha production and significantly improves functional recovery following traumatic spinal cord injury in rats. *J Neurotrauma* 16: 851-63
Bianchi K, Rimessi A, Prandini A, Szabadkai G, Rizzuto R. 2004. Calcium and mitochondria: mechanisms and functions of a troubled relationship. *Biochimica et biophysica acta* 1742: 119-31
Blight AR. 1985. Delayed demyelination and macrophage invasion: a candidate for secondary cell damage in spinal cord injury. *Central nervous system trauma : journal of the American Paralysis Association* 2: 299-315
Blight AR. 1992. Macrophages and inflammatory damage in spinal cord injury. *J Neurotrauma* 9 Suppl 1: S83-91
Blight AR. 1994. Effects of silica on the outcome from experimental spinal cord injury: implication of macrophages in secondary tissue damage. *Neuroscience* 60: 263-73
Bolanos JP, Moro MA, Lizasoain I, Almeida A. 2009. Mitochondria and reactive oxygen and nitrogen species in neurological disorders and stroke: Therapeutic implications. *Adv Drug Deliv Rev* 61: 1299-315
Bonfoco E, Krainc D, Ankarcrona M, Nicotera P, Lipton SA. 1995. Apoptosis and necrosis: two distinct events induced, respectively, by mild and intense insults with N-methyl-D-aspartate or nitric oxide/superoxide in cortical cell cultures. *Proceedings of the National Academy of Sciences of the United States of America* 92: 7162-6
Bracken MB, Shepard MJ, Hellenbrand KG, Collins WF, Leo LS, et al. 1985. Methylprednisolone and neurological function 1 year after spinal cord injury. Results of the National Acute Spinal Cord Injury Study. *Journal of neurosurgery* 63: 704-13
Bracken MB, Shepard MJ, Holford TR, Leo-Summers L, Aldrich EF, et al. 1997. Administration of methylprednisolone for 24 or 48 hours or tirilazad mesylate for 48 hours in the treatment of acute spinal cord injury. Results of the Third National Acute Spinal Cord Injury Randomized Controlled Trial. National Acute Spinal Cord Injury Study. *Jama* 277: 1597-604
Brand MD, Esteves TC. 2005. Physiological functions of the mitochondrial uncoupling proteins UCP2 and UCP3. *Cell Metab* 2: 85-93
Brand MD, Nicholls DG. 2011. Assessing mitochondrial dysfunction in cells. *The Biochemical journal* 435: 297-312
Braunwald E, Kloner RA. 1985. Myocardial reperfusion: a double-edged sword? *The Journal of clinical investigation* 76: 1713-9
Brown WM, George M, Jr., Wilson AC. 1979. Rapid evolution of animal mitochondrial DNA. *Proceedings of the National Academy of Sciences of the United States of America* 76: 1967-71
Brzezinska A. 2012. *US*

Buckman JF, Hernandez H, Kress GJ, Votyakova TV, Pal S, Reynolds IJ. 2001. MitoTracker labeling in primary neuronal and astrocytic cultures: influence of mitochondrial membrane potential and oxidants. *J Neurosci Methods* 104: 165-76

Burdon RH. 1995. Superoxide and hydrogen peroxide in relation to mammalian cell proliferation. *Free radical biology & medicine* 18: 775-94

Bygrave FL, Ash GR. 1977. Development of mitochondrial calcium transport activity in rat liver. *FEBS Lett* 80: 271-4

Cammer W, Bloom BR, Norton WT, Gordon S. 1978. Degradation of basic protein in myelin by neutral proteases secreted by stimulated macrophages: a possible mechanism of inflammatory demyelination. *Proceedings of the National Academy of Sciences of the United States of America* 75: 1554-8

Carlson SL, Parrish ME, Springer JE, Doty K, Dossett L. 1998. Acute inflammatory response in spinal cord following impact injury. *Experimental neurology* 151: 77-88

Carp H. 1982. Mitochondrial N-formylmethionyl proteins as chemoattractants for neutrophils. *The Journal of experimental medicine* 155: 264-75

Carta A, Calvani M. 1991. Acetyl-L-carnitine: a drug able to slow the progress of Alzheimer's disease? *Annals of the New York Academy of Sciences* 640: 228-32

Center NSCIS. 2016. Spinal Cord Injury (SCI) Facts and Figures at a Glance, University of Alabama, Birmingham, AL

Ch'ih JJ, Kalf GF. 1969. Studies on the biosynthesis of the DNA polymerase of rat liver mitochondria. *Arch Biochem Biophys* 133: 38-45

Chang J, Liu K, Chuang C, Wu S, Kuo S, Liu C. 2013a. Transplantation of Pep-1-labeled mitochondria protection against a 6-OHDA-induced neurotoxicity in rats. *The Changhua Journal of Medicine* 11: 8-17

Chang JC, Liu KH, Li YC, Kou SJ, Wei YH, et al. 2013b. Functional recovery of human cells harbouring the mitochondrial DNA mutation MERRF A8344G via peptide-mediated mitochondrial delivery. *Neurosignals* 21: 160-73

Chang JC, Wu SL, Liu KH, Chen YH, Chuang CS, et al. 2016. Allogeneic/xenogeneic transplantation of peptide-labeled mitochondria in Parkinson's disease: restoration of mitochondria functions and attenuation of 6-hydroxydopamine-induced neurotoxicity. *Translational research : the journal of laboratory and clinical medicine* 170: 40-56 e1-3

Chaplan SR, Bach FW, Pogrel JW, Chung JM, Yaksh TL. 1994. Quantitative assessment of tactile allodynia in the rat paw. *J Neurosci Methods* 53: 55-63

Cheeseman KH, Slater TF. 1993. An introduction to free radical biochemistry. *British medical bulletin* 49: 481-93

Chen H, Chomyn A, Chan DC. 2005. Disruption of fusion results in mitochondrial heterogeneity and dysfunction. *J Biol Chem* 280: 26185-92

Chen Y, Corriden R, Inoue Y, Yip L, Hashiguchi N, et al. 2006. ATP release guides neutrophil chemotaxis via P2Y2 and A3 receptors. *Science* 314: 1792-5

Cho YM, Kim JH, Kim M, Park SJ, Koh SH, et al. 2012. Mesenchymal stem cells transfer mitochondria to the cells with virtually no mitochondrial function but not with pathogenic mtDNA mutations. *PloS one* 7: e32778
Choi DW. 1985. Glutamate neurotoxicity in cortical cell culture is calcium dependent. *Neurosci Lett* 58: 293-7
Choi DW. 1988. Calcium-mediated neurotoxicity: relationship to specific channel types and role in ischemic damage. *Trends Neurosci* 11: 465-9
Clark MA, Shay JW. 1982. Mitochondrial transformation of mammalian cells. *Nature* 295: 605-7
Cohen DM, Patel CB, Ahobila-Vajjula P, Sundberg LM, Chacko T, et al. 2009. Blood-spinal cord barrier permeability in experimental spinal cord injury: dynamic contrast-enhanced MRI. *NMR in biomedicine* 22: 332-41
Cohen J, Scott R, Alikani M, Schimmel T, Munne S, et al. 1998. Ooplasmic transfer in mature human oocytes. *Mol Hum Reprod* 4: 269-80
Cohen J, Scott R, Schimmel T, Levron J, Willadsen S. 1997. Birth of infant after transfer of anucleate donor oocyte cytoplasm into recipient eggs. *Lancet* 350: 186-7
Collins LV, Hajizadeh S, Holme E, Jonsson IM, Tarkowski A. 2004. Endogenously oxidized mitochondrial DNA induces in vivo and in vitro inflammatory responses. *J Leukoc Biol* 75: 995-1000
Cossart P, Sansonetti PJ. 2004. Bacterial invasion: the paradigms of enteroinvasive pathogens. *Science* 304: 242-8
Coumans JV, Lin TT, Dai HN, MacArthur L, McAtee M, et al. 2001. Axonal regeneration and functional recovery after complete spinal cord transection in rats by delayed treatment with transplants and neurotrophins. *The Journal of neuroscience : the official journal of the Society for Neuroscience* 21: 9334-44
Cowan DB, Yao R, Akurathi V, Snay ER, Thedsanamoorthy JK, et al. 2016. Intracoronary Delivery of Mitochondria to the Ischemic Heart for Cardioprotection. *PloS one* 11: e0160889
Coyne TM, Marcus AJ, Woodbury D, Black IB. 2006. Marrow stromal cells transplanted to the adult brain are rejected by an inflammatory response and transfer donor labels to host neurons and glia. *Stem cells* 24: 2483-92
Cselenyak A, Pankotai E, Horvath EM, Kiss L, Lacza Z. 2010. Mesenchymal stem cells rescue cardiomyoblasts from cell death in an in vitro ischemia model via direct cell-to-cell connections. *BMC Cell Biol* 11: 29
Cunha FM, Caldeira da Silva CC, Cerqueira FM, Kowaltowski AJ. 2011. Mild mitochondrial uncoupling as a therapeutic strategy. *Curr Drug Targets* 12: 783-9
Cuzzocrea S, Riley DP, Caputi AP, Salvemini D. 2001. Antioxidant therapy: a new pharmacological approach in shock, inflammation, and ischemia/reperfusion injury. *Pharmacological reviews* 53: 135-59
David S, Bouchard C, Tsatas O, Giftochristos N. 1990. Macrophages can modify the nonpermissive nature of the adult mammalian central nervous system. *Neuron* 5: 463-9

Dawson VL, Dawson TM, London ED, Bredt DS, Snyder SH. 1991. Nitric oxide mediates glutamate neurotoxicity in primary cortical cultures. *Proceedings of the National Academy of Sciences of the United States of America* 88: 6368-71

Ding WX, Yin XM. 2012. Mitophagy: mechanisms, pathophysiological roles, and analysis. *Biol Chem* 393: 547-64

Donnelly DJ, Popovich PG. 2008. Inflammation and its role in neuroprotection, axonal regeneration and functional recovery after spinal cord injury. *Experimental neurology* 209: 378-88

Droge W. 2002. Free radicals in the physiological control of cell function. *Physiological reviews* 82: 47-95

Du H, Guo L, Fang F, Chen D, Sosunov AA, et al. 2008. Cyclophilin D deficiency attenuates mitochondrial and neuronal perturbation and ameliorates learning and memory in Alzheimer's disease. *Nat Med* 14: 1097-105

Ducker TB, Assenmacher DR. 1969. Microvascular response to experimental spinal cord trauma. *Surgical forum* 20: 428-30

Dumont RJ, Okonkwo DO, Verma S, Hurlbert RJ, Boulos PT, et al. 2001. Acute spinal cord injury, part I: pathophysiologic mechanisms. *Clinical neuropharmacology* 24: 254-64

Eguchi Y, Shimizu S, Tsujimoto Y. 1997. Intracellular ATP levels determine cell death fate by apoptosis or necrosis. *Cancer Res* 57: 1835-40

Elliott MR, Chekeni FB, Trampont PC, Lazarowski ER, Kadl A, et al. 2009. Nucleotides released by apoptotic cells act as a find-me signal to promote phagocytic clearance. *Nature* 461: 282-6

Elliott RL, Jiang XP, Head JF. 2012. Mitochondria organelle transplantation: introduction of normal epithelial mitochondria into human cancer cells inhibits proliferation and increases drug sensitivity. *Breast Cancer Res Treat* 136: 347-54

England JM, Attardi G. 1974. Expression of the mitochondrial genome in HeLa cells. XXI. Mitochondrial protein synthesis during the cell cycle. *J Mol Biol* 85: 433-44

Faden AI, Lemke M, Simon RP, Noble LJ. 1988. N-methyl-D-aspartate antagonist MK801 improves outcome following traumatic spinal cord injury in rats: behavioral, anatomic, and neurochemical studies. *J Neurotrauma* 5: 33-45

Fehlings MG, Nguyen DH. 2010. Immunoglobulin G: a potential treatment to attenuate neuroinflammation following spinal cord injury. *Journal of clinical immunology* 30 Suppl 1: S109-12

Ferguson AR, Hook MA, Garcia G, Bresnahan JC, Beattie MS, Grau JW. 2004. A simple post hoc transformation that improves the metric properties of the BBB scale for rats with moderate to severe spinal cord injury. *J Neurotrauma* 21: 1601-13

Fiskum G. 2000. Mitochondrial participation in ischemic and traumatic neural cell death. *J Neurotrauma* 17: 843-55

Fleming JC, Norenberg MD, Ramsay DA, Dekaban GA, Marcillo AE, et al. 2006. The cellular inflammatory response in human spinal cords after injury. *Brain : a journal of neurology* 129: 3249-69
Friedman J. 2011. *Oxidative Stress and Free Radical Damage in Neurology*. pp. 19-27. Humana Press. Viii, 323 pp.
Garg AD, Nowis D, Golab J, Vandenabeele P, Krysko DV, Agostinis P. 2010. Immunogenic cell death, DAMPs and anticancer therapeutics: an emerging amalgamation. *Biochimica et biophysica acta* 1805: 53-71
Ghiringhelli F, Apetoh L, Tesniere A, Aymeric L, Ma Y, et al. 2009. Activation of the NLRP3 inflammasome in dendritic cells induces IL-1beta-dependent adaptive immunity against tumors. *Nat Med* 15: 1170-8
Gilgun-Sherki Y, Rosenbaum Z, Melamed E, Offen D. 2002. Antioxidant therapy in acute central nervous system injury: current state. *Pharmacological reviews* 54: 271-84
Gill R, Lodge D. 1997. Pharmacology of AMPA antagonists and their role in neuroprotection. *International review of neurobiology* 40: 197-232
Gollihue JL, Patel SP, Mashburn C, Eldahan KC, Sullivan PG, Rabchevsky AG. 2017. Optimization of Mitochondrial Isolation Techniques for Intraspinal Transplantation Procedures. *J Neurosci Methods*
Gollihue JL, Rabchevsky AG. 2017. Prospects for therapeutic mitochondrial transplantation. *Mitochondrion*
Grillner S. 1975. Locomotion in vertebrates: central mechanisms and reflex interaction. *Physiological reviews* 55: 247-304
Griot C, Burge T, Vandevelde M, Peterhans E. 1989. Antibody-induced generation of reactive oxygen radicals by brain macrophages in canine distemper encephalitis: a mechanism for bystander demyelination. *Acta neuropathologica* 78: 396-403
Hadi B, Zhang YP, Burke DA, Shields CB, Magnuson DS. 2000. Lasting paraplegia caused by loss of lumbar spinal cord interneurons in rats: no direct correlation with motor neuron loss. *Journal of neurosurgery* 93: 266-75
Hall ED. 1995. Inhibition of lipid peroxidation in central nervous system trauma and ischemia. *Journal of the neurological sciences* 134 Suppl: 79-83
Hall ED, Braughler JM. 1982. Effects of intravenous methylprednisolone on spinal cord lipid peroxidation and Na+ + K+)-ATPase activity. Dose-response analysis during 1st hour after contusion injury in the cat. *Journal of neurosurgery* 57: 247-53
Hall ED, Braughler JM. 1993. Free radicals in CNS injury. *Research publications - Association for Research in Nervous and Mental Disease* 71: 81-105
Hall ED, Vaishnav RA, Mustafa AG. 2010. Antioxidant therapies for traumatic brain injury. *Neurotherapeutics* 7: 51-61
Hall ED, Yonkers PA, Horan KL, Braughler JM. 1989. Correlation between attenuation of posttraumatic spinal cord ischemia and preservation of tissue vitamin E by the 21-aminosteroid U74006F: evidence for an in vivo antioxidant mechanism. *J Neurotrauma* 6: 169-76

Han J, Han MS, Tung CH. 2013. A non-toxic fluorogenic dye for mitochondria labeling. *Biochimica et biophysica acta* 1830: 5130-5
Hayakawa K, Esposito E, Wang X, Terasaki Y, Liu Y, et al. 2016. Transfer of mitochondria from astrocytes to neurons after stroke. *Nature* 535: 551-5
Hayashi J, Tagashira Y, Yoshida MC. 1985. Absence of extensive recombination between inter- and intraspecies mitochondrial DNA in mammalian cells. *Exp Cell Res* 160: 387-95
Henriques ST, Castanho MA, Pattenden LK, Aguilar MI. 2010. Fast membrane association is a crucial factor in the peptide pep-1 translocation mechanism: a kinetic study followed by surface plasmon resonance. *Biopolymers* 94: 314-22
Hirschberg DL, Yoles E, Belkin M, Schwartz M. 1994. Inflammation after axonal injury has conflicting consequences for recovery of function: rescue of spared axons is impaired but regeneration is supported. *Journal of neuroimmunology* 50: 9-16
Hou S, Duale H, Cameron AA, Abshire SM, Lyttle TS, Rabchevsky AG. 2008. Plasticity of lumbosacral propriospinal neurons is associated with the development of autonomic dysreflexia after thoracic spinal cord transection. *The Journal of comparative neurology* 509: 382-99
Huang SF, Tsai YA, Wu SB, Wei YH, Tsai PY, Chuang TY. 2012. Effects of intravascular laser irradiation of blood in mitochondria dysfunction and oxidative stress in adults with chronic spinal cord injury. *Photomed Laser Surg* 30: 579-86
Hume RI, Dingledine R, Heinemann SF. 1991. Identification of a site in glutamate receptor subunits that controls calcium permeability. *Science* 253: 1028-31
Hunter DR, Haworth RA. 1979. The Ca2+-induced membrane transition in mitochondria. I. The protective mechanisms. *Archives of biochemistry and biophysics* 195: 453-9
Hunter DR, Haworth RA, Southard JH. 1976. Relationship between configuration, function, and permeability in calcium-treated mitochondria. *J Biol Chem* 251: 5069-77
Hutchison CA, 3rd, Newbold JE, Potter SS, Edgell MH. 1974. Maternal inheritance of mammalian mitochondrial DNA. *Nature* 251: 536-8
Ide T, Tsutsui H, Hayashidani S, Kang D, Suematsu N, et al. 2001. Mitochondrial DNA damage and dysfunction associated with oxidative stress in failing hearts after myocardial infarction. *Circ Res* 88: 529-35
Ishii T. 2014. Potential impact of human mitochondrial replacement on global policy regarding germline gene modification. *Reprod Biomed Online* 29: 150-5
Islam MN, Das SR, Emin MT, Wei M, Sun L, et al. 2012. Mitochondrial transfer from bone-marrow-derived stromal cells to pulmonary alveoli protects against acute lung injury. *Nat Med* 18: 759-65
Iyer SS, Pulskens WP, Sadler JJ, Butter LM, Teske GJ, et al. 2009. Necrotic cells trigger a sterile inflammatory response through the Nlrp3 inflammasome.

Proceedings of the National Academy of Sciences of the United States of America 106: 20388-93
Jia ZQ, Li G, Zhang ZY, Li HT, Wang JQ, et al. 2016. Time representation of mitochondrial morphology and function after acute spinal cord injury. *Neural regeneration research* 11: 137-43
Jin H, Kanthasamy A, Ghosh A, Anantharam V, Kalyanaraman B, Kanthasamy AG. 2014. Mitochondria-targeted antioxidants for treatment of Parkinson's disease: preclinical and clinical outcomes. *Biochimica et biophysica acta* 1842: 1282-94
Jin Y, McEwen ML, Nottingham SA, Maragos WF, Dragicevic NB, et al. 2004. The mitochondrial uncoupling agent 2,4-dinitrophenol improves mitochondrial function, attenuates oxidative damage, and increases white matter sparing in the contused spinal cord. *J Neurotrauma* 21: 1396-404
Jouaville LS, Pinton P, Bastianutto C, Rutter GA, Rizzuto R. 1999. Regulation of mitochondrial ATP synthesis by calcium: evidence for a long-term metabolic priming. *Proceedings of the National Academy of Sciences of the United States of America* 96: 13807-12
Katrangi E, D'Souza G, Boddapati SV, Kulawiec M, Singh KK, et al. 2007. Xenogenic transfer of isolated murine mitochondria into human rho0 cells can improve respiratory function. *Rejuvenation Res* 10: 561-70
Kaza AK, Wamala I, Friehs I, Kuebler JD, Rathod RH, et al. 2016. Myocardial rescue with autologous mitochondrial transplantation in a porcine model of ischemia/reperfusion. *J Thorac Cardiovasc Surg*
Kazama H, Ricci JE, Herndon JM, Hoppe G, Green DR, Ferguson TA. 2008. Induction of immunological tolerance by apoptotic cells requires caspase-dependent oxidation of high-mobility group box-1 protein. *Immunity* 29: 21-32
Keij JF, Bell-Prince C, Steinkamp JA. 2000. Staining of mitochondrial membranes with 10-nonyl acridine orange, MitoFluor Green, and MitoTracker Green is affected by mitochondrial membrane potential altering drugs. *Cytometry* 39: 203-10
King MP, Attardi G. 1988. Injection of mitochondria into human cells leads to a rapid replacement of the endogenous mitochondrial DNA. *Cell* 52: 811-9
Kitani T, Kami D, Kawasaki T, Nakata M, Matoba S, Gojo S. 2014a. Direct human mitochondrial transfer: a novel concept based on the endosymbiotic theory. *Transplant Proc* 46: 1233-6
Kitani T, Kami D, Matoba S, Gojo S. 2014b. Internalization of isolated functional mitochondria: involvement of macropinocytosis. *J Cell Mol Med* 18: 1694-703
Kjaerulff O, Kiehn O. 1996. Distribution of networks generating and coordinating locomotor activity in the neonatal rat spinal cord in vitro: a lesion study. *The Journal of neuroscience : the official journal of the Society for Neuroscience* 16: 5777-94
Koyanagi M, Brandes RP, Haendeler J, Zeiher AM, Dimmeler S. 2005. Cell-to-cell connection of endothelial progenitor cells with cardiac myocytes by

nanotubes: a novel mechanism for cell fate changes? *Circ Res* 96: 1039-41
Krajewska M, Rosenthal RE, Mikolajczyk J, Stennicke HR, Wiesenthal T, et al. 2004. Early processing of Bid and caspase-6, -8, -10, -14 in the canine brain during cardiac arrest and resuscitation. *Experimental neurology* 189: 261-79
Krajewski S, Krajewska M, Ellerby LM, Welsh K, Xie Z, et al. 1999. Release of caspase-9 from mitochondria during neuronal apoptosis and cerebral ischemia. *Proceedings of the National Academy of Sciences of the United States of America* 96: 5752-7
Kroemer G, Dallaporta B, Resche-Rigon M. 1998. The mitochondrial death/life regulator in apoptosis and necrosis. *Annual review of physiology* 60: 619-42
Krysko DV, Agostinis P, Krysko O, Garg AD, Bachert C, et al. 2011. Emerging role of damage-associated molecular patterns derived from mitochondria in inflammation. *Trends Immunol* 32: 157-64
Lafon-Cazal M, Pietri S, Culcasi M, Bockaert J. 1993. NMDA-dependent superoxide production and neurotoxicity. *Nature* 364: 535-7
Laird MD, Clerc P, Polster BM, Fiskum G. 2013. Augmentation of normal and glutamate-impaired neuronal respiratory capacity by exogenous alternative biofuels. *Transl Stroke Res* 4: 643-51
Lariccia V, Fine M, Magi S, Lin MJ, Yaradanakul A, et al. 2011. Massive calcium-activated endocytosis without involvement of classical endocytic proteins. *The Journal of general physiology* 137: 111-32
Levron J, Willadsen S, Bertoli M, Cohen J. 1996. The development of mouse zygotes after fusion with synchronous and asynchronous cytoplasm. *Hum Reprod* 11: 1287-92
Lewen A, Matz P, Chan PH. 2000. Free radical pathways in CNS injury. *J Neurotrauma* 17: 871-90
Lightowlers RN, Chinnery PF, Turnbull DM, Howell N. 1997. Mammalian mitochondrial genetics: heredity, heteroplasmy and disease. *Trends Genet* 13: 450-5
Lin HC, Liu SY, Lai HS, Lai IR. 2013. Isolated mitochondria infusion mitigates ischemia-reperfusion injury of the liver in rats. *Shock* 39: 304-10
Lin MT, Beal MF. 2006. Mitochondrial dysfunction and oxidative stress in neurodegenerative diseases. *Nature* 443: 787-95
Liu J, Head E, Gharib AM, Yuan W, Ingersoll RT, et al. 2002. Memory loss in old rats is associated with brain mitochondrial decay and RNA/DNA oxidation: partial reversal by feeding acetyl-L-carnitine and/or R-alpha -lipoic acid. *Proceedings of the National Academy of Sciences of the United States of America* 99: 2356-61
Lotze MT, Zeh HJ, Rubartelli A, Sparvero LJ, Amoscato AA, et al. 2007. The grateful dead: damage-associated molecular pattern molecules and reduction/oxidation regulate immunity. *Immunological reviews* 220: 60-81
Loy DN, Magnuson DS, Zhang YP, Onifer SM, Mills MD, et al. 2002. Functional redundancy of ventral spinal locomotor pathways. *The Journal of*

neuroscience : the official journal of the Society for Neuroscience 22: 315-23
Lucas DR, Newhouse JP. 1957. The toxic effect of sodium L-glutamate on the inner layers of the retina. *A.M.A. archives of ophthalmology* 58: 193-201
Luft R. 1994. The development of mitochondrial medicine. *Proceedings of the National Academy of Sciences of the United States of America* 91: 8731-8
MacDermott AB, Mayer ML, Westbrook GL, Smith SJ, Barker JL. 1986. NMDA-receptor activation increases cytoplasmic calcium concentration in cultured spinal cord neurones. *Nature* 321: 519-22
Magnuson DS, Lovett R, Coffee C, Gray R, Han Y, et al. 2005. Functional consequences of lumbar spinal cord contusion injuries in the adult rat. *J Neurotrauma* 22: 529-43
Magnuson DS, Trinder TC, Zhang YP, Burke D, Morassutti DJ, Shields CB. 1999. Comparing deficits following excitotoxic and contusion injuries in the thoracic and lumbar spinal cord of the adult rat. *Experimental neurology* 156: 191-204
Manev H, Favaron M, Guidotti A, Costa E. 1989. Delayed increase of Ca2+ influx elicited by glutamate: role in neuronal death. *Mol Pharmacol* 36: 106-12
Maragos WF, Rockich KT, Dean JJ, Young KL. 2003. Pre- or post-treatment with the mitochondrial uncoupler 2,4-dinitrophenol attenuates striatal quinolinate lesions. *Brain research* 966: 312-6
Masuzawa A, Black KM, Pacak CA, Ericsson M, Barnett RJ, et al. 2013. Transplantation of autologously derived mitochondria protects the heart from ischemia-reperfusion injury. *Am J Physiol Heart Circ Physiol* 304: H966-82
Matsushita T, Lankford KL, Arroyo EJ, Sasaki M, Neyazi M, et al. 2015. Diffuse and persistent blood-spinal cord barrier disruption after contusive spinal cord injury rapidly recovers following intravenous infusion of bone marrow mesenchymal stem cells. *Experimental neurology* 267: 152-64
Matz MV, Fradkov AF, Labas YA, Savitsky AP, Zaraisky AG, et al. 1999. Fluorescent proteins from nonbioluminescent Anthozoa species. *Nat Biotechnol* 17: 969-73
Mc LJ, Cohn GL, Brandt IK, Simpson MV. 1958. Incorporation of labeled amino acids into the protein of muscle and liver mitochondria. *The Journal of biological chemistry* 233: 657-63
McCord JM, Fridovich I. 1969. Superoxide dismutase. An enzymic function for erythrocuprein (hemocuprein). *J Biol Chem* 244: 6049-55
McCullers DL, Sullivan PG, Scheff SW, Herman JP. 2002. Mifepristone protects CA1 hippocampal neurons following traumatic brain injury in rat. *Neuroscience* 109: 219-30
McCully JD, Cowan DB, Emani SM, Del Nido PJ. 2017. Mitochondrial transplantation: From animal models to clinical use in humans. *Mitochondrion* 34: 127-34
McCully JD, Cowan DB, Pacak CA, Toumpoulis IK, Dayalan H, Levitsky S. 2009. Injection of isolated mitochondria during early reperfusion for cardioprotection. *Am J Physiol Heart Circ Physiol* 296: H94-H105

McEwen ML, Sullivan PG, Springer JE. 2007. Pretreatment with the cyclosporin derivative, NIM811, improves the function of synaptic mitochondria following spinal cord contusion in rats. *J Neurotrauma* 24: 613-24
Means ED, Anderson DK. 1983. Neuronophagia by leukocytes in experimental spinal cord injury. *Journal of neuropathology and experimental neurology* 42: 707-19
Merrill JE, Ignarro LJ, Sherman MP, Melinek J, Lane TE. 1993. Microglial cell cytotoxicity of oligodendrocytes is mediated through nitric oxide. *Journal of immunology* 151: 2132-41
Meyer RR, Simpson MV. 1970. Deoxyribonucleic acid biosynthesis in mitochondria. Purification and general properties of rat liver mitochondrial deoxyribonucleic acid polymerase. *J Biol Chem* 245: 3426-35
Michel RP, Cruz-Orive LM. 1988. Application of the Cavalieri principle and vertical sections method to lung: estimation of volume and pleural surface area. *J Microsc* 150: 117-36
Michelakis ED. 2008. Mitochondrial medicine: a new era in medicine opens new windows and brings new challenges. *Circulation* 117: 2431-4
Minamikawa T, Sriratana A, Williams DA, Bowser DN, Hill JS, Nagley P. 1999. Chloromethyl-X-rosamine (MitoTracker Red) photosensitises mitochondria and induces apoptosis in intact human cells. *Journal of cell science* 112 (Pt 14): 2419-30
Mizuno Y, Ohta S, Tanaka M, Takamiya S, Suzuki K, et al. 1989. Deficiencies in complex I subunits of the respiratory chain in Parkinson's disease. *Biochem Biophys Res Commun* 163: 1450-5
Morris MC, Deshayes S, Heitz F, Divita G. 2008. Cell-penetrating peptides: from molecular mechanisms to therapeutics. *Biol Cell* 100: 201-17
Murray PJ, Wynn TA. 2011. Protective and pathogenic functions of macrophage subsets. *Nature reviews. Immunology* 11: 723-37
Nakada K, Inoue K, Ono T, Isobe K, Ogura A, et al. 2001. Inter-mitochondrial complementation: Mitochondria-specific system preventing mice from expression of disease phenotypes by mutant mtDNA. *Nat Med* 7: 934-40
Nass S, Nass MM. 1963. Intramitochondrial Fibers with DNA Characteristics. Ii. Enzymatic and Other Hydrolytic Treatments. *The Journal of cell biology* 19: 613-29
Nicholls DG, Ferguson SJ. 2013. *Bioenergetics*. Amsterdam: Academic Press, Elsevier. xiv, 419 pages pp.
Noble LJ, Wrathall JR. 1989. Distribution and time course of protein extravasation in the rat spinal cord after contusive injury. *Brain research* 482: 57-66
Norenberg MD, Smith J, Marcillo A. 2004. The pathology of human spinal cord injury: defining the problems. *Journal of neurotrauma* 21: 429-40
Nunnari J, Suomalainen A. 2012. Mitochondria: in sickness and in health. *Cell* 148: 1145-59
Okano H, Ogawa Y, Nakamura M, Kaneko S, Iwanami A, Toyama Y. 2003. Transplantation of neural stem cells into the spinal cord after injury. *Seminars in cell & developmental biology* 14: 191-8

Olney JW. 1969. Brain lesions, obesity, and other disturbances in mice treated with monosodium glutamate. *Science* 164: 719-21
Olney JW, Sharpe LG. 1969. Brain lesions in an infant rhesus monkey treated with monsodium glutamate. *Science* 166: 386-8
Onopiuk M, Brutkowski W, Wierzbicka K, Wojciechowska S, Szczepanowska J, et al. 2009. Mutation in dystrophin-encoding gene affects energy metabolism in mouse myoblasts. *Biochem Biophys Res Commun* 386: 463-6
Pacak CA, Preble JM, Kondo H, Seibel P, Levitsky S, et al. 2015. Actin-dependent mitochondrial internalization in cardiomyocytes: evidence for rescue of mitochondrial function. *Biology open* 4: 622-6
Packer MA, Murphy MP. 1994. Peroxynitrite causes calcium efflux from mitochondria which is prevented by Cyclosporin A. *FEBS Lett* 345: 237-40
Patel SP, Gamboa JL, McMullen CA, Rabchevsky A, Andrade FH. 2009a. Lower respiratory capacity in extraocular muscle mitochondria: evidence for intrinsic differences in mitochondrial composition and function. *Invest Ophthalmol Vis Sci* 50: 180-6
Patel SP, Sullivan PG, Lyttle TS, Magnuson DS, Rabchevsky AG. 2012. Acetyl-L-carnitine treatment following spinal cord injury improves mitochondrial function correlated with remarkable tissue sparing and functional recovery. *Neuroscience* 210: 296-307
Patel SP, Sullivan PG, Lyttle TS, Rabchevsky AG. 2010. Acetyl-L-carnitine ameliorates mitochondrial dysfunction following contusion spinal cord injury. *Journal of neurochemistry* 114: 291-301
Patel SP, Sullivan PG, Pandya JD, Goldstein GA, VanRooyen JL, et al. 2014. N-acetylcysteine amide preserves mitochondrial bioenergetics and improves functional recovery following spinal trauma. *Experimental neurology* 257: 95-105
Patel SP, Sullivan PG, Pandya JD, Rabchevsky AG. 2009b. Differential effects of the mitochondrial uncoupling agent, 2,4-dinitrophenol, or the nitroxide antioxidant, Tempol, on synaptic or nonsynaptic mitochondria after spinal cord injury. *J Neurosci Res* 87: 130-40
Peng W, Cotrina ML, Han X, Yu H, Bekar L, et al. 2009. Systemic administration of an antagonist of the ATP-sensitive receptor P2X7 improves recovery after spinal cord injury. *Proceedings of the National Academy of Sciences of the United States of America* 106: 12489-93
Perry VH, Brown MC, Gordon S. 1987. The macrophage response to central and peripheral nerve injury. A possible role for macrophages in regeneration. *The Journal of experimental medicine* 165: 1218-23
Petruzzella V, Baggetto LG, Penin F, Cafagna F, Ruggiero FM, et al. 1992. In vivo effect of acetyl-L-carnitine on succinate oxidation, adenine nucleotide pool and lipid composition of synaptic and non-synaptic mitochondria from cerebral hemispheres of senescent rats. *Arch Gerontol Geriatr* 14: 131-44
Pettegrew JW, Levine J, McClure RJ. 2000. Acetyl-L-carnitine physical-chemical, metabolic, and therapeutic properties: relevance for its mode of action in Alzheimer's disease and geriatric depression. *Mol Psychiatry* 5: 616-32

Pica-Mattoccia L, Attardi G. 1971. Expression of the mitochondrial genome in HeLa cells. V. Transcription of mitochondrial DNA in relationship to the cell cycle. *J Mol Biol* 57: 615-21
Pica-Mattoccia L, Attardi G. 1972. Expression of the mitochondrial genome in HeLa cells. IX. Replication of mitochondrial DNA in relationship to cell cycle in HeLa cells. *J Mol Biol* 64: 465-84
Pitkanen S, Robinson BH. 1996. Mitochondrial complex I deficiency leads to increased production of superoxide radicals and induction of superoxide dismutase. *J Clin Invest* 98: 345-51
Plotnikov EY, Khryapenkova TG, Vasileva AK, Marey MV, Galkina SI, et al. 2008. Cell-to-cell cross-talk between mesenchymal stem cells and cardiomyocytes in co-culture. *J Cell Mol Med* 12: 1622-31
Polster BM, Basanez G, Etxebarria A, Hardwick JM, Nicholls DG. 2005. Calpain I induces cleavage and release of apoptosis-inducing factor from isolated mitochondria. *J Biol Chem* 280: 6447-54
Popovich PG, Guan Z, Wei P, Huitinga I, van Rooijen N, Stokes BT. 1999. Depletion of hematogenous macrophages promotes partial hindlimb recovery and neuroanatomical repair after experimental spinal cord injury. *Experimental neurology* 158: 351-65
Popovich PG, Horner PJ, Mullin BB, Stokes BT. 1996. A quantitative spatial analysis of the blood-spinal cord barrier. I. Permeability changes after experimental spinal contusion injury. *Experimental neurology* 142: 258-75
Priault M, Salin B, Schaeffer J, Vallette FM, di Rago JP, Martinou JC. 2005. Impairing the bioenergetic status and the biogenesis of mitochondria triggers mitophagy in yeast. *Cell death and differentiation* 12: 1613-21
Puca FM, Genco S, Specchio LM, Brancasi B, D'Ursi R, et al. 1990. Clinical pharmacodynamics of acetyl-L-carnitine in patients with Parkinson's disease. *Int J Clin Pharmacol Res* 10: 139-43
Rabchevsky AG, Fugaccia I, Sullivan PG, Blades DA, Scheff SW. 2002. Efficacy of methylprednisolone therapy for the injured rat spinal cord. *J Neurosci Res* 68: 7-18
Rabchevsky AG, Fugaccia I, Sullivan PG, Scheff SW. 2001. Cyclosporin A treatment following spinal cord injury to the rat: behavioral effects and stereological assessment of tissue sparing. *J Neurotrauma* 18: 513-22
Rabchevsky AG, Streit WJ. 1997. Grafting of cultured microglial cells into the lesioned spinal cord of adult rats enhances neurite outgrowth. *J Neurosci Res* 47: 34-48
Reardon S. 2016. 'Three-parent baby' claim raises hopes- and ethical concerns. *Nature News*
Rebbeck CA, Leroi AM, Burt A. 2011. Mitochondrial capture by a transmissible cancer. *Science* 331: 303
Reid RA, Moyle J, Mitchell P. 1966. Synthesis of adenosine triphosphate by a protonmotive force in rat liver mitochondria. *Nature* 212: 257-8
Ren Y, Young W. 2013. Managing inflammation after spinal cord injury through manipulation of macrophage function. *Neural plasticity* 2013: 945034

Riedl SJ, Salvesen GS. 2007. The apoptosome: signalling platform of cell death. *Nat Rev Mol Cell Biol* 8: 405-13
Rizzuto R, Brini M, De Giorgi F, Rossi R, Heim R, et al. 1996. Double labelling of subcellular structures with organelle-targeted GFP mutants in vivo. *Curr Biol* 6: 183-8
Rizzuto R, Brini M, Pizzo P, Murgia M, Pozzan T. 1995. Chimeric green fluorescent protein as a tool for visualizing subcellular organelles in living cells. *Curr Biol* 5: 635-42
Rizzuto R, Nakase H, Darras B, Francke U, Fabrizi GM, et al. 1989. A gene specifying subunit VIII of human cytochrome c oxidase is localized to chromosome 11 and is expressed in both muscle and non-muscle tissues. *J Biol Chem* 264: 10595-600
Robb EL, Winkelmolen L, Visanji N, Brotchie J, Stuart JA. 2008. Dietary resveratrol administration increases MnSOD expression and activity in mouse brain. *Biochem Biophys Res Commun* 372: 254-9
Rodriguez-Jimnez FJ, Alastrue-Agudo A, Erceg S, Stojkovic M, Moreno-Manzano V. 2012. FM19G11 favors spinal cord injury regeneration and stem cell self-renewal by mitochondrial uncoupling and glucose metabolism induction. *Stem cells* 30: 2221-33
Rogers GW, Brand MD, Petrosyan S, Ashok D, Elorza AA, et al. 2011. High throughput microplate respiratory measurements using minimal quantities of isolated mitochondria. *PloS one* 6: e21746
Rottenberg H, Scarpa A. 1974. Calcium uptake and membrane potential in mitochondria. *Biochemistry* 13: 4811-7
Rowland JW, Hawryluk GW, Kwon B, Fehlings MG. 2008. Current status of acute spinal cord injury pathophysiology and emerging therapies: promise on the horizon. *Neurosurgical focus* 25: E2
Rubartelli A, Lotze MT. 2007. Inside, outside, upside down: damage-associated molecular-pattern molecules (DAMPs) and redox. *Trends Immunol* 28: 429-36
Sauerbeck A, Pandya J, Singh I, Bittman K, Readnower R, et al. 2011. Analysis of regional brain mitochondrial bioenergetics and susceptibility to mitochondrial inhibition utilizing a microplate based system. *J Neurosci Methods* 198: 36-43
Saunders RD, Dugan LL, Demediuk P, Means ED, Horrocks LA, Anderson DK. 1987. Effects of methylprednisolone and the combination of alpha-tocopherol and selenium on arachidonic acid metabolism and lipid peroxidation in traumatized spinal cord tissue. *Journal of neurochemistry* 49: 24-31
Scheff SW, Rabchevsky AG, Fugaccia I, Main JA, Lumpp JE, Jr. 2003. Experimental modeling of spinal cord injury: characterization of a force-defined injury device. *J Neurotrauma* 20: 179-93
Schroder K, Tschopp J. 2010. The inflammasomes. *Cell* 140: 821-32
Selmaj K, Raine CS. 1988. Tumor necrosis factor mediates myelin damage in organotypic cultures of nervous tissue. *Annals of the New York Academy of Sciences* 540: 568-70

Senter HJ, Venes JL. 1978. Altered blood flow and secondary injury in experimental spinal cord trauma. *Journal of neurosurgery* 49: 569-78
Sheu SS, Nauduri D, Anders MW. 2006. Targeting antioxidants to mitochondria: a new therapeutic direction. *Biochimica et biophysica acta* 1762: 256-65
Shi X, Zhao M, Fu C, Fu A. 2017. Intravenous administration of mitochondria for treating experimental Parkinson's disease. *Mitochondrion* 34: 91-100
Shitara H, Kaneda H, Sato A, Iwasaki K, Hayashi J, et al. 2001. Non-invasive visualization of sperm mitochondria behavior in transgenic mice with introduced green fluorescent protein (GFP). *FEBS Lett* 500: 7-11
Sims NR, Muyderman H. 2010. Mitochondria, oxidative metabolism and cell death in stroke. *Biochimica et biophysica acta* 1802: 80-91
Singh IN, Sullivan PG, Deng Y, Mbye LH, Hall ED. 2006. Time course of post-traumatic mitochondrial oxidative damage and dysfunction in a mouse model of focal traumatic brain injury: implications for neuroprotective therapy. *Journal of cerebral blood flow and metabolism : official journal of the International Society of Cerebral Blood Flow and Metabolism* 26: 1407-18
Skulachev VP. 1998. Uncoupling: new approaches to an old problem of bioenergetics. *Biochimica et biophysica acta* 1363: 100-24
Smith RA, Adlam VJ, Blaikie FH, Manas AR, Porteous CM, et al. 2008. Mitochondria-targeted antioxidants in the treatment of disease. *Annals of the New York Academy of Sciences* 1147: 105-11
Sorice M, Circella A, Cristea IM, Garofalo T, Di Renzo L, et al. 2004. Cardiolipin and its metabolites move from mitochondria to other cellular membranes during death receptor-mediated apoptosis. *Cell death and differentiation* 11: 1133-45
Spees JL, Olson SD, Whitney MJ, Prockop DJ. 2006. Mitochondrial transfer between cells can rescue aerobic respiration. *Proceedings of the National Academy of Sciences of the United States of America* 103: 1283-8
Struck J, Uhlein M, Morgenthaler NG, Furst W, Hoflich C, et al. 2005. Release of the mitochondrial enzyme carbamoyl phosphate synthase under septic conditions. *Shock* 23: 533-8
Suen DF, Norris KL, Youle RJ. 2008. Mitochondrial dynamics and apoptosis. *Genes & development* 22: 1577-90
Sullivan PG, Krishnamurthy S, Patel SP, Pandya JD, Rabchevsky AG. 2007. Temporal characterization of mitochondrial bioenergetics after spinal cord injury. *J Neurotrauma* 24: 991-9
Sullivan PG, Rabchevsky AG, Waldmeier PC, Springer JE. 2005. Mitochondrial permeability transition in CNS trauma: cause or effect of neuronal cell death? *Journal of neuroscience research* 79: 231-9
Sullivan PG, Springer JE, Hall ED, Scheff SW. 2004. Mitochondrial uncoupling as a therapeutic target following neuronal injury. *J Bioenerg Biomembr* 36: 353-6
Sun Z, Hu L, Wen Y, Chen K, Sun Z, et al. 2013. Adenosine triphosphate promotes locomotor recovery after spinal cord injury by activating

mammalian target of rapamycin pathway in rats. *Neural regeneration research* 8: 101-10
Swerdlow RH, Khan SM. 2004. A "mitochondrial cascade hypothesis" for sporadic Alzheimer's disease. *Med Hypotheses* 63: 8-20
Tachibana M, Sparman M, Sritanaudomchai H, Ma H, Clepper L, et al. 2009. Mitochondrial gene replacement in primate offspring and embryonic stem cells. *Nature* 461: 367-72
Taoka Y, Okajima K, Uchiba M, Murakami K, Kushimoto S, et al. 1997. Role of neutrophils in spinal cord injury in the rat. *Neuroscience* 79: 1177-82
Tator CH. 1991. Review of experimental spinal cord injury with emphasis on the local and systemic circulatory effects. *Neuro-Chirurgie* 37: 291-302
Tator CH, Fehlings MG. 1991. Review of the secondary injury theory of acute spinal cord trauma with emphasis on vascular mechanisms. *Journal of neurosurgery* 75: 15-26
Tompkins AJ, Burwell LS, Digerness SB, Zaragoza C, Holman WL, Brookes PS. 2006. Mitochondrial dysfunction in cardiac ischemia-reperfusion injury: ROS from complex I, without inhibition. *Biochimica et biophysica acta* 1762: 223-31
Tondera D, Grandemange S, Jourdain A, Karbowski M, Mattenberger Y, et al. 2009. SLP-2 is required for stress-induced mitochondrial hyperfusion. *The EMBO journal* 28: 1589-600
Twig G, Elorza A, Molina AJ, Mohamed H, Wikstrom JD, et al. 2008a. Fission and selective fusion govern mitochondrial segregation and elimination by autophagy. *The EMBO journal* 27: 433-46
Twig G, Hyde B, Shirihai OS. 2008b. Mitochondrial fusion, fission and autophagy as a quality control axis: the bioenergetic view. *Biochimica et biophysica acta* 1777: 1092-7
Tymianski M, Tator CH. 1996. Normal and abnormal calcium homeostasis in neurons: a basis for the pathophysiology of traumatic and ischemic central nervous system injury. *Neurosurgery* 38: 1176-95
Ungvari Z, Labinskyy N, Mukhopadhyay P, Pinto JT, Bagi Z, et al. 2009. Resveratrol attenuates mitochondrial oxidative stress in coronary arterial endothelial cells. *Am J Physiol Heart Circ Physiol* 297: H1876-81
Valasani KR, Sun Q, Fang D, Zhang Z, Yu Q, et al. 2016. Identification of a Small Molecule Cyclophilin D Inhibitor for Rescuing Abeta-Mediated Mitochondrial Dysfunction. *ACS Med Chem Lett* 7: 294-9
Valasani KR, Vangavaragu JR, Day VW, Yan SS. 2014. Structure based design, synthesis, pharmacophore modeling, virtual screening, and molecular docking studies for identification of novel cyclophilin D inhibitors. *J Chem Inf Model* 54: 902-12
Visavadiya NP, Patel SP, VanRooyen JL, Sullivan PG, Rabchevsky AG. 2015. Cellular and subcellular oxidative stress parameters following severe spinal cord injury. *Redox Biol* 8: 59-67
Wang X, Arcuino G, Takano T, Lin J, Peng WG, et al. 2004. P2X7 receptor inhibition improves recovery after spinal cord injury. *Nature medicine* 10: 821-7

Wang X, Gerdes HH. 2015. Transfer of mitochondria via tunneling nanotubes rescues apoptotic PC12 cells. *Cell death and differentiation* 22: 1181-91
Weisiger RA, Fridovich I. 1973. Superoxide dismutase. Organelle specificity. *The Journal of biological chemistry* 248: 3582-92
Weissig V, Boddapati SV, Cheng SM, D'Souza GG. 2006. Liposomes and liposome-like vesicles for drug and DNA delivery to mitochondria. *Journal of liposome research* 16: 249-64
Wigler M, Perucho M, Kurtz D, Dana S, Pellicer A, et al. 1980. Transformation of mammalian cells with an amplifiable dominant-acting gene. *Proceedings of the National Academy of Sciences of the United States of America* 77: 3567-70
Winklhofer KF, Haass C. 2010. Mitochondrial dysfunction in Parkinson's disease. *Biochimica et biophysica acta* 1802: 29-44
Winterbourn CC. 1995. Toxicity of iron and hydrogen peroxide: the Fenton reaction. *Toxicol Lett* 82-83: 969-74
Wisniewski HM, Bloom BR. 1975. Primary demyelination as a nonspecific consequence of a cell-mediated immune reaction. *The Journal of experimental medicine* 141: 346-59
Wolman L. 1965. The Disturbance of Circulation in Traumatic Paraplegia in Acute and Late Stages: A Pathological Study. *Paraplegia* 2: 213-26
Wrathall JR, Teng YD, Choiniere D. 1996. Amelioration of functional deficits from spinal cord trauma with systemically administered NBQX, an antagonist of non-N-methyl-D-aspartate receptors. *Experimental neurology* 137: 119-26
Xiong Y, Gu Q, Peterson PL, Muizelaar JP, Lee CP. 1997. Mitochondrial dysfunction and calcium perturbation induced by traumatic brain injury. *J Neurotrauma* 14: 23-34
Xiong Y, Hall ED. 2009. Pharmacological evidence for a role of peroxynitrite in the pathophysiology of spinal cord injury. *Experimental neurology* 216: 105-14
Xu W, Chi L, Xu R, Ke Y, Luo C, et al. 2005. Increased production of reactive oxygen species contributes to motor neuron death in a compression mouse model of spinal cord injury. *Spinal cord* 43: 204-13
Yamada Y, Akita H, Kamiya H, Kogure K, Yamamoto T, et al. 2008. MITO-Porter: A liposome-based carrier system for delivery of macromolecules into mitochondria via membrane fusion. *Biochimica et biophysica acta* 1778: 423-32
Yamada Y, Akita H, Kogure K, Kamiya H, Harashima H. 2007. Mitochondrial drug delivery and mitochondrial disease therapy--an approach to liposome-based delivery targeted to mitochondria. *Mitochondrion* 7: 63-71
Yang YW, Koob MD. 2012. Transferring isolated mitochondria into tissue culture cells. *Nucleic Acids Res* 40: e148
Young W, Koreh I. 1986. Potassium and calcium changes in injured spinal cords. *Brain research* 365: 42-53
Zhang Q, Itagaki K, Hauser CJ. 2010a. Mitochondrial DNA is released by shock and activates neutrophils via p38 map kinase. *Shock* 34: 55-9

Zhang Q, Raoof M, Chen Y, Sumi Y, Sursal T, et al. 2010b. Circulating mitochondrial DAMPs cause inflammatory responses to injury. *Nature* 464: 104-7

VITA

Jenna L. (VanRooyen) Gollihue
Birthplace: Denver, CO, USA

Education:

2011- present	PhD Candidate	Department of Physiology University of Kentucky, Lexington, KY
2008	Bachelor of Science	Food Science and Technology Texas A&M University, College Station, TX

AWARDS AND HONORS:

- Thomas V Getchell Memorial Award, Cash travel award, University of Kentucky, November 2016
- NIH F31 Fellowship award-NIH F31NS093904-01A1, April 1, 2016-September 30, 2017
- Michael Goldsberger Poster Cash Award, Top poster prize award, Annual National Neurotrauma Symposium, Lexington KY, June 26-29, 2016
- Poster Cash Award, 4th Annual Kentucky Chapter Meeting, American Physiological Society, Lexington, KY, March 24, 2016
- Travel Award Recipient, 22nd Annual American Society for Neural Therapy and Repair Conference, Clearwater, FL April 30-May 2 2015
- Poster Cash Award, Bluegrass Society for Neuroscience Day, Lexington KY, March 25, 2015
- NIH Predoctoral Fellowship- Neurobiology of CNS Injury and Repair Training Grant (5T32NS077889) 2014- 2016
- KSCHIRT Training Fellowship 2013-2014
- Deans Honor Roll Texas A&M University 2008

Publications:

Jenna L. Gollihue, Samir P. Patel, Charles Mashburn, Khalid C. Eldahan and Alexander G. Rabchevsky. (2017) Optimization of Mitochondrial Isolation Techniques for Intraspinal Transplantation Procedures. *Journal of Neuroscience Methods.* Epub 2017 May 23 DOI: 10.1016/j.jneumeth.2017.05.023

Jenna L. Gollihue and Alexander G. Rabchevsky. (2017) Prospects for Therapeutic Mitochondrial Transplantation. *Mitochondrion.* 2017 May 19 DOI: 10.1016/j.mito.2017.05.007

Patel S.P., Cox D.H., **VanRooyen J.L**., Bailey W.M., Geldenhuys W.J., Gensel J.G., Sullivan P.G. and Rabchevsky A.G. (2017) Pioglitazone Treatment Following Spinal Cord Injury Maintains Acute Mitochondrial Integrity and Increases Chronic Tissue Sparing and Functional Recovery. Exp Neurol. 293 (2017) 74–82. Epub 2017 March 30 DOI: 10.1016/j.expneurol.2017.03.021

Nishant P. Visavadiya, Samir P. Patel, **Jenna L. VanRooyen**, Patrick G. Sullivan, Alexander G. Rabchevsky (2015) Cellular and Subcellular Oxidative Stress Parameters Following Severe Spinal Cord Injury. *Redox Biology* PMID:26760911, PMCID: PMC4712315

Samir P Patel, Taylor D. Smith, **Jenna L. VanRooyen**, David Powell, David H. Cox, Patrick G. Sullivan, Alexander G. Rabchevsky. (2015) Serial Diffusion Tensor Imaging In Vivo Predicts Long-Term Functional Recovery and Histopathology in Rats Following Different Severities of Spinal Cord Injury. (2015) *J. Neurotrauma* 33(10):917-928. PMID: 26650623

Patel S.P., Sullivan P.G., Pandya J.D., Goldstein G.A., **VanRooyen J.L.**, Yonutas H.M, Eldahan K.C., Morehouse J., Magnuson D.S.K., Rabchevsky A.G. (2014) N-acetylcysteine amide preserves mitochondrial bioenergetics and improves functional recovery following spinal trauma. *Exp Neurol.* PMID: 24805071

Head E., Murphey H.L., Dowling A.L., McCarty K.L., Bethel S.R., Nitz J.A., Pleiss M., **Vanrooyen J**., Grossheim M., Smiley J.R., Murphy M.P., Beckett T.L., Pagani D., Bresch F., Hendrix C.(2012) A combination cocktail improves spatial attention in a canine model of human aging and Alzheimer's disease. *J Alzheimers Dis*. 2012;32(4):1029-42 PMID:22886019

Oral Presentations:

Gollihue J.L., Patel S.P., Eldahan K.C., Cox D.H., Rabchevsky A.G. "Transplanted Mitochondria Maintain Cellular Respiration after Contusion Spinal

Cord Injury", *Annual Physiology Department Retreat*, University of Kentucky, Lexington, KY. August 5, 2016.

VanRooyen J.L., Patel S.P., Eldahan K.C., Smith T.L., Cox D.H., Rabchevsky A.G. "Mitochondrial Transplantation to Restore Cellular Bioenergetics after Spinal Cord Injury." *22nd Annual American Society for Neural Therapy and Repair Conference*, Clearwater, FL. April 30-May 2, 2015

Presentations (Posters/Abstracts):

Gollihue J.L. , Patel S.P., Mashburn C., Eldahan K.C., Cox D., Sullivan P.G. and Rabchevsky A. G**.** "Mitochondrial transplantation into the injured spinal cord improves cellular respiration" *1st Annual Clinical-Translational Research Symposium*, Kentucky Neuroscience Institute, UK Albert B. Chandler Hospital, Lexington, KY, September 2016.

VanRooyen J.L., Patel S., Mashburn C., Eldahan K., Cox D., Sullivan P. and Rabchevsky A. "Transplanted mitochondria significantly maintain cellular respiration after acute contusion spinal cord injury" *The 34th Annual National Neurotrauma Society Symposium*, Lexington, KY, July 2016. *J. Neurotrauma* 33(13): A-8, T01-10.

VanRooyen J.L., Patel S.P., Mashburn C., Eldahan K.C., Cox D., Sullivan P.G., Rabchevsky A.G. "Restoration of Cellular Bioenergetics after Mitochondrial Transplantation into the Injured Spinal Cord" *Bluegrass Society for Neuroscience Day*, Lexington, KY, July 2016.

VanRooyen J.L., Patel S.P., Eldahan K.C., Cox D., Rabchevsky A.G. "Mitochondrial Transplantation into the Injured Spinal Cord Improves Bioenergetic Integrity." *Keystone Symposium on Mitochondrial Dynamics, Steamboat Springs*, CO. April 3-7 2016

VanRooyen J.L., Patel S.P., Mashburn C., Eldahan K.C., Cox D., Sullivan P.G., Rabchevsky A.G. "Transplantation of Mitochondria to Maintain Overall Respiration after Contusion Spinal Cord Injury*" 4th Annual Meeting of Kentucky Chapter American Physiological Society*, Lexington, KY. March 24 2016

Eldahan K.C., **VanRooyen J.L**., Patel S.P., and Rabchevsky A.G. "Pharmacological Manipulation of Maladaptive Plasticity to Prevent Autonomic Dysreflexia" *International Symposium on Neural Regeneration Annual Conference*, Pacific Grove, CA. November 2015

Patel S.P., **VanRooyen J.L.,** Sullivan P.G. and Rabchevsky A.G. "Synergistic Effects of β-Hydroxybutyrate and Acetyl-L-Carnitine on Mitochondrial Function

after Spinal Cord Injury." *National Neurotrauma Society Annual Conference*, Santa Fe, NM. June 2015

VanRooyen J.L., Patel S.P., Eldahan K.C., Smith T.L., Cox D.H., Rabchevsky A.G. "Mitochondrial Supplementation after Spinal Cord Injury Maintains Cellular Bioenergetics." *Bluegrass Society for Neuroscience Day*, Lexington, KY. March 25 2015

Patel S.P, **VanRooyen J.L.,** Visavadiya N.P., Smith T.L., Sullivan P.G. and Rabchevsky A.G. "Treatment with Ketone Bodies Preserves Mitochondrial Function and Reduces Oxidative Stress Following Contusion Spinal Cord Injury." *Society for Neuroscience Annual Conference*, Washington, D.C. November 2014

Rabchevsky A.G., Eldahan K.C., **VanRooyen J.L**., Wang C.Y., Smith T.L., Cox D.H. and Patel S.P. "Gabapentin Management of Autonomic Dysreflexia: Effects on Systemic Inflammation." *Society for Neuroscience Annual Conference*, Washington, D.C. November 2014

Patel S.P., Sullivan P.G., Yonutas H.M., **VanRooyen J.L.**, Eldahan K.C. and Rabchevsky A.G. "Effects of Continuous N-Acetylcysteine Amide (NACA) Treatment on Acute and Chronic Pathophysiology After Contusion Spinal Cord Injury" *Society for Neuroscience Annual Conference*, San Diego, CA. November 2013

Rabchevsky A.G., Eldahan K.C., Nall D.A., **VanRooyen J.L.**, Wang C.Y. and Patel S.P. "Influences of Inflammation and Gabapentin on the Severity of Autonomic Dysreflexia in Relation to the Expression of Inflammatory Cytokines in both Visceral and Neural Tissues" *Society for Neuroscience Annual Conference*, San Diego, CA. November 2013

Rabchevsky A.G., Eldahan K.C., **VanRooyen J.L.**, Kline IV R.H., and Patel S.P. "Mitigation of Autonomic Dysreflexia by Gabapentin Treatment after Complete Spinal Cord Injury: Effects on pERK Expression in Spinal Cord Neurons and Neuroglial Cells" *Society for Neuroscience Annual Conference*, New Orleans, LA. October 2012

VanRooyen J.L., Patel S.P., Kline IV R.H., Mashburn C., and Rabchevsky A.G., "Transplantation of Exogenous Mitochondria into Culture Cell Lines" *University of Kentucky Integrated Biomedical Science Orientation*, Lexington, KY. August 2012

VanRooyen J.L., Patel S.P., Kline IV R.H., Mashburn C, and Rabchevsky A.G., "Transplantation of Exogenous Mitochondria into Culture Cell Lines" *University of Kentucky Physiology Department retreat*, Jabez, KY. July 2012